Journal of the
OPTICAL SOCIETY
of AMERICA

VOLUME 40, NUMBER 2 FEBRUARY, 1950

Detection of Tracks and Stars in Nuclear Track Plates*

E. H. LAND, G. BIRD, AND W. A. SHURCLIFF
Research Laboratory, Polaroid Corporation, Cambridge, Massachusetts
(Received Nobember 22, 1949)

Tracks and stars in nuclear track plates are usually found by ordinary bright-field microscope procedures affording limited field of view and requiring continual focusing up and down. Standard dark-field illumination schemes fail due to background scattering by fog grains. A rotating-azimuth, planar, dark-field, illumination scheme has been developed which provides sufficient contrast so that low magnification (50 to 100 times) may be used. The field of view is thereby increased to 2 to 4 mm and the depth of field becomes comparable to the total thickness of the emulsion.

1. INTRODUCTION

IN studies of cosmic rays and nuclear reactions considerable use is currently being made of nuclear track plates, whose special emulsions are particularly suited to recording tracks of fast charged particles such as alpha-particles, protons, and mesons.[1,2] In the exposed and developed plate, a typical track, which may be a few microns to a few millimeters in length, consists of a co-linear array of silver grains perhaps 0.3 to 0.5 microns in diameter. The distance between successive grains is random, being typically 0.2 to 2 microns. A track is usually reasonably straight except along the terminal segment where the particle's velocity was small. A track may make any angle with the plane of the emulsion, although tracks roughly paralleling the emulsion are ordinarily best suited to careful study.

Typical emulsions, after being developed, fixed, and dried, are 40 to 90 microns in thickness. (Recently developed emulsions are even thicker.) They contain besides individual tracks and stars, a random array of silver grains comprising the "fog" background.

Microscopes are used to detect and locate interesting tracks, and to analyze them. Analysis involves high resolution and high magnification, and will not be discussed here. The problem of detection will be discussed, and a new, dark-field, low magnification detection scheme will be described.

2. LIMITATIONS TO USUAL DETECTION METHODS

Tracks are usually detected by means of a microscope having ordinary bright-field illumination. Since, in this method, the track can appear only as a row of black grains on a white background, there is the obvious requirement that the grains be resolved; otherwise the track may entirely escape notice. This requirement requires (a) moderately high magnification, such as 150 to 300, (b) correct focus within perhaps 3 to 10 microns, and (c) full attention of the observer—not only to see the grains, but also to distinguish grains comprising a track from grains comprising the fog. In the case of weak, steeply-pitched tracks (tracks making a considerable angle with the plane of the emulsion), the observer must vary the focus through a considerable range and mentally integrate suspected track segments noticed for successive positions of focus. The general result is that the field of view is usually less than 1 mm in diameter, and each area of the plate must be inspected carefully for perhaps 10 to 30 positions of focus. It is not surprising, therefore, that one to three days of meticulous effort may be required to detect all the tracks on a single 1×3-in. plate.

Use of ordinary dark-field illumination is seldom advantageous. Tracks can be seen by this method (as rows of white specks on a dark background) if high resolution and high magnification are used. But if the

* This work was done under sub-contract to the Brookhaven National Laboratory which is a prime contractor of the AEC.
[1] C. F. Powell and G. P. S. Occhialini, *Nuclear Physics in Photographs* (Clarendon Press, Oxford, 1947).
[2] H. Yagoda, *Radioactive Measurements with Nuclear Emulsions* (John Wiley and Sons, Inc., New York, 1949).

attempt is made to use this method with low magnification, scattering by the fog grains forms a practically continuous background tending to mask all but the very strongest tracks.

3. ROTATING-AZIMUTHAL PLANAR DARK-FIELD ILLUMINATION METHOD

When this laboratory was first presented by the Nuclear Track Group of the Brookhaven National Laboratory with the problem of finding a simpler method of detecting tracks and stars in nuclear track plates, the thought occurred to one of us (E.H.L.) that the dark-field method might be significantly improved by illuminating a given track *only by light perpendicular thereto*. The track might then scatter especially strongly, whereas the fog would not. By slowly changing the azimuth of the planar dark-field beam, tracks of different azimuths would gleam successively.† Thus in the course of a short interval, of the order of one second, all tracks within the field of view would be detected.

This scheme was tried and found effective. It proved to be especially effective using an objective lens of small numerical aperture (0.17 to 0.25) and low over-all magnification (50 to 100 times).

It was found that the angle between the illuminating ray and the vertical (microscope axis) was important. Even a strong track gleamed only moderately brightly when the illuminating ray (in the prescribed vertical plane) was nearly horizontal; but it gleamed very brightly when the ray was directed upward at an angle of 25° to 45° from the vertical.

Figure 1 indicates schematically the most satisfactory design as applied to a Leitz CTA binocular microscope with Abbe condenser of N.A. 1.2. Heart of the system is a small rotating sector located just below the lower lens of the condenser. The sector has two 15° openings 180° apart. The openings do not extend inward as far as the $\frac{1}{8}$-in. axial shaft, but are blocked off close to that shaft by a double-wedge diaphragm indicated in the figure. The diaphragm is adjusted so that no ray passing first the sector and then the nuclear track plate makes an angle of less than, say, 25° with the vertical.

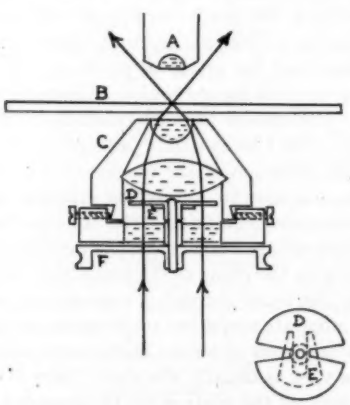

FIG. 1. Schematic general design, and detail of sector. *A*: objective lens; *B*: nuclear track plate; *C*: condenser lens; *D*: sector; *E*: double-wedge diaphragm; *F*: pulley.

The sector shaft is supported by a bearing mounted along the axis of a thick Lucite disk which is mounted centered on the base of the Abbe condenser. The lower end of the shaft is attached to a pulley rotated at approximately $\frac{1}{2}$ rev./sec. by a rubber belt driven by a variable speed motor.

The entire aperture of the condenser is filled with light proceeding vertically upward from the plane sub-stage mirror. A wide aperture (3 in.) microscope lamp with ground glass is placed 1 cm from the sub-stage mirror.

Using an objective lens of numerical aperture 0.17, an over-all magnification of 50 to 100 times, and with the illumination system well centered, the fog background in a typical emulsion of 200-micron nominal thickness appears unobtrusive and essentially static, while individual tracks gleam and disappear alternately. The width of the field of view is 2 to 4 mm, and the useful depth of field is perhaps 50 to 100 microns. Using an intermediate adjustment of the focus, strong tracks may be seen at any depth in the emulsion; thus steeply pitching strong tracks and strong tracks as long as 2 to 3 mm may be seen in their entireties at a single glance. By their blinking on and off, tracks call attention to themselves conveniently; stars are particularly conspicuous, appearing almost like rotating spoked wheels.

In foggy emulsions, weak tracks may escape notice despite use of the rotating azimuthal illumination scheme. The scheme is, of course, completely unsuited to *analysis* of tracks, as analysis requires high resolution and high magnification. But for use in locating strong tracks and stars, and especially for locating stars in "minimum ionization" plates, the method appears to have merit. The Nuclear Track Group at the Brookhaven National Laboratory has found,[3] in the case of minimum ionization plates, that stars may be located approximately five times more rapidly than by the usual, bright-field method.

Since the rotating azimuthal illumination system employs an objective lens of low numerical aperture, the working distance is large, being of the order of 1 cm. Thus plates may be examined from the back as well as from the front, which is an advantage in studying tracks in the deeper layers of thick emulsions which are foggy or optically inhomogeneous. It is also possible to

† We are indebted to our colleague Dr. C. D. West for pointing out to us that planar dark-field illumination was used over 30 years ago to show the non-spherical nature of certain particles studied under the ultramicroscope. See F. Weigert *Optische Methoden der Chemie* (Akademische Verlagsgesellschaft MBH, Leipzig, 1927) p. 412–417; also H. Siedentopf, Z. wiss. Mikroskop. **29**, 1 (1912).

[3] Private communication.

look through one or more plates to view an underlying plate, offering the possibility, which may or may not be of value, of viewing *in a stack* plates which have been exposed as a stack.

4. DISCUSSION OF THE IMPROVED SIGNAL-TO-BACKGROUND RATIO

The explanation for the improvement in signal-to-background (track-to-fog) ratio is easily stated. The individual silver grains, having diameters less than the wave-length of light, scatter light in all directions. For a number of randomly located grains (fog), there is only one direction in which constructive interference occurs among the scattered wavelets, this being the "straight-ahead" direction. Thus little fog-scattered light reaches the objective lens, which is 25° to 45° from the straight-ahead direction in the design described. For the grains comprising a straight horizontal track, however, and at the instant when the illuminating plane is perpendicular to the track, constructive interference occurs in all directions perpendicular to the track. Because the microscope axis is perpendicular to the track, the amount of light scattered by the track toward the objective lens and thence into the observer's eye is considerable.‡ Thus the track appears bright and the fog appears relatively dark. And conversely, when the illuminating plane is *parallel* to the track, *destructive* interference may be found in the direction of the objective, so that the track may be entirely invisible or may even "reverse," that is, appear darker than the fog. This phenomenon is, of course, advantageous as it increases the amplitude of the blinking and accentuates the noticeability of the track.

These pronounced interference effects do not occur, of course, when the numerical aperture and magnification are increased to the point where the individual grains are clearly resolved.

The situation regarding tracks which are steeply pitched is also easily understood. Consider a straight track comprising many grains which are arranged colinearly but with random separations. Assume that the track makes an angle A with the vertical, and that A is greater than 20°. Assume further that the illuminating ray makes an angle of 40° with the vertical. Now we may imagine a very small, two-dimensional, plane mirror which (a) intersects the track, (b) makes an angle of 20° with the vertical, and (c) is perpendicular to the plane determined by the illuminating ray and the microscope axis. Obviously this mirror will specularly reflect the illuminating ray toward the objective lens. That is, interference is constructive (in the vertical direction) for light scattered from all the various area elements of the mirror.

Now it is clear that if the illuminating ray and the mirror are continually rotated together about the microscope axis, the track and mirror will occasionally coincide. These occasions are clearly the occasions when the track will be seen to gleam; the track may then be regarded as a specularly-reflecting portion of a two-dimensional specularly-reflecting mirror.

When $A=90°$ (track horizontal), there are two azimuths of the mirror for which the mirror and track coincide, these two aximuths being, of course 180° apart. When $90°>A>20°$, there are still two azimuths for which coincidence occurs, but they are no longer 180° apart.¶

These inferences are borne out by observation. In many-pronged stars whose prongs pitch to different extents, prongs of different plan-view azimuth may gleam at the same instant or at widely different instants, depending on the relative magnitudes and sign of pitch.

This work was supported by a contract with the Brookhaven National Laboratory. We wish to thank the Nuclear Track Group of that laboratory for its advice and encouragement, and for lending us representative nuclear track plates.

‡ More detailed consideration shows that, since the track grains have appreciable diameters (0.3 to 0.5 microns) and may depart from strict co-linearity by this same order of magnitude, constructive interference should be considerably more pronounced for generally forward scattering than for backward or lateral scattering. It is for this reason that the illuminating rays are arranged to have directions within roughly 45° of the direction of the center of the objective lens.

¶ If $A=20°$, there will be just one azimuth for which coincidence occurs; when $A<20°$, coincidence cannot occur.

The Measurement of Unresolved, Single Particles of Uniform Thickness by Means of Variable Phase Microscopy*

HAROLD OSTERBERG AND GILBERT E. PRIDE
American Optical Company, Research Laboratory, Stamford, Connecticut
(Received September 30, 1949)

The adjustments of a variable phase microscope control two variable experimental parameters, specifically the phase difference δ between and the amplitude transmission ratio h of the conjugate and complementary areas of the diffraction plate or its polanret equivalent. It is shown that the center of the sharply focused diffraction image of a single unresolved particle can be brought to zero intensity by a definite choice of the parameters h and δ. The relations which exist among the required choice of h, δ, the area and the optical properties of the particle are derived and specialized to various classes of particles. These relations permit the computation of the area and one or more optical properties of the particle from the observed values of the parameters h, δ. Observations made upon opaque particles with a modified polanret microscope are described and found to be in accord with the theory. The radii of these particles ranged from 0.5 to 0.15 times the Airy limit of the test objective.

I. INTRODUCTION

INFORMATION gained with the aid of a light microscope about the area and the optical properties of an unresolved particle must be deduced from the properties of the diffraction image of the particle. An unresolved particle is defined for the purposes of the following discussion as one whose effective radius R_0 is less than one-half of the Airy limit of the microscope objective. πR_0^2 is equal to the area A of the particle. It is assumed that the particle is not unduly oblong. The most important optical properties of the particle are: g, the ratio of the amplitude transmission of the particle to the amplitude transmission of its surround and Δ, the optical path difference between the particle and surround. Other properties of the particle, for example its thickness and volume, can often be determined when A, g and Δ have been measured.

The following method for measuring the properties R_0, g and Δ of a particle is basically photometric although auxiliary photometric equipment is not essential. The photometric attack has been chosen because more precise information about the area and optical properties of the particle can be gained from the diffraction image by photometric measurements than by linear measurements.

If the particle is viewed in a variable phase microscope such as the polanret[1] microscope, the appearance of the diffraction image varies with the amplitude transmission ratio h and the phase difference δ of the two zones of the diffraction plate or its polanret equivalent. The quantities h and δ will be called the polanret settings whether the settings are made with a polanret system or any other system of continuously variable phase microscopy. Theory shows that it is always possible to find a polanret setting h_1, δ_1 for which the energy density at the center of the diffraction image (i.e., at the diffraction head) is zero. If the system scatters light, the diffraction head will still be darkest at this polanret setting. With a polanret microscope, h and δ can be varied continuously and independently toward the particular setting h_1, δ_1 at which the diffraction head is darkest as judged either visually or photometrically. If δ_1 is increased by π, a second polanret setting h_1, $(\delta_1+\pi)$ is obtained at which the diffraction head appears brightest. When the dark and bright settings are judged visually, the dark setting can be made the more critically. Furthermore, the bright setting does not provide essentially new information even though it constitutes a second polanret setting. From the dark setting of the polanret microscope, therefore, two experimental parameters h_1 and δ_1 are available. In principle, these two parameters can be expected to permit the determination of A and g when Δ is known or of A and Δ when g is known. With opaque particles, $g=0$ and Δ is not significant so that one polanret setting provides more than enough experimental parameters for determining the single unknown A.

It will be shown that the dark settings h_1, δ_1 depend upon the properties of the unresolved particle and that the functional relationships among the experimental parameters h_1, δ_1 and the unknowns A, g and Δ are suitable for determining the unknowns from the experimental parameters. When all of the three properties A, g and Δ are unknown, it is possible to determine the three unknowns by securing a second polanret dark setting after suitable variations have been made in either the refractive index or in the amplitude transmission of the medium surrounding the particle.

The theory and method will be specialized to particles whose amplitude and phase transmissions are uniform except when the particle is substantially opaque. The amplitude and phase transmission of the surround is assumed to be uniform. The theory, in its most general form, includes the effects of spherical aberration but the specialized equations are restricted to microscope objectives of the Airy type.[2]

* Presented at the New York meeting of the Optical Society of America, February 21, 1947.

[1] H. Osterberg, J. Opt. Soc. Am. **37**, 726 (1947).

[2] H. Osterberg and F. C. Wissler, J. Opt. Soc. Am. **39**, 558 (1949), Eqs. (27) and (28).

II. THE AMPLITUDE AND PHASE EQUATION

The object plane X_0,Y_0 and the image plane X,Y are conjugate as in Fig. 1. The object plane contains an unresolved particle of area A and of constant, complex amplitude and phase transmission f_0. The constant complex number f_1 denotes the amplitude and phase transmission of the surround. The particle will be located upon the optical axis in order to simplify the analysis. A monochromatic source of light is focused as in Köhler illumination upon a diaphragm which is placed adjacent to the first focal plane of the substage condenser. The opening in this diaphragm is focused upon the conjugate area (see Fig. 1) of the diffraction plate or its polanret equivalent. The optical direction cosines of the normals of the practically plane waves which are incident upon the object plane are denoted by p_0,q_0. The optical direction cosines of the rays in the axial cone of the image space are denoted by p,q. $P(p,q)$ is the usual pupil function.[3]

Let $F_0(x,y,p_0,q_0)$ denote the amplitude and phase distribution produced over the image plane by the incidence upon the object plane of the wave front whose normal has the optical direction cosines p_0,q_0. It has been shown[4] that

$$F_0(x,y,p_0,q_0)=F_u(x,y,p_0,q_0)+F_d(x,y,p_0,q_0), \quad (1)$$

in which

$$M^2F_u(x,y,p_0,q_0)=f_1\exp[2\pi i(p_0x+q_0y)/M]P((p_0/M),(q_0/M)) \quad (2)$$

and in which

$$F_d=(f_0-f_1)\int\int\exp[2\pi i(p_0x_0+q_0y_0)]U(x-Mx_0,y-My_0)dx_0dy_0. \quad (3)$$

The integral (3) extends over the area of the particle. The primary diffraction integral U is given by

$$U(x,y)=\int\int P(p,q)\exp[2\pi i(px+qy)]dpdq; \quad (4)$$

$$p^2+q^2\leqq n^2\sin^2\vartheta_m=\sin^2\vartheta_m\equiv\rho_m^2. \quad (4.1)$$

All distances in Eqs. (2) to (4) are to be measured in number of wave-lengths and are therefore dimensionless. Equation (2) is valid when the field of view in the object space extends over a large number of wave-lengths.

When the particle is located upon the optical axis and when its radius does not exceed one-half of the Airy limit of resolution of the microscope objective, Eq. (3) may be replaced by the simpler expression

$$F_d(x,y,p_0,q_0)=fAU(x,y) \quad (5)$$

in which A is the area of the particle and in which

$$f\equiv f_0-f_1. \quad (6)$$

[3] H. Osterberg and J. E. Wilkins, Jr., J. Opt. Soc. Am. 39, 553 (1949).

[4] H. Osterberg and F. C. Wissler, J. Opt. Soc. Am. 39, 558 (1949).

From Eqs. (1), (2) and (5)

$$M^2F_0(x,y,p_0,q_0)=f_1\exp[2\pi i(p_0xq_0y)/M]+P((p_0/M),(q_0/M))+fM^2AU(x,y). \quad (7)$$

Since $U(x,y)$ approaches zero rapidly as x or y or both become large,

$$|M^2F_0(x,y,p_0,q_0)|^2\rightarrow|f_1|^2|P((p_0/M),(q_0/M))|^2 \quad (8)$$

as x or y become large. Such points x,y fall outside of the geometrical image of the particle. Accordingly, Eq. (8) determines the constant partial energy density over that portion of the geometrical image of the surround which is not adjacent to the geometrical image of the particle.

III. THE TOTAL ENERGY DENSITY

The total energy density $G(x,y)$ in the image plane is given[5] by

$$G(x,y)=\int\int(S(p_0,q_0))/(n_0^2-p_0^2-q_0^2)\times|F_0(x,y,p_0,q_0)|^2dp_0dq_0 \quad (9)$$

in which the integration extends over optical direction cosines of the rays incident upon the object plane. $S(p_0,q_0)$ is proportional to the energy density of the source of light. $F_0(x,y,p_0,q_0)$ is determined from Eq. (7).

From Eq. (4)

$$U(0,0)=\int\int P(p,q)dpdq. \quad (10)$$

From Eqs. (7), (9), and (10) the energy density $G(0,0)$ at the diffraction head is therefore

$$G(0,0)=\frac{1}{M^4}\int\int\frac{S(p_0,q_0)}{n_0^2-p_0^2-q_0^2}\left|f_1P\left(\frac{p_0}{M},\frac{q_0}{M}\right)+fM^2A\int\int P(p,q)dpdq\right|^2dp_0dq_0. \quad (11)$$

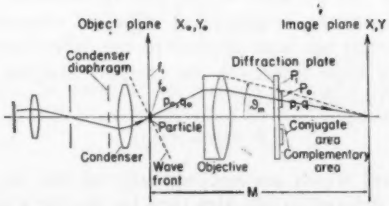

FIG. 1. The essential elements of the phase microscope and their denotation. The refractive indices of the object and image spaces are, respectively, n_0 and $n=1$. The conjugate area of the diffraction plate coincides with the geometrical image of the opening in the condenser diaphragm. The complementary comprises the remaining area of the diffraction plate. It is supposed that the diffraction plate is variable in the sense that the optical path difference between its conjugate and complementary areas and the light transmission ratio of these areas can be varied.

[5] H. Osterberg, J. Opt. Soc. Am. 38, 685 (1948), Eq. (19).

From Eqs. (8) and (9) the total energy density $G(\infty)$ at a point far removed from the diffraction head assumes the constant value

$$G(\infty)=\frac{|f_1|^2}{M^4}\int\int\frac{S(p_0,q_0)}{n_0^2-p_0^2-q_0^2}\left|P\left(\frac{p_0}{M},\frac{q_0}{M}\right)\right|^2 dp_0dq_0. \quad (12)$$

If the conjugate area of the diffraction plate is opaque, $S(p_0,q_0)|P((p_0/M),(q_0/M))|^2=0$ and $G(\infty)=0$. This case of schlieren microscopy will be excluded.

The consequences of Lambert's law have not been incorporated in current theories of phase microscopy. The effect of employing a source of illumination which does not radiate with spherical symmetry is to modify the source-function $S(p_0,q_0)$. An advantage of this method of measuring unresolved particles is that the method is practically independent of the choice of source-function provided that the source has sufficiently great intensity for the purpose of obtaining an illuminated background of adequate energy density $G(\infty)$.

IV. THE GENERAL CONDITION FOR ZERO ENERGY DENSITY AT THE DIFFRACTION HEAD

Apart from the trivial case in which $S(p_0,q_0)=0$, it follows directly from Eq. (11) that the condition for zero energy density at the diffraction head is

$$f_1P((p_0/M),(q_0/M))+fM^2A\int\int P(p,q)dpdq=0. \quad (13)$$

It will be supposed that the pupil function $P(p,q)$ is chosen so that

$$\int\int P(p,q)dpdq\neq 0. \quad (14)$$

It has been shown[3] that

$$P(p,q)=c(p,q)\psi(p,q) \quad (15)$$

in which $c(p,q)$, the coating function, is a complex number which specifies the change produced in the amplitude and phase transmission of the diffraction plate by the presence of the coating material on the diffraction plate. In particular, $c(p,q)=1$ when no coating material has been applied to the diffraction plate. For Airy type objectives the complex function $\psi(p,q)$ reduces to unity so that

$$P(p,q)=c(p,q). \quad (16)$$

Objectives which are not normally of the Airy type may be reduced to the Airy type by placing a properly coated correction plate adjacent to the diffraction plate of phase microscopy.

The schlieren case $P((p_0/M),(q_0/M))=0$ is a solution of Eqs. (13) and (14) when $f_1\neq 0$ and when either f or A is equal to zero. Cases in which $f=0$ or $A=0$ are trivial because the particle ceases to have real physical significance. Consequently, no significant loss of generality is incurred by the exclusion of the schlieren case.

Since Eq. (13) must hold for the family of optical direction cosines of the rays which are incident upon the object plane and since the integral of Eq. (13) is a constant for a given choice of pupil function $P(p,q)$, it follows that $P((p_0/M),(q_0/M))$ must be constant. Now the optical direction cosines p_0/M, q_0/M belong to the rays which pass through the conjugate area. A necessary physical condition for the realization of zero energy density at the diffraction head is therefore that the pupil function shall be constant for points which belong to the conjugate area. Correspondingly, if the objective is of the Airy type in accordance with Eq. (16), the diffraction plate must be coated uniformly over its conjugate area. It will be supposed for purposes of simplicity and definiteness that also the complementary area is either uncoated or coated uniformly in the case of diffraction plates which are used with Airy type objectives. In polanret microscopy an actual coating is not present but the phase and amplitude transmission produced over the plane conjugate to the condenser diaphragm is equivalent to that produced by the coating on the corresponding diffraction plate.

Since opaque surrounds are not of general interest, the following equations will be specialized to the case

$$f_1\neq 0. \quad (17)$$

Since $f=f_0-f_1$, Eq. (13) may be rewritten after division by f_1 in the form

$$P_0+M^2A[g\exp(-i\Delta)-1]\int\int P(p,q)dpdq=0, \quad (18)$$

in which

$$P_0\equiv P((p_0/M),(q_0/M)) \quad (19)$$

and in which

$$g\exp(-i\Delta)\equiv f_0/f_1. \quad (20)$$

g is physically the ratio of the amplitude transmission of the particle to the amplitude transmission of the surround and Δ is the optical path difference between the particle and surround considered positive when the optical path of the particle exceeds that of the surround. P_0 is a complex number which specifies the value of the pupil function over the conjugate area of the diffraction plate.

Let

$$T_c\equiv\int\int dpdq \quad (21)$$

in which the integral is taken over the axial bundle of rays which pass through the conjugate zone of the diffraction plate. Then

$$\int\int P(p,q)dpdq=P_0T_c+P_1\int\int(P(p,q)/P_1)dpdq$$

$$=P_0T_c+P_1Q \quad (22)$$

in which

$$Q \equiv \int\int [P(p,q)/P_1]\,dp\,dq, \tag{23}$$

where the integral is taken over the axial bundle of rays which pass through the complementary zone of the diffraction plate. The constant complex number P_1 is preferably chosen as the value of the pupil function at some point in the complementary zone. With an Airy type objective $P(p,q)/P_1$ is equal to unity provided that the complementary area has been coated uniformly.

When Eq. (22) is combined with Eq. (18) the condition for zero energy at the diffraction head becomes

$$P_0+P_0M^2AT_c[g\exp(-i\Delta)-1] +P_1QM^2A[g\exp(-i\Delta)-1]=0. \tag{24}$$

This result applies to all objectives. If the objective has spherical aberration, the conjugate area of the diffraction plate can be chosen as a small zone about the optical axis. The permissible area of the zone is limited by the requirement that the phase variation produced over the zone by spherical aberration shall be negligible in order that P_0 shall be substantially constant.

It will be supposed henceforth that the complementary area of the diffraction plate is never opaque so that

$$P_1 \neq 0. \tag{25}$$

Division of Eq. (24) by P_1 is then permissible. Let

$$h\exp(-i\delta) \equiv P_0/P_1. \tag{26}$$

By definition P_1 is the value of the pupil function over a selected portion of the complementary zone. h is physically the ratio of the amplitude transmission of the conjugate zone to the amplitude transmission of the selected portion of the complementary zone and δ is the optical path difference between the conjugate zone and the selected portion of the complementary zone. δ is considered as positive when the optical path of the conjugate zone exceeds that of the selected portion of the complementary zone. If the objective is of the Airy type whose conjugate and complementary zones are coated uniformly, h is simply the ratio of the amplitude transmission of the conjugate area of the diffraction plate to the amplitude transmission of the complementary area and δ is the optical path difference between these two areas of the diffraction plate. From Eqs. (24) and (26) the zero condition may be stated in the more useful form

$$h\exp(-i\delta)+M^2AT_ch\exp(-i\delta)[g\exp(-i\Delta)-1] +M^2AQ[g\exp(-i\Delta)-1]=0. \tag{27}$$

The following pair of simultaneous conditions for zero energy density at the diffraction head is obtained by equating the real and imaginary parts of the left hand member of Eq. (27) to zero.

$$\begin{aligned} \alpha h\cos\delta-\gamma h\sin\delta-M^2AQ(1-g\cos\Delta)&=0;\\ \alpha h\sin\delta+\gamma h\cos\delta+M^2AQg\sin\Delta&=0; \end{aligned} \tag{28}$$

in which

$$\begin{aligned} \alpha &\equiv 1-M^2AT_c(1-g\cos\Delta);\\ \gamma &\equiv M^2AT_cg\sin\Delta. \end{aligned} \tag{29}$$

Equations (28) may be solved for the polanret setting h, δ at which the diffraction head is darkest. The result is

$$\begin{aligned} h &= M^2AQ(g^2-2g\cos\Delta+1)^{\frac{1}{2}}/(\alpha^2+\gamma^2)^{\frac{1}{2}};\\ \sin\delta &= -g\sin\Delta/(g^2-2g\cos\Delta+1)^{\frac{1}{2}}(\alpha^2+\gamma^2)^{\frac{1}{2}};\\ \cos\delta &= [1-g\cos\Delta-M^2AT_c(g^2-2g\cos\Delta+1)]/\\ &\qquad [(g^2-2g\cos\Delta+1)(\alpha^2+\gamma^2)]^{\frac{1}{2}}; \end{aligned} \tag{30}$$

with

$$\alpha^2+\gamma^2=1-2M^2AT_c(1-g\cos\Delta) +M^4A^2T_c^2(g^2-2g\cos\Delta+1). \tag{31}$$

V. THE ZERO CONDITIONS WITH AIRY TYPE OBJECTIVES

The conditions for obtaining zero energy density at the diffraction head will henceforth be called the zero conditions. The chief advantage gained by the use of an Airy type objective for measuring unresolved particles is due to the property that Airy type objectives are free of spherical aberration. When the objective is substantially free of spherical aberration, it is a relatively simple matter to adjust the microscope for sharpest focus of the diffraction image of the unresolved particle from a knowledge of how the diffraction image behaves about the state of sharpest focus. For example, the diffraction image of an opaque particle varies symmetrically about the state of sharpest focus. It is essential to make the polanret dark settings at or near the state of sharpest focus because the zero conditions have been derived under the supposition that the object plane X_0,Y_0 and the image plane X,Y are conjugate.

Since $P(p,q)/P_1=1$ with Airy type objectives, it follows from Eq. (32) that Q reduces to

$$Q = \int\int dp\,dq, \tag{32}$$

in which the integration extends over the bundle of axial rays which are intercepted by the complementary area. Let

$$T \equiv \int\int dp\,dq, \tag{33}$$

in which the integration extends over the entire bundle of axial rays intercepted by the aperture of the objective. Then

$$Q = T - T_c, \tag{34}$$

with T_c defined as in Eq. (21). The most general zero conditions for Airy type objectives are now obtained by replacing Q by $(T-T_c)$ in Eqs. (30). The zero con-

ditions so obtained depend only upon the numerical values of the parameters T and T_c. Two different methods of illuminating the object plane are therefore equivalent provided only that T and T_c are alike in both methods. In particular, no advantage is gained by the use of an annular opening in the diaphragm of the substage condenser. For purposes of mechanical and optical simplicity it is preferable to choose the opening in the condenser diaphragm as a circle centered on the optical axis. The conjugate and complementary areas are then related as in Fig. 2. T_c and T are accordingly given by

$$T_c=\int_0^{\rho_1}\int_0^{2\pi}\rho d\phi d\rho=\pi\rho_1^2; \tag{35}$$

$$T=\int_0^{\rho_m}\int_0^{2\pi}\rho d\phi d\rho=\pi\rho_m^2; \tag{36}$$

in which ρ_1 and ρ_m are respectively the numerical apertures of the conjugate area and of the objective with respect to the image space of the objective. Thus

$$N.A.=|M|\rho_m, \tag{37}$$

where $N.A.$ denotes the usual numerical aperture of the objective and M is the magnification ratio.

VI. THE ZERO CONDITIONS FOR AIRY TYPE OBJECTIVES WHOSE CONJUGATE AREAS ARE MODERATELY OR NEGLIGIBLY SMALL

The difficulties of determining the properties of the unresolved particle from the polanret dark settings h, δ can be reduced greatly by the choice of small conjugate areas. The main disadvantage accompanying the use of small conjugate areas is a reduction of the level of illumination in the diffraction image of the particle.

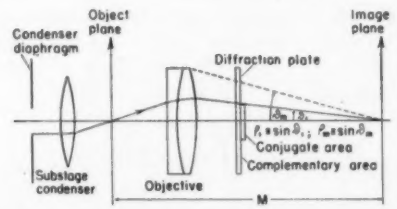

FIG. 2. The preferred system. The opening in the condenser diaphragm and the conjugate area are circular and are centered upon the optical axis. For greatest ease in interpreting the polanret dark settings, the opening in the condenser diaphragm will be made so small that $\rho_1 \ll \rho_m$.

The maximum value $(M^2AT_c)_m$ of M^2AT_c can be estimated in the following manner. The radius R of the Airy limit in the image space is given by $R=3.8317/2\pi\rho_m$. Since the greatest effective radius $(R_0)_m$ of the unresolved particle shall be one-half Airy unit as measured in the object space, $(R_0)_m=3.8317/4\pi|M|\rho_m$. Correspondingly, the greatest area A_m of the particle is

$$A_m=\pi 3.8317^2/16\pi^2M^2\rho_m^2. \tag{38}$$

From Eqs. (35) and (38), $(M^2AT_c)_m=3.8317^2\rho_1^2/16\rho_m^2$ or approximately,

$$(M^2AT_c)_m=\rho_1^2/\rho_m^2. \tag{39}$$

If, therefore, the conjugate area is chosen so small that $\rho_1 \leqq 0.3\rho_m$, the term containing the factor $M^4A^2T_c^2$ in Eq. (31) is negligible except for unusual values of g and Δ. Hence

$$(\alpha^2+\gamma^2)^{\frac{1}{2}}=[1-2M^2AT_c(1-g\cos\Delta)]^{\frac{1}{2}}\rightarrow 1-M^2AT_c(1-g\cos\Delta) \tag{40}$$

when the conjugate areas are moderately small. The polanret dark settings are then computed from Eqs. (30) and (40).

A marked simplification is obtained when the conjugate area is made so small that

$$T_c \ll T \quad \text{or} \quad \rho_1^2 \ll \rho_m^2. \tag{41}$$

It follows from Eqs. (39) and (41) that all terms containing the factor M^2AT_c in Eqs. (30) and (40) may be dropped. Then from Eqs. (30), (40), (36) and (37) the zero conditions are readily shown to assume the form

$$h=\pi A(N.A.)^2(g^2-2g\cos\Delta+1)^{\frac{1}{2}}; \tag{42.1}$$

$$\sin\delta=-g\sin\Delta/(g^2-2g\cos\Delta+1)^{\frac{1}{2}}; \tag{42.2}$$

$$\cos\delta=(1-g\cos\Delta)/(g^2-2g\cos\Delta+1)^{\frac{1}{2}}. \tag{42.3}$$

In summary, the polanret setting h, δ for zero energy density at the diffraction head is related to the properties A, g and Δ of the unresolved particle and to $N.A.$, the numerical aperture of the objective, in accordance with Eqs. (42) when the conjugate area of the diffraction plate is so small that Eq. (41) is satisfied.

VII. SOME GENERAL THEOREMS

Since $P(p_0/M,q_0/M)$ is constant, it follows from Eq. (11) that with Airy type objectives

$$G(0,0):|h\exp(-i\delta)+M^2AT_ch\exp(-i\delta)[g\exp(-i\Delta)-1]+M^2A(T-T_c)[g\exp(-i\Delta)-1]|^2. \tag{43}$$

If h_1, δ_1 is the polanret setting for which $G(0,0)=0$, it can be shown from Eq. (43) that h_1, $(\delta_1+\pi)$ is the polanret setting for which $G(0,0)$, the energy density at the diffraction head, is a maximum.

If h is set at any value and if δ is varied, then $G(0,0)$ is a minimum when $\delta=\delta_1$.

If δ is set at any value near $\delta=\delta_1$ and if h is varied, then $G(0,0)$ is a minimum when $h=h_1$.

These theorems are in agreement with experiment. On the validity of these theorems hinges the experimental possibility of finding h_1, δ_1 with rapidity and certainty from successive variations in h and δ.

VIII. SPECIALIZATION OF THE ZERO CONDITION TO DEFINITE CLASSES OF PARTICLES

The following specializations apply to systems whose conjugate areas are so small that Eqs. (42) are valid or approximate.

Class A: Opaque Particles

For opaque particles the amplitude transmission ratio g between the particle and surround vanishes. When $g=0$, Eqs. (42) reduce to the simple result

$$h=\pi A(N.A.)^2; \tag{44.1}$$

$$\delta=0. \tag{44.2}$$

The diffraction head in the image of an opaque particle is therefore darkest for the polanret setting $h=\pi A(N.A.)^2$, $\delta=0$. As determined by Eq. (44.1), the area, A, of the particle is given in number of squared wave-lengths.

Let the effective radius R_0 of the particle be written in the form

$$R_0=Kr_a^0=0.6098K/N.A. \tag{45}$$

in which $r_a^0=0.6098/N.A.$ is the Airy limit of resolution in number of wave-lengths with reference to the object space. K is then physically the effective radius of the particle expressed in Airy units r_a^0. From Eqs. (44) and (45)

$$h=3.670K^2.$$

It will be noted that h is nearly equal to unity when the effective radius of the particle is one-half Airy unit. Since polanret h-settings can be made with precision in the neighborhood of $h=1$, this method of measuring the area of a small opaque particle is effective when the particle has become too small to be measured in other microscopes. With the use of light sources of high intensity in conjunction with optical systems whose scattering power has been minimized, it may become possible to make polanret settings on particles whose effective radius is only 0.05 of the Airy limit of the microscope objective.

Class B: Particles for which $g=1$

Particles belong to the class for which $g=1$ when their light transmission is equal to that of their surround. Eqs. (42) now reduce to the form

$$h=2\pi A(N.A.)^2|\sin\Delta/2|; \tag{47}$$

$$\sin\delta=-sgn(\sin\Delta/2)\cos\Delta/2; \tag{48.1}$$

$$\cos\delta=|\sin\Delta/2|; \tag{48.2}$$

in which $sgn x\equiv x/|x|$. From Eqs. (48)

$$\delta=\Delta/2-\pi/2, \quad 0<\Delta<2\pi; \tag{49.1}$$

$$\delta=\Delta/2+\pi/2, \quad -2\pi<\Delta<0. \tag{49.2}$$

The well-known discontinuity of π-radians in δ at $\Delta=0$ appears also in the polanret dark or bright setting for the diffraction head with particles of the class $g=1$.

Δ expressed in radians or degrees and the area A expressed in numbers of squared wave-lengths may be computed consecutively from Eqs. (49) and (47). Alternately, the effective radius K of the particle may be computed in Airy units from the relation

$$h=7.34K^2|\sin\Delta/2|. \tag{50}$$

As an example of the sensitivity of the method, when $\Delta=30°$ and $K=\frac{1}{2}$, $h=0.476$ and $\delta=-75°$. Since h-settings of 0.5 can be made with considerable certainty and since the polanret error in the δ-setting falls in the neighborhood of $\leqq 5°$, both K and Δ can be measured reliably for particles whose Δ-value is so small that the image of the particle exhibits poor contrast in the biological microscope.

Case C: Particles of Low Amplitude Transmission Ratio g

When g is so small that all terms containing g^2 may be neglected in the binomial expansion of $(g^2-2g\cos\Delta+1)^{\frac{1}{2}}$, Eqs. (42) are closely approximated by the result

$$h=\pi A(N.A.)^2(1-g\cos\Delta); \tag{51.1}$$

$$\delta=-g\sin\Delta. \tag{51.2}$$

If the polanret dark setting δ is zero for a given particle no matter in which fluid the particle is immersed, the particle is opaque for purposes of microscopy. The method is therefore capable of ascertaining whether or not an unresolved particle is opaque. Since the relative energy transmission of the particle is g^2, the amplitude transmission ratio g is much greater than the corresponding energy transmission ratio when g is small.

Equations (51) do not permit the determination of the three unknowns A, g and Δ from a single dark polanret setting. Several methods of attack are possible, however, for obtaining the necessary second polanret setting when the observer is at liberty to alter either the refractive index or the amplitude transmission of the surround. As an example, suppose that the refractive index of the surround is held constant while its amplitude transmission is varied by the admixture of an absorbing material whose particles are much too small to be detected microscopically. It follows from Eq. (42.1) that $dh/dg=0$ when $g=\cos\Delta$ and that, correspondingly, h is a minimum when Δ lies in the interval $-\pi/2<\Delta<\pi/2$. Provided that Δ falls well within this interval, it will be possible to vary the absorption of the surround until the observed h-value reaches a minimum at the polanret setting for zero energy density at the diffraction head. Let this polanret setting be recorded as h_2, δ_2 and let the corresponding unknown value of g

be denoted by g_2. Then from Eqs. (42)

$$h_2=\pi A(N.A.)^2|\sin\Delta|;$$
$$\sin\delta_2=-sgn(\sin\Delta)\cos\Delta; \tag{52.1}$$

$\cos\delta_2=|\sin\Delta|$. Whence

$$\delta_2=\Delta-\pi/2, \quad 0<\Delta<\pi/2; \tag{52.2}$$

$$\delta_2=\pi/2-\Delta, \quad \pi/2<\Delta<0. \tag{52.3}$$

Let the polanret dark setting with the particle in its original surround be recorded as h_1, δ_1 and let the corresponding unknown value of g be denoted by g_1. From Eqs. (51)

$$h_1=\pi A(N.A.)^2(1-g_1\cos\Delta); \tag{53.1}$$

$$\delta_1=-g_1\sin\Delta. \tag{53.2}$$

An examination of Eqs. (52) and (53) shows that Δ is determined from Eqs. (52.2) and (52.3), that g_1 is determined by Eq. (53.2) and that the area A of the particle can be determined from either Eq. (52.1) or (53.1). Furthermore, $g_2=\cos\Delta$. In principle, therefore, the unknowns A, g and Δ can be determined from two properly chosen polanret dark settings.

On the other hand, the above example can be varied by keeping g constant and altering the refractive index of the surround until the dark polanret setting h is a minimum. The condition for the minimum is then derived from the statement $dh/d\Delta=0$. Instead of Eqs. (52), another pair of equations will be obtained from Eqs. (42). Again, one is not restricted to basing the measurements of A, g and Δ on a search for maxima or minima of the polanret dark setting h. A search for maxima or minima of the polanret dark setting δ can lead to increased convenience or precision in measuring A, g and Δ for some particles. The technique of searching for maxima or minima in either h or δ at the polanret dark settings has the important advantage that it does not require a knowledge of the refractive index or of the transmission per unit thickness of either the particle or surround in order to determine A, g and Δ.

Case D: Particles and Surrounds Whose Refractive Indices Are Known

Frequently the refractive indices of the particles and surround are known from the bulk values. Suppose that the thickness and the amplitude transmission of the particle are unknown, that the amplitude transmissions of the immersion fluids are practically unity and that the refractive indices of the set of fluids are known together with that of the particle. Let n, n_1 and n_2 denote the refractive indices of the particle, the first immersion fluid and of the second immersion fluid, respectively. The amplitude transmission ratio g will be practically the same with both immersion fluids but Δ_2 will differ from Δ_1 in accordance with the relation

$$\Delta_2=\Delta_1(n_1-n_2)/(n-n_1). \tag{54}$$

Let the polanret dark setting with the first and second fluids be recorded as h_1, δ_1 and h_2, δ_2, respectively. From Eqs. (42) the governing relations are

$$h_j=\pi A(N.A.)^2(g^2-2g\cos\Delta_j+1)^{\frac{1}{2}}; \tag{55.1}$$

$$\sin\delta_j=-g\sin\Delta_j/(g^2-2g\cos\Delta_j+1)^{\frac{1}{2}}; \tag{55.2}$$

$$\cos\delta_j=(1-g\cos\Delta_j)/(g^2-2g\cos\Delta_j+1)^{\frac{1}{2}}; \tag{55.3}$$

$j=1$ or 2.

Since Eqs. (55.2) and (55.3) are not independent, Eqs. (55) constitute four simultaneous equations for the four unknowns A, g, Δ_1 and Δ_2. If the physical measurements of h_1, h_2, δ_1 and δ_2 are self-consistent, Δ_1 and Δ_2 will be in close agreement with Eq. (54).

The following variation of the above procedure involves simpler calculations. Let n_1 be chosen sufficiently different from n so that δ_1 differs from 0 or π by about 5 times the polanret error in the δ_1-setting. The product $t(n-n_1)/2\pi=\Delta_1$, with the thickness t of the particle expressed in wave-lengths,is then large enough so that the optical path difference Δ_1 is appreciably different from zero. Let the second immersion fluid be selected such that $n_2=n$. Consequently, $\Delta_2=0$ and

$$h_2=\pi A(N.A.)^2|g-1|; \tag{56.1}$$

$$\delta_2=0 \text{ or } \pi. \tag{56.2}$$

It can be seen from Eqs. (55.2) and (55.3) that for $\Delta_2=0$, $\delta_2=0$ or π according as $g<1$ or as $g>1$. In other words, the polanret dark setting δ_2 determines whether $g<1$ or >1. Hence

$$h_2=\pi A(N.A.)^2\begin{cases}(1-g), & \delta_2=0;\\ (g-1), & \delta_2=\pi.\end{cases} \tag{57}$$

Equations (55) with $j=1$ and Eq. (57) form three independent simultaneous equations for determining the three unknowns A, g and Δ_1. Let

$$a=h_2/h_1-\cos\delta_1\cos\delta_2;$$
$$b=(h_2/h_1)^2-2(h_2/h_1)\cos\delta_1\cos\delta_2+1. \tag{58}$$

It can be shown† that

$$\sin\Delta_1=2a\sin\delta_1\cos\delta_2/b; \tag{59.1}$$

$$1/g=1-2ah_2/h_1b. \tag{59.2}$$

Equation (59.1) has the two solutions Δ_1 and $(\pi-\Delta_1)$ in the interval $0<\Delta_1<2\pi$ or $-2\pi<\Delta_1<0$. The correct solution satisfies the relation

$$a\cos\delta_2\sin\Delta/\sin\delta_1+\cos\Delta=1. \tag{60}$$

When Δ_1 and g have been determined from Eqs. (58), (59) and (60) the area A of the particle in number of squared wave-lengths can be computed from Eq. (57).

† The authors are indebted to J. E. Wilkins, Jr. for this statement of the solution.

The thickness t of the particle in number of wave-lengths is given by the relation

$$t=2\pi\Delta_1/(n-n_1), \qquad (61)$$

where Δ_1 is expressed in radians. Since t and A are thus determined, the volume of the particle becomes known.

As a numerical example, given the polanret dark settings $h_1=0.5$, $h_2=0.2$, $\delta_1=+45°$ and $\delta_2=0$, it follows that $g=0.7075$, $\Delta_1=46°57'$ and $\pi A(N.A.)^2=0.6838$. If the numerical aperture of the objective is equal to unity, the area of the particle is 0.218 squared wave-lengths and the effective radius of the particle is 0.263 wave-lengths.

IX. EXPERIMENTS WITH OPAQUE PARTICLES

Opaque particles are ideal test particles for checking the validity of the method. The test particles were formed by placing a small glubule of mercury in a drop of clarite on a microscope slide and by pressing or tamping upon the cover slip until the globule disintegrated into a large set of microscopic globules.

The experimental arrangement for measuring unresolved particles is illustrated in Fig. 3. The system is an adaptation of the polanret microscope. A mercury arc was filtered for 5461A and was focused upon a small circular aperture centered on the optical axis and located at the first focal plane of a doublet which served as substage condenser. This circular aperture was imaged upon the central, circular zone of the micoid disk assembly which consisted of a quarter-wave plate, two orthogonal zonal polarizers and cemented cover plates. The projected image of the circular aperture in the condenser diaphragm was slightly smaller than the central zone of the micoid disk. The ratio of the radius of the central zone to the radius of the clear aperture of the objective in the plane of the micoid disk was chosen as approximately 0.1. Correspondingly, $(\rho_1/\rho_m)^2=0.01$ or $(\rho_1/\rho_m)^2\ll 1$ as in Eq. (41). Consequently, Eqs. (44) and (45) could be used with negligible error for interpreting the experimental data.

A 25 mm focus objective having a measured numerical aperture of 0.146 and negligible spherical aberration was selected for observations in the polanret microscope. The diameters of the mercury particles were measured directly in a separate, standard microscope

TABLE I. Measurements of the radii R in wave-lengths for several mercury particles.

Particle	R (direct)	R (polanret)	R/Airy limit
1	2.36	2.34	0.56
2	1.97	2.18	0.47
3	1.77	1.67	0.42
4	1.46	1.27	0.35
5	1.18	1.18	0.28
6	1.01	1.08	0.24
7	0.985	1.02	0.235
8	0.83	0.99	0.20
9	0.76	0.85	0.18

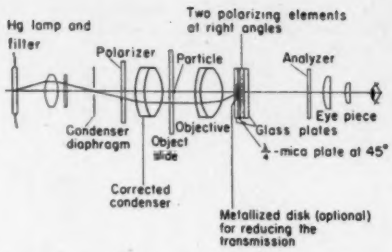

FIG. 3. The modified polanret system for measuring unresolved particles.

equipped with objectives having numerical apertures from 0.95 to 1.30. The selected mercury test particles were small enough that their images appeared as diffraction patterns in the polanret microscope but were large enough that their images were well resolved by the auxiliary objectives of high numerical aperture. In this way the radii R of the particles were measured from the properties of the diffraction image in the polanret microscope and were compared with the corresponding radii measured by the conventional method employing objectives of high numerical aperture.

Diffraction images which are formed by objectives whose spherical aberration is negligible vary symmetrically above and below the plane of sharpest focus. Hence no difficulty was encountered in setting the polanret microscope for the state of sharpest focus. In the plane of sharpest focus the energy density at the diffraction head was a minimum with opaque particles at the polanret phase setting $\delta=0$ as required by Eq. (44.2). When the polanret setting h,δ for darkest diffraction head had been determined for a given opaque particle, the diffraction head became brightest by altering δ alone to the polanret setting h, $(\delta+\pi)$. This behavior is in agreement with the theorems of Section VII. The experimental error in setting the polarizer for darkest diffraction heads fell within the range $\pm 2.5°$ from the zero position. The corresponding uncertainty in δ is $\pm 5°$. With the smaller mercury particles the h-settings became increasingly difficult to make because the diffraction images show poorer contrast with decreasing area of the particles. These preliminary observations are in qualitative agreement with the theory.

Some typical results of the measurements with spherical particles of mercury are listed in Table I. The radii R of the particles in wave-lengths are given in the second and third columns from the direct and the polanret measurements, respectively. The direct measurements were made with the auxiliary objectives of high numerical aperture. These directly measured radii are regarded as the known values. They have been divided to obtain the last column by the Airy limit, $0.6098/N.A.$, expressed in wave-length where $N.A.$ is the numerical aperture of the objective in the polanret system. The smallest measured radius in Table I is equal to 0.18 of the Airy limit of the polanret

TABLE II. Measurement of a selected particle by six observers. The direct measurement of the radius of this particle is 1.57 wave-lengths.

Observer	R in λ (polanret)
1	1.69
2	1.57
3	1.69
4	1.60
5	1.58
6	1.52

TABLE III. Precision measurements of a selected particle.

Method of measurement	Average R	Probable error of the mean
Direct	1.66λ	0.01λ
Polanret	1.63λ	0.01λ

objective. Still smaller radii could have been measured by means of the polanret system whose objective had the numerical aperture 0.146. For these smaller radii an electron microscope is required in order to obtain sufficiently reliable direct readings for the purpose of comparison with the polanret measurements. Indeed, it would be desirable to check the entire range of polanret measurements of Table I with a well-calibrated electron microscope. Assuming that the polanret system can be adapted successfully to objectives having the numerical aperture 1.40, it will be possible to measure opaque particles whose radii are nearly one-tenth of those listed in Table I. In adapting this method of variable phase microscopy to objectives of high numerical aperture, one has the choice either of modifying the objective so as to reduce it to the Airy type objective or of taking into account the known departure of the objective from the Airy type upon the interpretation of the polanret settings.

In order to determine a practical limit of the smallest measurable radius R by means of this polanret method, the following experiments were performed. An aluminum film having the light transmission of 0.005 was added to the conjugate area of the micoid disk assembly of Fig. 3 for the purpose of obtaining a smaller h-value at a given setting of the amplitude controlling knob of the polanret microscope. After some practice, repeatable settings were made upon particles whose computed radii fell in the neighborhood of 0.07 of the Airy limit of the polanret objective of $N.A.$ 0.146. The practical limit may prove to be below 0.07 of the Airy limit with objectives of higher numerical aperture employed in conjunction with monochromatic light sources of high intensity.

The polanret determinations of Table II indicate the spread in the measurement of the radius of the same particle by six different observers. The greatest deviation from the mean is only 5.6 percent of the mean although four of the observers were new.

As an additional experiment, a particle of favorable radius was measured by the authors with the greatest possible care. A study of several auxiliary objectives showed that a 2 mm focus, $N.A.$ 1.30 apochromat enabled the best direct measurement of the radius of the particle. The results of Table III are based in each case upon twenty readings. The direct measurement of the radius of the particle is subject to the systematic error involved in choosing the edge of the geometrical image of the particle. Observations upon the diffraction image showed that the directly measured value of the radius cannot exceed 1.80λ and that the true radius must be near 1.66λ. The criterion finally used for determining the location of the edge was to set the micrometer indicator near the region of apparent discontinuity or most rapid change in the energy density with monochromatic illumination.

The correction factor by which the polanret R-value must be multiplied in order to account for the neglected terms in $(\rho_1/\rho_m)^2$ is 1.002. This correction factor is not large enough to alter the rounding off of the value $R=1.63\lambda$. The use of the simplified Eq. (44.1) is therefore justified.

X. CONCLUSIONS

(1) It is possible to measure the area and the optical properties of single, unresolved particles of uniform thickness with the aid of a suitably modified variable phase microscope. The optical properties include the optical path difference between and the light transmission ratio of the particle and its surround.

(2) The modified phase microscope is preferably of the continuously variable type such as the polanret microscope whose objective is of the Airy type. When ease of interpretation is desirable, the conjugate area of the diffraction plate or its polanret equivalent must be small as compared with the complementary area. Means should be provided for indicating the phase difference δ between and the amplitude transmission ratio h of the conjugate and complementary areas.

(3) For measuring unresolved particles, it suffices to determine experimentally the polanret setting h, δ at which the central portion of the sharply focused diffraction image of the particle appears darkest as judged visually or photometrically. The properties of the particle may then be computed from the experimental parameters h and δ provided that the number of unknown properties does not exceed two.

(4) When the number of unknown properties of the particle is greater than two, as may be the case with transmitting particles, it is possible in principle to obtain the required number of experimental parameters by making a second polanret dark setting after having altered the light transmission or the refractive index of the medium surrounding the particle.

(5) The method is particularly simple and effective as applied to the measurement of the area of opaque particles. The particle is opaque when the polanret

dark setting of the phase parameter δ is zero no matter in which fluid the particle is immersed. The area of the particle is proportional to the polanret dark setting of the amplitude ratio, h. The restriction of uniform thickness does not apply to opaque particles. Such particles can have any shape provided that they are not unduly oblong.

(6) Observations upon opaque particles are in close accord with theory.

(7) It was found experimentally that the method as applied to an objective of $N.A.=0.146$ is capable of measuring the area of opaque particles which are too small to be measured in the bright field microscope with an objective whose $N.A.=1.30$. With the use of light sources of high intensity in conjunction with optical systems of low scattering power, it is expected that the method will be capable of measuring opaque particles whose effective radii approach 0.05 of the Airy limit of the microscope objective. The modified polanret microscope used in these experiments was constructed for the purpose of testing the principles of the method. It is not yet available commercially.

Society for Applied Spectroscopy

THE Society for Applied Spectroscopy of the Metropolitan New York area has scheduled monthly meetings at the Socony-Vacuum Training Center, 63 Park Row, New York City. Meetings are held on the first Tuesday evening of each month. The schedule for the remainder of the first half of this year includes: March 7—"Vacuum Ultraviolet Spectroscopy," Dr. Janice A. Cutler, Markite Company. April 4—"Geometrical Optics of Spectrograph Slit Irradiation," Dr. Robert Bell, Lucius Pitkin, Inc., May 2—"Theory and Demonstrations of Emission Spectrograph Optics and the New Read Stigmatic Mounting," Dr. Harry S. Read, Harry S. Read Company.

A special two-day session including a Symposium on Spectroscopic Sources is scheduled for May 26 and 27. Information on regular meetings and the special session can be obtained from the program chairman, Dr. Harold K. Hughes, Socony-Vacuum Laboratories, 412 Greenpoint Avenue, Brooklyn 22, New York.

A Simple Method for Evaluation of Atomic and Ionic Ground States

MAYER B. GOREN
Department of Chemistry, Northeastern University, Boston, Massachusetts
(Received November 2, 1949)

A simple, direct method is detailed for evaluating the lowest energy term arising from any electronic configuration. Only a single solution is obtained and no other allowed terms can be derived. The method entails assignment of magnetic quantum numbers to electrons in uncompleted shells, according to a uniform scheme and summation of these quantum numbers algebraically to afford a number, the absolute value of which is definitive for L. With the aid of a simple diagrammatic scheme both the resultant L and S vectors defining the ground state can be seen at a glance. The method is valid for ionic ground states and is illustrated with a number of examples for atomic and ionic configurations. All terms calculated are in agreement with the established values, and the conclusion seems permissible that the method can be applied with confidence toward prediction of ionic ground states as yet undetermined experimentally.

THE evaluation of atomic ground states by classical methods can at times become a tedious procedure, for even simple atomic configurations can lead to lengthy vector summations in the effort to evaluate all of the allowed terms on the basis of resultant angular momentum, L. When all of the allowed terms are determined, one can, on the basis of Hund's rule, select the ground state by choosing the level of maximum multiplicity, and of configurations having the same multiplicity, selecting the one of largest L-value.

The following, however, contains a detailed description of a very simple method for the evaluation of atomic ground states, and also for the determination of the ground term for ionized atoms. In each instance, only a single solution is obtained, and no other allowed terms can be determined.

In brief, instead of compounding the angular momentum vectors l, to determine the resultant angular momentum L, the magnetic quantum numbers m are added algebraically to define L, according to the following scheme, which is based on the well-known conditions that

(1) An s-electron has allowable m-values of zero only, and therefore makes no contribution to L.
(2) A p-electron ($l=1$) has m-values $-1, 0, 1$.
(3) A d-electron ($l=2$) has m-values $-2, -1, 0, 1, 2$; etc.

The first electron in a p sub-shell is arbitrarily assigned an m-value of -1; the second, 0; and the third, 1. A fourth p-electron is paired with the first, canceling contributions to L; a fifth p-electron is paired with the second. In a similar fashion, the first electron in a d-shell is assigned an m-value of -2; the second, -1; 0, 1, and 2 to the third, fourth, and fifth electrons respectively. The sixth electron is paired with the first; the seventh, with the second, etc. A simple check notation is employed to indicate the configuration.

Nitrogen has the electronic configuration $1s^2 2s^2 2p 2p 2p$. Considering only the incomplete sub-shells, we write for the three p electrons

p: −1 0 1
* * *

TABLE I. Fourth period.

Element	Configuration	Notation	$\|\Sigma m\|$	S	Ground term
V	$(A)3d^3 4s^2$	d: −2 −1 0 1 2 * * *	3	3/2	^4F
Cr	$(A)3d^5 4s^1$	s: 0; d: −2 −1 0 1 2 * * * * *	0	6/2	^7S
Mn	$(A)3d^5 4s^2$	d: −2 −1 0 1 2 * * * * *	0	5/2	^6S
Fe	$(A)3d^6 4s^2$	d: −2 −1 0 1 2 * * * * * *	2	4/2	^5D
Co	$(A)3d^7 4s^2$	d: −2 −1 0 1 2 * * * * * * *	3	3/2	^4F

TABLE II. Sixth period.[a]

Element and configuration	Notation	$\|\Sigma m\|$	S	Ground term[a]
Sm: (Pd)$4f^6 5s^2 5p^6 5d^1 6s^2$	f: −3 −2 −1 0 1 2 3 * * * * * * d: −2 −1 0 1 2 *	7	6/2	^7K
Eu: (Pd)$4f^7 5s^2 5p^6 5d^1 6s^2$	f: −3 −2 −1 0 1 2 3 * * * * * * * d: −2 −1 0 1 2 *	5	7/2	^8H
Gd: (Pd)$4f^7 5s^2 5p^6 5d^1 6s^2$	f: −3 −2 −1 0 1 2 3 * * * * * * * * d: −2 −1 0 1 2 *	2	8/2	^9D
Tb: (Pd)$4f^8 5s^2 5p^6 5d^1 6s^2$	f: −3 −2 −1 0 1 2 3 * * * * * * * * d: −2 −1 0 1 2 *	5	7/2	^8H
Yb: (Pd)$4f^{13} 5s^2 5p^6 5d^1 6s^2$	f: −3 −2 −1 0 1 2 3 * * * * * * * * d: −2 −1 0 1 2 *	5	2/2	^2H

[a] Ground terms were computed on the basis of the electronic configurations employed, which involve d-electrons and which were chosen in order to illustrate the compounding of non-equivalent electrons; the term values calculated are therefore in agreement with those of Hund (F. Hund, *Linienspektren und periodisches System der Elemente* (Julius Springer, Berlin, 1927)). Some of these configurations are now known to correspond to metastable states, and not to the ground state; the true or most probable configurations (W. F. Meggers, Science 105, 514 (1947)) for the group chosen are:

Pm: $4f^5 6s^2$: ^6H
Sm: $4f^6 6s^2$: ^7F
Eu: $4f^7 6s^2$: ^8S
Gd: (as given above)
Tb: $4f^8 6s^2$: ^6H
Yb: $4f^{14} 6s^2$: ^1S

The lowest energy terms calculated (by the method under discussion) from these configurations are in agreement with the given values.

TABLE III.

Element and configuration		Notation	$\lvert\Sigma m\rvert$	S	Ground term
C I	$1s^2 2s^2 2p 2p$				
C II	$1s^2 2s^2 2p$	p: −1 0 1 ; *	1	1/2	^2P
C III	$1s^2 2s^2$	0	0	0	^1S
Kr I	(A)$3d^{10} 4s^2 4p^6$				
Kr II	$4s^2 4p^5$	p: −1 0 1 ; * * *	1	1/2	^2P
Kr III	$4s^2 4p^4$	p: −1 0 1 ; * * *	1	2/2	^3P
Rh I	(Kr)$4d^8 5s$				
Rh II	(Kr)$4d^8$	d: −2 −1 0 1 2 ; * * * * *	3	2/2	^3F
Rh III[a]	(Kr)$4d^7$	d: −2 −1 0 1 2 ; * * * * *	3	3/2	^4F
Fe I	(A)$3d^6 4s^2$				
Fe II	(A)$3d^6 4s$	s: 0; d: −2 −1 0 1 2 ; * * * * *	2	5/2	^6D
Fe III[b]	(A)$3d^6$	d: −2 −1 0 1 2 ; * * * * *	2	4/2	^5D
Fe V	(A)$3d^4$	d: −2 −1 0 1 2 ; * * * *	2	4/2	^5D

[a] Predicted state.
[b] Edlen and Swings, Astrophys. J. 95, 532 (1942).

wherein an asterisk indicates that this particular quantum level is occupied.

Again, oxygen has the configuration $1s^2 2s^2 2p^2 2p 2p$, and would be designated

p: −1 0 1
* * *
*

indicating that the fourth p-electron cancels the contribution of the first to L.

When the occupied levels have been assigned according to this notation, the algebraic sum of all terms not occupied by two electrons (asterisks) is taken. The absolute value of this sum is the L-value which defines the ground state.

Thus, summing up the terms in the case of nitrogen: −1, 0, 1 equals zero, equals L. Therefore the ground state is S. Three electrons have uncompensated spin (uncancelled contribution to L), so that the resultant S vector is 3/2, and $2S+1=4$. The ground term of nitrogen is therefore ^4S.

To illustrate with oxygen

$$L=|\Sigma m|=|1,0|=1.$$

Therefore the ground state is P. There are two unpaired electrons, hence a ^3P state.

In instances where there exist two incomplete sub-shells (non-equivalent electrons), as in the rare earths, each incomplete sub-shell is compounded separately, and the absolute values of the algebraic sums are added to define the resultant L. To illustrate:

Promethium:† (Pd core) $4f^4 5s^2 5p^6 5d^1 6s^2$

Only the $4f$ and $5d$ sub-shells are incomplete. For the d-shell we write

d: −2 −1 0 1 2 $\quad |\Sigma m|=|-2|$ or 2
*

For the f-shell we write

f: −3 −2 −1 0 1 2 3 $\quad |\Sigma m|=|-6|$ or 6
* * * *

Σm total $=L=6+2=8$.

The term is therefore L (since J is omitted as a term); there are five unpaired electrons, so the ground state is ^6L (*cf.*, however, footnotes † of text and footnote a of Table II).

To illustrate further, let us select five successive elements in the fourth period and five rare earths as shown in Tables I and II.

The determination of the ground terms for ionized atoms follows the same scheme in general, and can be summed up by the following rules:

1. Write the electronic configuration of the unionized atom.
2. Remove the requisite number of electrons from the level of highest principal quantum number, and in that level, from the sub-shell of highest orbital quantum number, in order to obtain the configuration of the ionized atom.‡
3. Sum up the magnetic quantum numbers as in the previous instances.

The method can be illustrated with several elements picked at random as shown in Table III.

All ground terms computed by this method (other than predicted for unknown ionic states) are in agreement with the accepted ground terms for the elements described. The expectation seems permissible, therefore, that predicted values based on this method may also be proved correct in the future, and that the procedure may be adopted for the computing of ionic ground states as yet undetermined.

ACKNOWLEDGMENT

The author acknowledges with thanks the encouragement and interest offered by Professor Otto Oldenberg of Harvard University, who initially suggested the application of this method for the evaluation of ionic ground states.

† The configuration selected is probably a metastable state; *cf.* footnote a of Table II.

‡ An essentially identical rule has been formulated by Meggers (*op. cit.*), with the comment that the rule is not a universal one, and that certain exceptions are encountered, for instance in the rare earths. Thus Lu I, which has the configuration $4f^{14}5d^1 6s^2$ affords on ionization Lu II: $4f^{14}6s^2$, a ^1S term (Meggers and Scribner, *Bur. Standards J. Research* 5, 73 (1930)). On the basis of rule 2 above, Lu II would be assigned the configuration $4f^{14}5d^1 6s^1$, which would give rise to a ^3D term. This term was established by Meggers and Scribner along with ^1D and ^3F, all of which have been characterized, however, as metastable states.

A D.C. Arc Source and Automatic Controller*

G. H. FETTERLEY AND W. M. HAZEL
Research Laboratory, Norton Company, Niagara Falls, Canada

(Received November 17, 1949)

An effective source of direct current having any desired output up to 45 amperes at 150 volts is described, being characterized by small size, light weight, low cost, and negligible maintenance. While it has superseded all other d.c. sources, regardless of cost, in the Norton Company laboratories, it is particularly recommended where cost is an important consideration. It is also a useful auxiliary unit where highly refractory materials are analyzed regularly, since these materials are sometimes difficult to volatilize completely with the familiar multipurpose type of source. An automatic current controller is also described as a separate unit, and can be used to hold the current within ±0.5 ampere at any selected value between 5 and 15 amperes.

THE RECTIFIER

THE Norton Company manufactures abrasives and refractories, and nearly all the samples analyzed spectrographically are highly resistant to volatilization. As a result, the d.c. arc has proved to be the only practical excitation source for use in this laboratory. After several years of experience with motor-generators, the rectifier described below was assembled, principally as a stand-by unit. It proved to be so satisfactory that the motor-generator has been completely superseded. This equipment cost less than $100, including the labor of assembly, can be carried easily by one man, and has required no maintenance in several years of constant use. Having no moving parts, it is silent in operation, and is small and light enough to be placed in a corner of the laboratory or under a table.

The circuit diagram of the rectifier is shown in Fig. 1 and a photograph in Fig. 2. The components are mounted on a 20-in.×20-in.×3-in. chassis of 10-gauge sheet steel. The wooden base with casters, visible in Fig. 2, is an added refinement, no longer used.

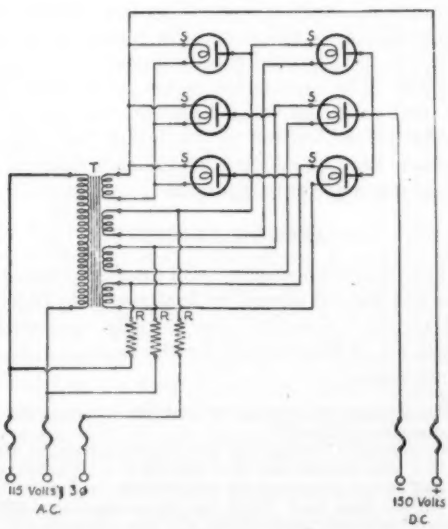

FIG. 1. Rectifier circuit.

The 15-ampere mercury vapor tubes are type CE-203, made by the Continental Electric Company of Geneva, Illinois. They mount in standard Mogul sockets. Note that in every case the d.c. output connection is taken from the shell side of the socket, marked *S* in the diagram. Brass strip was used in the filament circuits to carry the heavy current. The transformer was made to order, with one 2.5-volt, 66-ampere and three 2.5-volt, 22-ampere windings. The total rated output capacity of the six tubes in this connection is 45 amperes d.c. The resistors marked *R* are wound on a 20-in.×12-in.×$\frac{1}{4}$-in. Transite sheet with $\frac{3}{16}$ in.×0.013 in. Chromel A ribbon. They reduce the load on the main control rheostat normally used in the d.c. arc circuit, and positively prevent reverse conduction by the rectifiers and the resulting annoyance of blown fuses. As seen in Fig. 2 they are mounted well out in the open where they can readily dissipate the heat evolved.

The following formulas will be found useful by anyone who wants to assemble a similar unit:

$$\text{R.m.s. a.c. volts per leg in star connection} = 0.428(V+12) \quad (1)$$

$$\text{R.m.s. a.c. volts per phase in delta-connection} = 0.740(V+12) \quad (2)$$

$$\text{Peak inverse voltage on rectifiers} = 1.05(V+12) \quad (3)$$

$$\text{Lowest frequency in output ripple} = 6\times \text{ supply frequency} \quad (4)$$

$$\text{Peak ripple voltage without filter} = +4.7 \text{ percent and } -9.3 \text{ percent} \quad (5)$$

$$\text{Peak plate current per tube} = I \quad (6)$$

$$\text{Average current per tube} = 0.33I \quad (7)$$

$$V = 1.35\times \text{r.m.s. voltage per phase} - 12 \quad (8)$$

$$I = V/(RL+2.2R) \quad (9)$$

* Presented at the Buffalo meeting of the Optical Society of America, October, 1949.

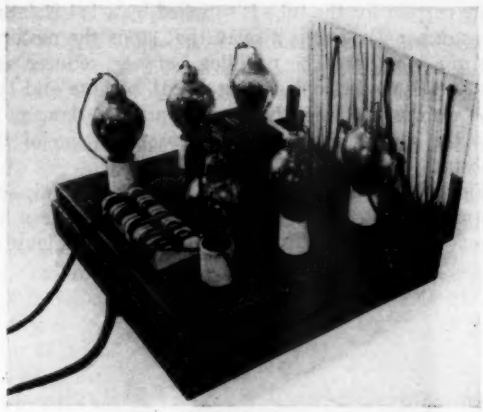

FIG. 2. Photograph of rectifier.

where, $-V$=d.c. output voltage under no-load conditions; I=d.c. output current; RL=load resistance, consisting normally of the arc and a rheostat in series; R=limiting resistors shown in Fig. 1.

An example will illustrate the process of design. Suppose that 115 volt, three phase current is available and that currents from 8 to 15 amperes will be required. The voltage drop across the arc will be about 60 volts, and will not vary much with arc current.

(1) From Eq. (8), $V=1.35\times115-12=143$v.

(2) Assume that the arc control rheostat is near its minimum resistance, say 1 ohm, when the maximum current of 15 amperes is being drawn. Then the arc will have a resistance of $60/15=4$ ohms, and $RL=5$ ohms.

(3) Substitute for I, V, and RL in Eq. (9) and solve for R. Then $R=2.1$ ohms.

(4) Consider the minimum current of 8 amperes. Substitute for I, V, and RL in Eq. (9) and solve for RL. Then $RL=13$ ohms.

(5) Since the arc resistance is now $60/8=7.5$ ohms, the remainder of 5.5 ohms must be made up by the rheostat. Allowing a margin for error, use 7 ohms.

(6) The final design then calls for 2.1 ohms for R, and a control rheostat in the d.c. circuit having a maximum resistance of 7 ohms and a current-carrying capacity of 15 amperes.

THE CONTROLLER

Some time after the rectifier had been installed, the need for an automatic current controller began to be felt. An ingenious and apparently very effective controller had already been described by Green and Kuper.[1] This device, based on the properties of resonant circuits, was out of the question since it required components that were totally unavailable just at the end of the war. It also appeared to be better suited to high voltages and low currents than to the other extreme. Another design has been described recently by Potter and Scott.[2] Using completely electronic control throughout, it offers the ultimate in current regulation, but requires a large array of tubes to pass reasonably high d.c. currents. The device described here is simple, rugged, and can be designed to handle large currents if desired. Being partly mechanical in action, it can not compare in speed of response with the two pieces of equipment noted above. However, when a mechanical hand on the rheostat is sufficient for the purpose, this controller will add considerably to accuracy and convenience in the use of the d.c. arc.

The controller is essentially a motor-driven rheostat in series with the arc. It comprises three functional units as follows:

(1) A zero temperature coefficient fixed resistor in series with the arc to generate a d.c. voltage proportional to the arc current.

(2) A rheostat in series with the arc with the sliding contact driven by a small reversible d.c. motor and speed reducer.

(3) A device to enable the voltage generated in (1) to control the motor in (2). The d.c. voltage is balanced against an adjustable fixed voltage from a battery, and the difference is applied to the grid of a thyratron. The plate current of the latter controls, by means of a DPDT relay, the direction of rotation of the motor.

As a result of the operation of the electromechanical feedback loop described above, the current hunts continuously within a maximum range of about ±0.5 ampere with the selected value at the center of the range. The effective average current, integrated over an exposure, is evidently much closer to the control-center value than 0.5 ampere, though how much closer has not been determined.

Figure 3 shows the controller circuit with some of the details omitted for clarity. Enough is given for an elec-

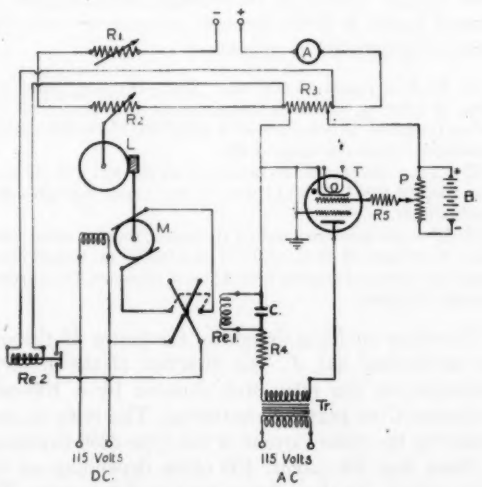

FIG. 3. Controller circuit.

[1] Green and Kuper, Rev. Sci. Inst. 11, 250 (1940).

[2] E. V. Potter and A. Scott, Rev. Sci. Inst. 18, 722 (1947).

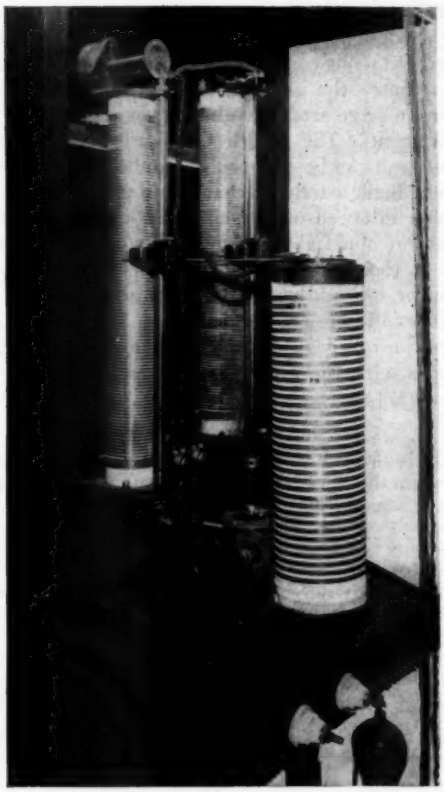

FIG. 4. Back view of motor drive and rheostats.

trical engineer to complete the design, and blueprints and photographs of the actual equipment will be supplied by this laboratory on request. Note that the arc current passes in series through an ammeter and three resistors designated as follows:

(1) *R*1 is a Jagabi "Lubri-tact" 20-in. rheostat, rated at 6 ohms, 14 amperes, with a right-angle screw drive controlled by a dial on the panel. It is set at such a value that the desired control is obtained within the range of *R*2.

(2) *R*2 is a rheostat of the same type as *R*1, but with its screw drive coupled to a 1/20 hp 1750 r.p.m. d.c. motor through a 50:1 speed reducer.

(3) *R*3 is the zero temperature coefficient resistor noted previously. It consists of 44 ft. of 0.375 in.×0.0089 in. Copel[3] ribbon wound on a grooved ceramic form 4¼ in. in diameter. Its resistance is about 3.0 ohms.

The slider on *R*2 is driven by the motor *M* through the mechanical link *L*. The direction of the motor is controlled by the relay Rel, shunted by a 100-mfd. condenser *C* to prevent chattering. The relay is controlled by the plate current of the type 2050 thyratron *T*. Note that *R*4 (about 100 ohms depending on the relay coil) limits the tube current to 0.2 ampere. The plate current for the tube is supplied by a 1:1 isolating transformer *Tr*. *Re*2 is a relay that stops the motor if the arc goes out. The coupling between reducer and rheostat is made from a short length of hose and two hose clamps, left slightly loose to prevent damage in case the slider should try to go past the end of the rheostat.

Figure 4 shows, left to right, *R*1, *R*2, and *R*3, also the motor and speed reducer. *Re*2 can also be seen between *R*1 and *R*2, just above the motor. Figure 5

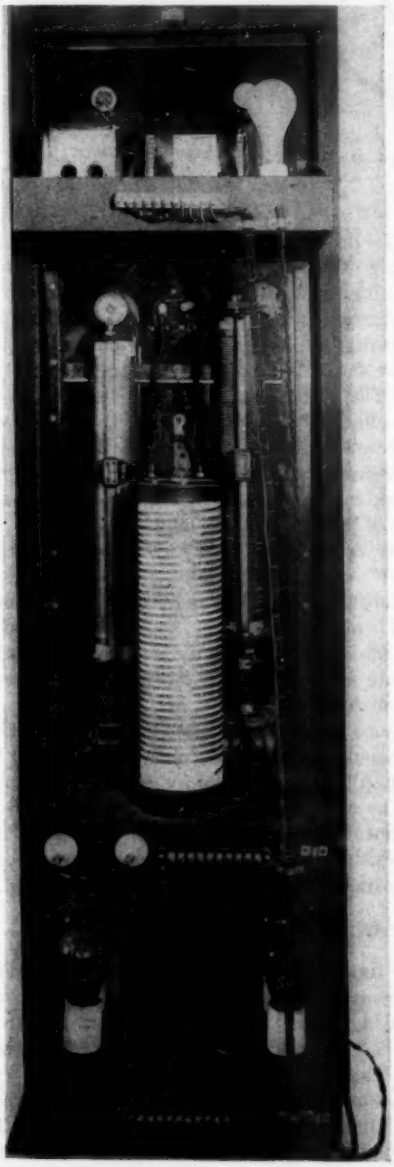

FIG. 5. Back view of controller.

[3] Made by Hoskins Manufacturing Company, Lawton and Kinnison Avenue, Detroit, Michigan.

shows a back view of the entire assembly. The bottom shelf houses a single phase rectifier of standard design to supply d.c. for the motor. This rectifier is essentially redundant, as indicated below, and would be omitted in a redesign.

The thyratron and associated equipment are mounted on the top shelf in Fig. 5. The voltage developed across *R3* by the arc current is balanced against an adjustable voltage obtained from the 45-volt battery *B* and the 500,000-ohm potentiometer *P*. The difference is applied to the control grid of the type 2050 thyratron *T* through a 100,000-ohm fixed resistor *R5*. The plate current of the thyratron controls the direction of rotation of the motor *M* by means of the DPDT relay *Rel*.

After the controller was completed and tested, it was found that it introduced so much resistance into the arc circuit that *R* (see rectifier section) had to be reduced to zero. The following procedure is therefore recommended for possible users of this design:

(1) If the rectifier is to be used alone, incorporate the three a.c. line resistors *R* as described.

(2) If the rectifier is to be used with this controller, omit *R* and connect the tubes directly to the a.c. line through the usual fuses.

(3) If the second alternative is taken, the 140–150-volt d.c. output of the rectifier can be used to run the motor, preferably with some series resistance to reduce the effect of the somewhat excessive voltage.

In operation, the terminals at the top of Fig. 3 are connected in series with the arc, making sure that the polarity of the voltage developed by the arc current is actually as indicated by the + and − signs. A trial arc is drawn and *P* adjusted until the desired current is obtained. The potentiometer will need occasional readjustment as the battery runs down. It will also usually be necessary to set *R1* in order to have the range of operation of *R2* come near the center of its range with no danger of the slider hitting the end. Note also that the motor must be polarized always to rotate in such a direction as to compensate for departures from the correct current, and not to accentuate them.

Errata: The Luminescence of Photo-Conducting Phosphors

[J. Opt. Soc. Am. 39, 935 (1949)]

G. F. J. GARLICK AND A. F. GIBSON
Physics Department, University of Birmingham, Birmingham, England

ON page 938, Table VI, last column, the energy values W should be 0.24 and 0.23, and not 0.42 and 0.23.

Reducing Stray Light Errors in the Hunter Multipurpose Reflectometer

D. J. Troy, Jr. and L. G. Glasser
Engineering Research Laboratory, Engineering Department, E. I. du Pont de Nemours and Company, Inc., Wilmington, Delaware
(Received October 10, 1949)

The use of the Hunter multipurpose reflectometer for color measurement has been limited, particularly at low reflectances, by inaccuracies arising chiefly from stray light in the optical system. A baffle is described whose installation greatly reduces stray light, so that its effect may be ignored above 2 percent reflectance. A method is also described for making corrections for stray light in those cases where its effect cannot be neglected. Application of these two procedures permits the Hunter reflectometer to furnish useful data down to reflectances of 0.1 percent.

THE Hunter multipurpose reflectometer is an instrument that may be used to measure color. The measurements that can be made with it provide information on hiding power and opacity; whiteness, yellowness, and blueness of near whites; and color co-ordinates in various standard color systems. With careful handling and use, the instrument can measure barely perceptible color differences. Furthermore, it has sufficient sensitivity to detect and measure small differences in color between very dark samples.

The usefulness of the instrument has been limited by inaccuracies arising mostly from stray light in the optical system. Other scale inaccuracies are present, but these are quite small and, if necessary, they can usually be taken into account by methods described by Hunter.[1] A method is described here for reducing stray light, so that its contribution to the reflectance readings may be ignored in most cases. A method for calculating scale corrections to be applied to reflectance readings to eliminate the effects of stray light, is also described.

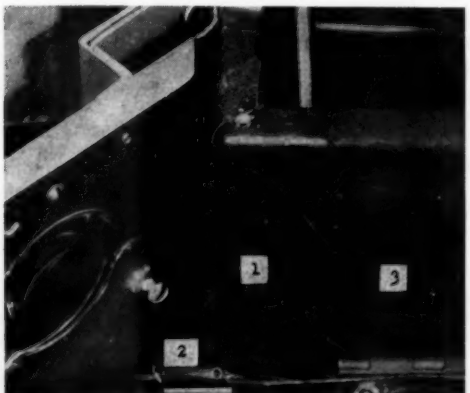

FIG. 1. Stray-light baffle. Baffle 1 intercepts stray light from the support of comparison-beam mirror 2 and prevents stray-light from entering the measuring photo-cell tunnel 3.

[1] R. S. Hunter, J. Research Nat. Bur. Stand. 25, 581 (1940).

Most of the stray light is the result of scattering by the glass support of the small oblique mirror that divides the light between the measuring and comparison beams. The installation of a baffle (Fig. 1) between the mirror and the measuring photo-cell reduces the stray light by 60–90 percent at reflectance scale readings between 0.08 and 0.20, where stray light is most serious. When the stray light baffle is installed, scale corrections are reduced to ± 0.002 for reflectances above 2 percent, and for many purposes corrections of this magnitude may be ignored. Figure 2 shows how the scale corrections are reduced when the baffle is installed.

Some means is still needed to determine the corrections for reflectances lower than 2 percent. Among the calibrated standards supplied with the instrument there is only one in the range below 2 percent, so that this range is not adequately covered. A method has been devised for calculating the corrections at these low reflectance values.

The method is based on the following considerations. When the reflectance of a sample is to be measured, the measuring photocell is moved towards or away from the illuminated sample to make the current i_r, generated by the specimen reflected light, exactly equal to a fixed current, I, supplied by the comparison photo-cell. The scale attached to the movable photo-cell is calibrated directly in reflectance. Thus as the cell is moved back and forth with a given sample in place, i_r is inversely proportional to the reflectance scale reading S. When the instrument is balanced,

$i_r = I$ and $S = S_b$, the scale reading at balance.

It follows therefore that

$$\begin{aligned} S_b/S &= i_r/I \\ (S_b - S)/S &= -(I - i_r)/I \\ \Delta S/S &= -\Delta i_r/I \\ I &= S\cdot(-\Delta i_r/\Delta S). \end{aligned} \tag{1}$$

If the instrument scale has been correctly ruled and there is no stray light, then S_b, the scale reading at balance, is equal to the true reading, S_t, corresponding to the reflectance of the sample.

Consider the case, however, where the amount of the stray light is appreciable. As before, the current, i_r,

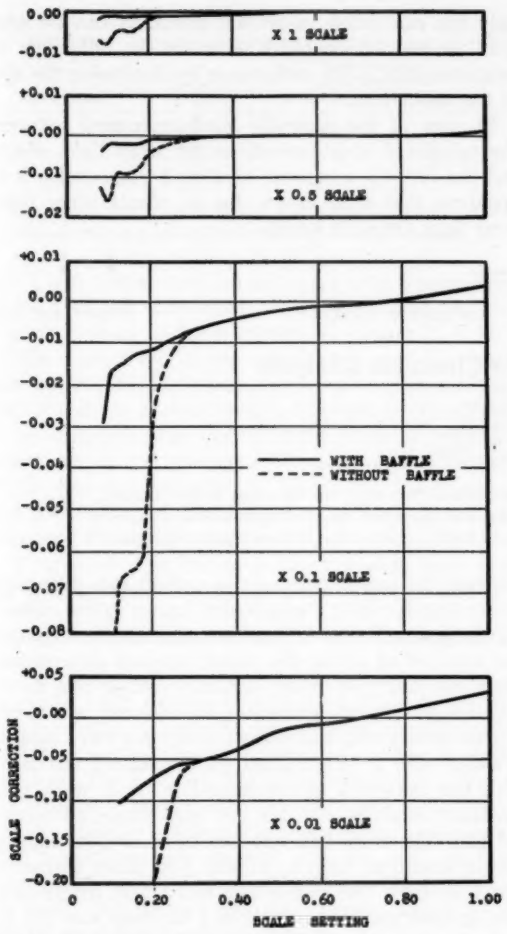

FIG. 2. Reduction of scale corrections by stray light elimination.

generated by the specimen reflected light will equal the comparison cell current, I, when $S=S_t$. But the instrument will not balance at this setting, since the total current in the measuring photo-cell has been increased by i_s, the stray light current. The instrument will balance, however, at a scale setting S_b, where $i_r+i_s=I$, or $i_r=I-i_s$. Since i_r is inversely proportional to S:

$$S_t/S_b=(I-i_s)/I$$

or

$$(S_t-S_b)/S_b=-i_s/I.$$

The scale correction, δ, is defined as $\delta=S_t-S_b$; hence

$$\delta=-S_b\cdot i_s/I. \qquad (2)$$

This equation permits computation of the scale correction for any scale reading. Values of i_s and I must be known. The magnitude of I is constant for any specific range of the instrument (×1, ×0.5, ×0.1, ×0.01). It may be determined from Eq. (1) by standardizing the instrument in the customary manner, then moving the photo-cell to produce a conveniently readable galvanometer deflection. The galvanometer deflection is Δi, the change in scale reading is ΔS, and the scale reading in the off-balance position is S. The value of I for any other range is obtained by multiplying the value for the ×1 scale by the filter factor for the range in question.

The stray light current, i_s, which varies with the scale setting, may be measured by completely masking the comparison photo-cell, placing a light trap at the sample port, and reading the galvanometer deflection at various scale settings. Since i_s need be measured only once, a light trap may be conveniently improvised by darkening the room, removing the cover from the sample port to allow the incident light to escape from the instrument and draping a black cloth in front of the sample port but several inches back, to shield the photo-cell from any light in the room.

It is usually desirable to decrease the scale corrections by making the correction equal zero for some medium scale reading, S_0, e.g., 0.500 or 0.700. This can be done by artificial adjustment of the value of I for a particular range. I is increased by an amount equal to i_{s0}, the stray light current at the scale reading S_0. All the other measured values of stray light current are then decreased by an amount equal to i_{s0} and scale corrections are calculated using Eq. (2).

The ×0.01 scale is not obtainable directly by insertion of a neutral filter. It is more convenient in this case to adjust the instrument to read correctly on the calibrated standard that has a reflectance between 0 and 1 percent. The measured stray light currents are

TABLE I. Comparison of measured and calculated scale corrections.

Sample reflectance	Scale multiplier		Scale reading	Measured scale correction	Calculated scale correction
(a) Before installing stray light baffle					
0.205	×1		0.208	−0.003	−0.002
0.145	×1		0.150	−0.005	−0.005
0.0878	×1		0.096	−0.008	−0.008
0.205	×0.5	(0.538)	0.381	0.000	−0.001
0.0878	×0.5		0.169	−0.006	−0.004
0.0244	×0.1	(0.072)	0.350	−0.011	−0.007
0.0061	×0.1		0.150	−0.065	−0.068
0.002	×0.01		0.272	—	−0.072
0.001	×0.01		0.228	—	−0.128
(b) After installing stray light baffle					
0.205	×1		0.207	−0.002	−0.001
0.145	×1		0.146	−0.001	−0.001
0.0878	×1		0.089	−0.001	−0.002
0.205	×0.5	(0.538)	0.379	+0.002	−0.001
0.0878	×0.5		0.164	−0.001	−0.002
0.0244	×0.1	(0.072)	0.341	−0.002	−0.007
0.0061	×0.1		0.104	−0.019	−0.017
0.002	×0.01		0.255	—	−0.055
0.001	×0.01		0.180	—	−0.080

then decreased by an amount equal to the stray light currents at the scale reading at which the instrument is standardized, and I is increased by the same amount.

The calculated and measured scale corrections are compared in Table I. In general the agreement is good, particularly in the case of large scale corrections where the greatest accuracy is needed. Since the corrections for the $\times 0.01$ scale could not be determined experimentally, because of the lack of standards of reflectance, only the calculated values are given. It can be seen that the use of the baffle increases the reliability of measurements at low reflectance by decreasing the size of the corrections.

In view of the generally good agreement between the calculated scale corrections for stray light effects and the directly measured total scale corrections, it is apparent that scale errors due to effects other than stray light are quite small.

JOURNAL OF THE OPTICAL SOCIETY OF AMERICA VOLUME 40, NUMBER 2 FEBRUARY, 1950

A New Source for Spectro-Chemical Analysis

ARTHUR G. ROUSE
Department of Physics, Saint Louis University, Saint Louis, Missouri
(Received October 3, 1949)

An induction heater is used to evaporate the sample held in a carbon cup, and the vapor is then excited by a spark. The two main functions of a source, evaporation and excitation, are thus separately controlled. A study of the boiling point temperature of the sample can be used to differentiate elements and compounds.

THE sources most commonly used for spectro-chemical analysis are the a.c. spark and the d.c. arc. It is generally agreed that the d.c. arc, because of its high electrode temperature is sensitive to trace impurities, but because of fluctuations of the arc, the line intensities in the spectrum are not accurately reproducible. The a.c. spark, on the other hand, is not so sensitive to trace impurities, but because of the good averaging process obtained in the several hundred flashes in a single exposure the line intensities are much more reproducible. Some characteristics of a source employing induction heating and which gives promise of combining the desirable high temperature of the arc with the averaging process of the spark are described in this paper.

THE SPARK INDUCTION HEATER SOURCE

A carbon cup which serves as a sample holder is heated by a 200-kc sec.$^{-1}$ induction heater having a 5-kw maximum plate dissipation. A variac adjusts the plate voltage of the induction heater tubes which controls the power output of the unit and this in turn controls the temperature of the carbon cup. Effective power transfer from the induction heater to the carbon cup is obtained when the coil surrounding the cup and the cup are of about the same physical dimensions. Since the tank coil of the induction heater was much larger than the cup, a coupling transformer[1] was used. The secondary of this coupling transformer was a copper cylinder with a longitudinal gap, mounted coaxially with the tank coil and surrounding it. A work coil mounted coaxially with the cup was connected across the gap. The work coil was five turns of $\frac{1}{8}$-in. copper tubing wound to form a cylinder $\frac{1}{2}$-in. inner diameter and 1 in. long. The carbon cup was a $\frac{3}{4}$-in. length of a $\frac{1}{4}$-in. carbon rod. An axial hole $\frac{3}{8}$ in. deep was cut in one end with a No. 13 drill to form a crater for holding the sample.

TABLE I.*

Spectrogram	Crater depth	Variac voltage	Temperature of cup °C	Line intensity (arbitrary units) Zn3345A	Cd3466A
a	$\frac{1}{8}$ in.	0	100	2	3
b	$\frac{1}{8}$ in.	5	—	2	3
c	$\frac{1}{8}$ in.	10	—	2	3
d	$\frac{1}{8}$ in.	15	—	2	3
a	$\frac{3}{8}$ in.	25	700–720	0	0
b	$\frac{3}{8}$ in.	30	770–790	0	1
c	$\frac{3}{8}$ in.	35	820–840	0	3
d	$\frac{3}{8}$ in.	40	880–900	1	3
e	$\frac{3}{8}$ in.	45	950–970	2	3

* Data taken from spectrograms of a Zn-Cd sample in a $\frac{1}{8}$-in. and a $\frac{3}{8}$-in. crater.

The vapor issuing from the carbon cup was excited by an a.c. spark between the carbon cup and a carbon rod placed above the open cup. Electrical contact with the cup for this spark was made by a metal plug fitted into a hole in the bottom. The plug also served as the mechanical support for the cup. The conventional spark excitation circuit was used with a resistance in the primary circuit (R), and a capacitance (C) in parallel with the gap in the secondary circuit (V). Circuit (a) involved $R=5$ ohms, $C=0.03$ mf, $V=2500$ volts; Circuit (b) $R=5$ ohms, $C=0.004$ mf, $V=6000$ volts.

An iron-constantan thermocouple was inserted into a hole in the cup for temperature measurements in some instances.

EXPERIMENTAL

Powdered samples of from 50 mg to 200 mg were placed in the crater in the carbon cup. The variac controlling the induction heater was set at some voltage

[1] Editor's column, Radio Craft 19, 36 (1948).

TABLE II.*

Spectrogram	Variac voltage	Line intensity (arbitrary units) Zn3345A	Cd3466A
a	29	3	0
b	30	3	0
c	31	3	0
d	32	4	3

* Data taken from a series of spectrograms of a $ZnCl_2$-Cd sample.

and 1 min. was allowed for an equilibrium temperature to be attained. The spark was then turned on, the shutter in front of the spectrograph (Hilger E. 9.307/26256) opened for 15 sec. then closed and the spark was turned off. The process was repeated at a higher plate voltage or another sample was used. Spectrograms to be compared were on the same plate to minimize variations in the photographic development process which was not temperature controlled. Pre-sparking and pre-heating of the cup before adding the sample decreased the background.

A series of experiments of the following type were made to determine the performance of the source.

1. Effect of secondary voltage V and capacitance C

The energy supplied to the cup by the spark must be made much smaller than that supplied by the induction heater in order to maintain an approximately constant temperature of the sample during a single exposure. The simplest way of decreasing the power of the spark is to decrease the capacitance C. As a typical datum, with $C=0.004$ mf, the temperature as measured with a thermocouple inserted into the cup, changed from 800°C to 830°C during the 15 sec. the spark was on (induction heater also on). Larger values of C caused greater temperature changes.

A large secondary voltage V permits the use of a longer spark gap which resulted in a smaller condensation of the vapor on the upper electrode. The condensed material sometimes closed the smaller gaps. The values of V used were 2500 volts and 6000 volts; the latter was more satisfactory.

2. Shape of the carbon cup

If the crater is made shallow ($\frac{1}{8}$ in.) the spark appears to strike directly on the sample and lines of all the elements in the sample appear even when the temperature as indicated by the thermocouple is low (about 100°C). It is possible that the temperature is much higher at the point where the spark terminates causing local vaporization, or the sample material may enter the discharge as a result of ionic bombardment. With a deeper crater in the cup ($\frac{3}{8}$ in.) and the sample material in only the bottom of the crater, the lines of an element do not appear in the spectrum until the thermocouple indicates a temperature almost equal to the boiling point temperature of the sample. This indicates that the induction heater is supplying a major portion of the power necessary for evaporation. See Table I.

3. Mixture of 2 or more elements in the sample in a $\frac{3}{8}$-in. crater

The second part of Table I shows data taken from a series of spectrograms of the sample in a $\frac{3}{8}$-in. crater at increasing induction heater plate voltage. The sample consists of equal weights of Cd and Zn filings. Cd with a boiling point temperature of 767°C first appears in spectrogram (b), Zn with a boiling point temperature of 907°C first appears in spectrogram (d). The order of appearance of the spectra of the elements in a series of these spectrograms taken at increasing temperatures of the sample is the same as the order of the boiling point temperature of the elements in the sample. The spectra of Cd, Zn, and Pb taken in various combinations of 2 or 3 at a time have appeared in the order of the boiling point temperatures.

4. Mixtures of chemical compounds in the sample

As noted above, in a sample which is a mixture of elements the spectra of those elements appear in a series of spectrograms taken at increasing temperature in the order of the boiling point temperatures of the elements. It is found that if the sample is a mixture of compounds, the spectra appear in the order of the boiling point temperatures of the compounds. Using a sample of $CdBr_2$ and ZnI_2 the Zn lines appear before the Cd lines because ZnI_2 has the lower boiling point temperature. This is just the reverse of the order when the sample is a mixture of Cd and Zn. This means that the spark-induction heater source can be used for a qualitative analysis of the chemical composition, in that a mixture of Zn with Cd can be readily distinguished from a mixture of $CdBr_2$ and ZnI_2. Various compounds have been distinguished in this way.

5. Boiling point temperatures

Spectroscopic measurements of boiling point temperatures have been made by Richardson[2] using a moving plate technique. It was considered that the spark-induction heater source might have some advantage for such measurements. Since it has been noted that spectra appear in the order of the boiling point temperatures, a thermocouple was used to measure the temperature of the cup at a point close to the sample. By keeping the power supplied by the spark small and the sample at the bottom of the rather deep cup, the temperature as measured by the thermocouple when the line appeared and the boiling point temperature were approximately equal. For example, Zn of boiling point temperature 907°C appears in the spectrum when the thermocouple indicates a temperature of 880°C–900°C. See Table I.

[2] D. Richardson, *Proceedings of the Fifth Summer Conference on Spectroscopy and its Applications* (John Wiley and Sons, Inc., New York, 1938).

The question of the least difference in boiling point temperatures of two substances which can be detected was partially answered by using a mixture of Cd of boiling point temperature 767°C and $ZnCl_2$ of boiling point temperature 732°C. The order of appearance of the Cd and Zn lines is very apparent in the spectrograms, the data for which are summarized in Table II. A difference of 35°C in the boiling point temperature therefore is readily detected, which is a smaller difference than that indicated by Richardson.

The spectrograms of a mixture of $CdSO_4+H_2O$ (C.P. obtained from Heil Chemical Company) with Zn show the Zn lines appearing after the Cd lines while a mixture of $CdSO_4+H_2O$ with $ZnCl_2$ show the Zn lines appearing before the Cd lines. Quite obviously $CdSO_4+H_2O$ used must have a boiling point temperature (or a decomposition temperature) between that of Zn (907°C) and $ZnCl_2$ (732°C). The estimated boiling point temperature of $CdSO_4$ from the spectrograms is 820°C.

6. Sensitivity to trace impurities

Standard Zn samples containing 0.005 percent Cd and 0.002 percent Pb and supplied by the American Zinc Company of America were used in the sensitivity and reproducibility tests. Spectrograms were obtained using the induction heater plus spark as a source, with the spark alone between electrodes made of the sample, and with the d.c. arc as the source. The Cd lines appeared when the spark-induction heater source was used, they did not appear when the spark without induction heater was used and they sometimes appeared in the d.c. arc and with about the same relative intensity as in the spark-induction heater source. The sensitivity of the spark-induction heater source surpasses that of the spark used and is about the same as that of the d.c. arc.

7. Reproducibility of line intensity

Quantitative spectro-chemical analysis requires a constant ratio of line intensities of the various constituents in a sample when that sample is analyzed several times. Eight exposures were made of a single sample of Zn containing 0.0076 percent Pb, the temperature of the cup being high enough for simultaneous vaporization of the two elements. The line densities were measured on a non-recording densitometer and the ratio $\log(Pb_{2833})/Zn_{2670})$ was computed. This ratio had an average deviation from the mean of 7 percent. This is a somewhat smaller deviation than that reported for the arc and larger than that for the spark. It is considered however, that much of the variation is due to the photographic process used and that much of the variation could be eliminated by using photoelectric recording to by-pass the photographic process.

The spark induction heater as a source for spectra-chemical analysis gives promise of combining controlled evaporation with the averaging process of the spark. This source can be used to measure the boiling point temperatures of sample elements or compounds. The boiling point temperature information can be used to differentiate elements and compounds under certain conditions.

The author is deeply indebted to Sr. Wilma, Sr. Constance, and Sr. Sylvia, who made the laboratory observations and to the Physics Staff for many helpful suggestions.

Munsell Renotations Used to Study Color Space of Hunter and Adams*

DOROTHY NICKERSON
United States Department of Agriculture, Production and Marketing Administration, Washington, D. C.
(Received November 22, 1949)

The colorimetric scales of recent Hunter and Adams proposals are studied in terms of the smoothed curves of the Munsell renotation space. Three conversion tables prepared provide: I.C.I. (X, Y, Z) data; Adams' chromatic value data; Hunter's a and b. Each table extends to the theoretical hue, value, and chroma limits of the original table. Such use of Munsell renotation data makes it possible to visualize the color spacing of the coordinates of any color measuring instrument that is based upon or related to the I.C.I. system, and makes it possible to understand instrument results in terms of color experience, and thus assess the accuracy and precision of an instrument in terms of standard colorimetric practice and known color tolerance.

FOLLOWING early work of Judd on uniform chromaticity scales, Judd, Hunter, and Scofield developed a chromaticity diagram, with gray placed at the origin of the coordinates (α,β), that has been widely used in the paint and ceramic industries in connection with Hunter's tristimulus colorimeters.[1,2] In 1948 Hunter reported an instrument[3,4] designed to read directly in terms of adjusted formulas that give a diagram in which the chromaticity coordinates (a, b) are related to the I.C.I. tristimulus coordinates X, Y, Z for C illuminant as follows:

$$\begin{aligned} a &= 175 f_Y(1.02X - Y) \\ b &= 70 f_Y(Y - 0.847Z) \end{aligned} \tag{1}$$

$$R_d = 100Y \tag{2a}$$

$$L = f_Y R_d. \tag{2b}$$

Lightness (L) is based on the rate of change ($f_Y R_d$) of lightness with reflectance and this formula is the best approximation to the Munsell value function that Hunter could incorporate into his instrument circuit: $f_Y = 0.51[(21+20Y)/(1+20Y)]$. In the Hunter formula f_Y replaces the Munsell value function used for a similar purpose in Adams "chromatic value" formulas.[5-7] Actually the Hunter formulas are closer to Adams "chromatic valence" than to "chromatic value."

The factors 1.02 applied to X and 0.847 applied to Z are necessary in order to place the neutral point for C illuminant at zero.† The constants provide scale units of the order of a small but commercially important color difference. The "a" scale is 2.5 times that of the "b" scale in order that constant chroma may plot as near to a circle as possible. In the Adams formulas for "chromatic value," the Munsell value function (V) is applied separately to the three components X, Y, Z for a given illuminant, and the resulting V_X, V_Y, V_Z uniquely define a color, the differences $(V_X - V_Y)$ and $(V_Z - V_Y)$ being zero for an achromatic color. The $(V_X - V_Y)$ difference is similar to Hunter's "a," and $(V_Z - V_Y)$ to "b" with reversed sign: $(V_X - V_Y)$ is plotted 2.5 times the scale of $(V_Z - V_Y)$. Adams formulas for chromatic value are given in a form comparable to the Hunter formulas:

$$\begin{aligned} a_A &= (V_X - V_Y) \\ b_A &= 0.4(V_Z - V_Y) \\ V &= \text{Munsell value function}[8] \end{aligned}$$

The Adams formula gives better all-over results than the Hunter formulas in terms of uniform chromaticity[9] because the value function is applied separately to X, Y, Z while in the Hunter formula it can be applied only to Y if one is to have an instrument that is direct reading in terms of a and b. The circuit of the Hunter instrument is arranged so that a and b readings are related to f_Y when R_d is the first factor measured.

In order to understand the colorimetric scales of the Hunter and Adams‡ proposals they have been studied in terms of the smoothed curves of the Munsell renotation space.[10]

Three conversion tables have been prepared, each to correspond with Table I of the 1943 report.[10] Three new

* Presented at the Buffalo meeting of the Optical Society of America (October, 1949).

[1] R. S. Hunter, J. Opt. Soc. Am. **30**, 536 (1940); J. Research Nat. Bur. Stand. **25**, 581 (1940), (RP1345).

[2] R. S. Hunter, J. Opt. Soc. Am. **32**, 509 (1942); Nat. Bur. Stand. (U. S. Circ.) C429 (1942).

[3] R. S. Hunter, J. Opt. Soc. Am. **38**, 661(A) (1948).

[4] R. S. Hunter, J. Opt. Soc. Am. **38** 1094(A) (1948).

[5] E. Q. Adams, J. Opt. Soc. Am. **32**, 168 (1942).

[6] E. Q. Adams, J. Opt. Soc. Am. **36**, 717(A) (1946).

[7] D. Nickerson, "Interrelation of color specifications" (U. S. Department of Agriculture, February, 1947), 45 pp., processed; Pap. Trade J. **125**, 153 (1947).

† When using the 10 or 30 ordinate method of calculating I.C.I. data from spectrophotometric curves, the totals for X, Y, Z can be used directly before multiplication of X and Z factors to adjust them for the illuminant. The factors 1.02 and 0.847 are the reciprocals of the X_C and Z_C numbers 0.9804 and 1.1810.

[8] Newhall, Nickerson, and Judd, J. Opt. Soc. Am. **33**, 385 (1943), Table II, p. 406; the formula is a quintic parabola, p. 417.

[9] R. W. Burnham, J. Opt. Soc. Am. **38**, 387 (1949).

‡ Adams suggested recently a modification of his $(V_X - V_Y)$, $(V_Z - V_Y)$ formula by applying the value function to the average of the tristimulus values (e.g., $V[(X+Y)/2]$, and $V[(Z+Y)/2]$. He says there are two explanations for the use of average rational tristimulus values in computing chromatic value: (1) the actual retinal primaries are only half as saturated as the primaries chosen for the I.C.I. standard observer; (2) not all the "irrationality" in the value has been introduced at the stage in which "complementation" takes place, and averaging the values makes just about the right allowance for this.

[10] Newhall, Nickerson, and Judd, J. Opt. Soc. Am. **33**, 385 (1943).

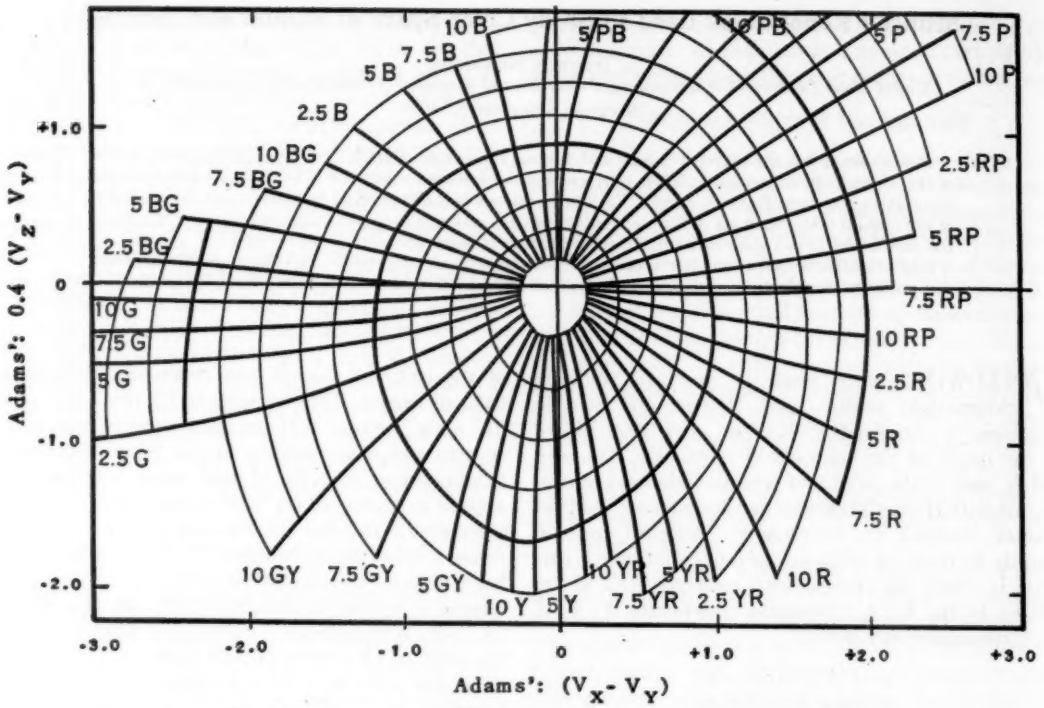

FIG. 1. Munsell renotations for 5/ value converted to Adams' "chromatic value" diagram.

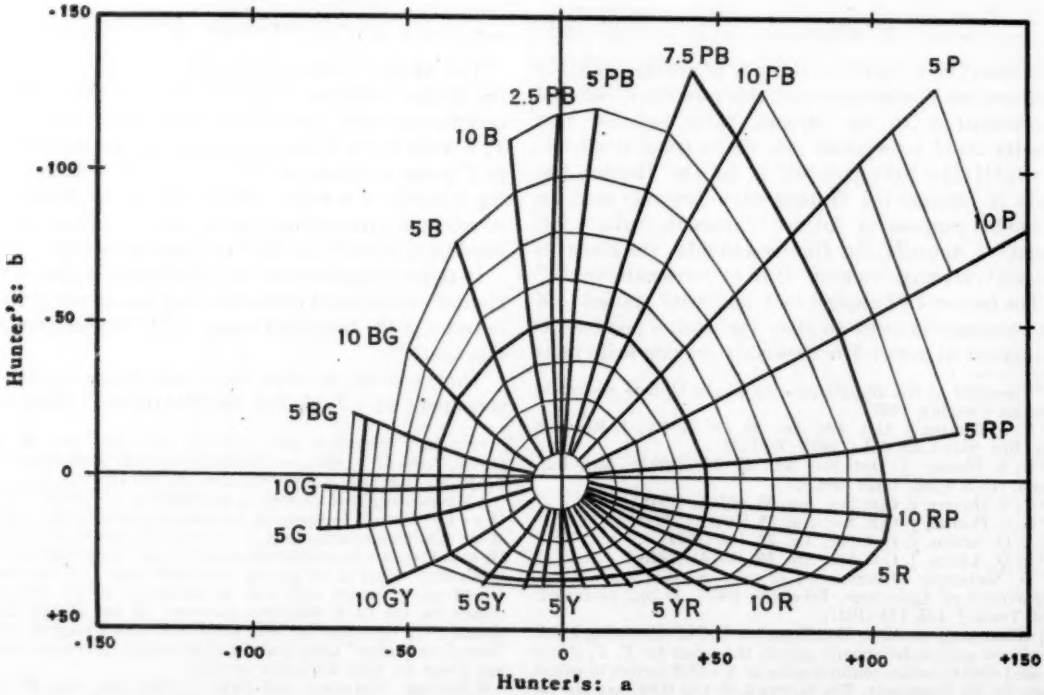

FIG. 2. Munsell renotations for 5/ value converted to Hunter (a, b)-diagram: $a = 175 f_Y(1.02X - Y)$; $b = 70 f_Y(Y - 0.847Z)$.

TABLE I. Data on five papers in the cotton color range based on measurements on the G. E. spectrophotometer and on the Hunter color and color-difference meter.

Munsell prod. No.	Based on spectrophotometric measurements[a] I.C.I. tristimulus values			Munsell renotations			Hunter coordinates			Based on color-difference meter[b] Hunter coordinates		
	X	*Y*	*Z*	*H*	*V*	*C*	% R_d	$+a$	$+b$	% R_d	$+a$	$+b$
1607	0.6835	0.6981	0.7312	2.5Y	8.57	0.8	69.8	−0.2	6.6	69.5	0.4	6.5
	0.6808	0.6954	0.7311	2.5Y	8.56	0.8	69.5	−0.2	6.4			
1608	0.6705	0.6826	0.6895	1.5Y	8.49	1.2	68.3	0.3	8.4	68.1	0.9	8.5
	0.6726	0.6848	0.6895	1.5Y	8.50	1.2	68.5	0.3	8.6			
1604	0.6476	0.6586	0.6404	1.0Y	8.37	1.5	65.9	0.4	10.0	65.6	1.1	10.4
	0.6467	0.6577	0.6404	1.0Y	8.36	1.5	65.8	0.4	10.0			
1605	0.5762	0.5829	0.4738	1.0Y	7.95	2.8	58.3	1.1	16.7	57.6	2.2	17.4
	0.5797	0.5871	0.4789	1.0Y	7.98	2.8	58.7	1.0	16.7			
1606	0.4937	0.5013	0.4696	1.5Y	7.47	1.6	50.1	0.6	10.5	48.7	1.2	10.4
	0.4969	0.5044	0.4744	1.5Y	7.48	1.6	50.4	0.6	10.4			

[a] The second measurement is taken with the samples oriented through 90°.
[b] Average of 10 measurements.

conversion tables are thus available, one providing tristimulus data (X, Y, Z), a second Adams "chromatic value" data, a third Hunter's a and b, each series extending to the hue, value, and chroma limits of the original tables, except that the Hunter data are given for 20 instead of 40 hues on values other than 5/. These tables are too extensive for general publication, but a limited number of copies are available on request.

Full series of diagrams have been drawn and studied for the Hunter and Adams formulas. They indicate that for constant chromas both the Hunter and Adams diagrams depart from circles toward an ovoid shape. Typical diagrams are given for value 5/ in Figs. 1 and 2. The Adams ovoid is flat on the blue side, the yellows being extended in comparison with the reds, greens, and blues, with chroma separations quite consistently well spaced for all values and all hues. The Hunter ovoid is flat on the yellow side, the blues being extended in comparison to the yellow, with red and green between; near neutral the chromas are fairly well spaced, but as higher chromas are reached the spacing contracts between the yellows, and between high chroma greens, but expands in the blues, somewhat less in the reds. This is a logical result of the way in which the f_Y function must be applied to accord with present limitations of the Hunter instrument if it is to provide a direct-reading instrument.

The data described have been obtained in the course of a study of the applicability of the new Hunter color and color-difference meter to the colorimetry of cotton grade standards work. There is little hue change in the color of raw cottons, therefore a study of the relation of color to cotton grades can be made on a two-dimensional diagram in which Munsell value and chroma are used as coordinates. A generally similar diagram can be made in terms of Hunter's reflectance (R_d) and "$+b$," the "$+b$" being the direction of yellowness on his instrument, thus providing a scale in the yellows that is related to the chroma of yellows. The range of raw cotton colors is extremely limited, and for the portion of color space referring to cotton the Hunter formulas have been carefully studied in relation to results obtained on his direct-reading instrument.

A series of five papers were painted several years ago

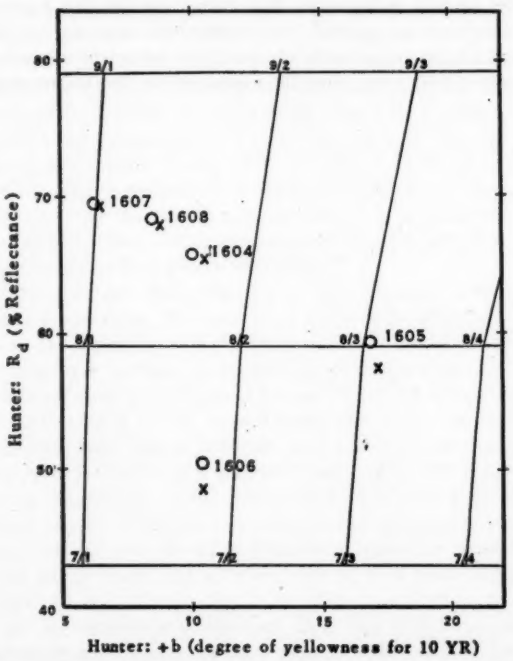

FIG. 3. Five color samples in the cotton color range plotted on Hunter scales R_d and $+b$ (percent reflectance and degree of yellowness) according to data calculated (○) from NBS spectrophotometric measurements, and from direct measurements (×) of the same samples on the Hunter color and color-difference meter. Munsell renotation points for 10 YR 7–9 value, 1–4 chroma, indicate the size of color difference involved. Applying photometric scale corrections for this instrument makes agreement between theory and direct colorimetric measurement in this color range quite satisfactory.

to match specified colors in the cotton color range. For this study they were spectrophotometered by the National Bureau of Standards in 1948. Two curves were made for each sample, the second curve for the sample oriented at 90° from its first position. In all cases the samples were backed with black. I.C.I. data calculated for Illuminant *C* are listed in Table I for each curve separately. The Hunter formulas (1) and (2a) were applied to these data. The samples were then measured on the Hunter color and color-difference meter. Both sets of data are plotted in Fig. 3, the calculated results as open circles, the measured results as crosses. The measurements plotted were made in the fall of 1948; those reported in Table I were made in September, 1949, following adjustments of the "*a*" coordinate of the instrument.

To help judge the size of the visual color differences involved, points representing renotations for Munsell 10 YR 7–9 values, 1–4 chromas are indicated. It is known that the particular instrument on which these measurements were made has an unusually large photometric scale error. With agreement set for 80 percent, the difference amounts to almost 1.0 percent at about 60 percent reflectance, and as much as 1.6 percent at 40 percent reflectance. If a correction for this known difference is applied, the agreement between results calculated on a basis of spectrophotometric measurements and those directly measured on the instrument is very good. Originally the *a*, or red-green differences, did not check as well as the R_d and *b* differences, but part of this now has been corrected (the instrument used was No. 3, a very early model). Since only R_d and *b* measurements are necessary for cotton work, the agreement seems quite good enough when coupled with its very adequate precision of readings, to make this direct-reading instrument a very practical one for use in measuring cotton color.

The data obtained in this study are reported because it is believed that this method of using Munsell renotation space in investigating the relation of color space systems, or the applicability of a single instrument to a particular problem, is one that others may find useful in studying other instruments or other portions of color space.

In summary, it is believed that a knowledge of the visual color spacing of the coordinates used to express the results of any color measuring instrument makes it possible to understand the instrument results in terms of color experience, and to assess the accuracy and precision of the instrument in terms of standard colorimetric practice and known color tolerances. Use of the Munsell renotation data makes it possible to obtain this knowledge for any instrument or system that is in any way based upon or related to the I.C.I. system of colorimetry.

Empirical Convergence Correction of Depolarization Measurements*

D. H. RANK AND R. E. KAGARISE
Spectroscopy Laboratory, Pennsylvania State College, State College, Pennsylvania
(Received October 26, 1949)

A spiral mercury arc light source of the low pressure variety and 2-kilowatt power dissipation is described. The use of this powerful but geometrically undesirable arrangement for making depolarization measurements is investigated. Calculations of convergence errors using the polarized incident light method of Edsall and Wilson indicate a linear convergence correction of measured ρ-values. Measurement of depolarization values of Raman lines whose ρ-value is accurately known confirms the theoretical calculation of convergence correction. From the results moderately accurate ρ-values can be obtained by this method by using an empirical correction curve.

IT has been shown by Douglas and Rank[1] that it is possible to make extremely precise depolarization measurements using the method of polarized incident light. This method, which efficiently produces polarized incident light in the scattering tube, involves focusing the light from the arc by means of refracting or reflecting devices. The effectiveness of this system for the production of strong spectra depends upon the intrinsic brilliancy of the arc stream rather than the total flux produced by the lamp.

We have recently made use of low pressure lamps for the excitation of Raman spectra which have very superior spectral characteristics, i.e., extremely sharp lines, low continuous background and a very large reduction in intensity of lines arising from singlet transitions. Some of these desirable properties of low pressure lamps have been discussed by Rank and McCartney.[2] However, the arc stream in this type of intense low pressure lamp completely fills the tube and does not concentrate in the center as is the case with high pressure discharges, the result being that the intrinsic brilliancy of this lamp is much smaller than that of the high pressure lamp.

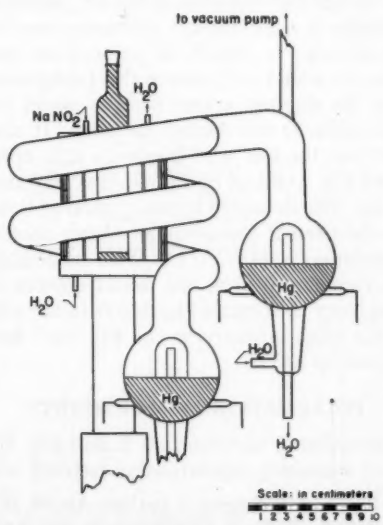

FIG. 1. Scaled drawing of light source, scattering tube, filter and cooling arrangement.

The result of the diffuseness of the discharge from a low pressure lamp is that when using the method of polarized incident light in the manner described by Douglas and Rank,[1] the spectra produced are only of about $\frac{1}{3}$ the intensity of those obtained with high pressure commercial lamps of similar geometry and operated at the same wattage. If one is doing photographic work, the loss of intensity is not too serious and can be compensated by increasing the exposure time by an appropriate factor. Theoretically, for direct photoelectric measurements, it is only necessary to increase the time constant in the electrical circuit to make up for the above mentioned decrease in intensity. There are, however, numerous reasons why it is undesirable to make the time constant excessively large when scanning the spectrum photoelectrically.

The spectral characteristics of low pressure lamps make it desirable that this type of lamp be efficiently used for depolarization measurements. It is necessary to employ a method of sample illumination which depends on total flux output of the source for the intensity of scattering if one is to use most effectively the low pressure type lamp. Menzies and Skinner[3] have recently described a new source arrangement which depends completely on flux output for its efficiency. The effectiveness of the Menzies and Skinner arrangement is obtained by the use of a cylindrical reflector coated with MgO which has a reflectivity of 97.8 percent at 4360A.†

It is immediately obvious that the light source arrangement of Menzies and Skinner[3] can be used for precise depolarization measurements if the method of Edsall and Wilson[4] is employed in conjunction with the

* This research was carried out on Contract N6onr-269, Task V, of the ONR.

[1] A. E. Douglas and D. H. Rank, J. Opt. Soc. Am. 38, 281 (1948).

[2] D. H. Rank and J. S. McCartney, J. Opt. Soc. Am. 38, 279 (1948).

[3] A. C. Menzies and J. Skinner, J. Sci. Inst. 26, 299 (1949).

† W. C. Price of King's College, London, had been using this source developed by Menzies and Skinner and has through private communication very kindly informed one of us (D.H.R.) concerning the excellent performance of his apparatus.

[4] J. T. Edsall and E. B. Wilson, Jr., J. Chem. Phys. 6, 124 (1938).

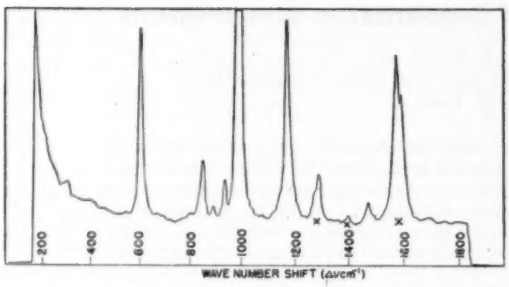

FIG. 2. Reproduction of record made with the photoelectric spectrograph of the Raman spectrum of benzene excited by means of the λ4358 group of mercury lines. Lines marked with an *X* are excited by λ4047 because of insufficient thickness of $NaNO_2$ filter. Slit width 12 cm^{-1}.

modifications described by Crawford and Horowitz[5] to render the light perpendicularly incident on the sample tube and reduce the convergence error to a relatively innocuous value. However, these baffles will also greatly reduce the efficiency of the extremely high reflectance diffuse reflector to an extent which would probably completely nullify the gain over use of a metallic reflector.

LIGHT SOURCE ARRANGEMENT

A source arrangement has been developed which incorporates most of the desirable features of various previously described sources. We shall show both theoretically and experimentally that good depolarization measurements can be made in a relatively simple manner. Light source, scattering tube and filter arrangement are shown, drawn to scale, in Fig. 1. This arrangement shown in Fig. 1 is surrounded by a cylindrical water-cooled metallic cylinder coated with MgO on its inside surface. The mercury vapor lamp is a "Toronto" type lamp constructed of Pyrex glass, the electrodes being water cooled as indicated in the figure.‡

The particular lamp shown in Fig. 1 operates on the 220-volt d.c. line with suitable ballast resistance and passes a current of 27 amperes with a voltage drop of 75 volts across the lamp. Since the lamp consumes 2 kilowatts, it is obvious that a large amount of luminous flux is produced. This flux has most desirable spectral characteristics since the lamp operates at low pressures. It can be seen that the geometry of the apparatus is such that the light source, which almost completely envelopes the scattering tube, is brought into the closest proximity to the sample, consistent with adequate filtering of the radiation. The effect of the MgO coated reflector is to increase the output of scattered light by a factor of 3 over that obtained without a reflector. We have made use of various filter and sample tube arrangements other than that shown in Fig. 1. Sample tubes of 10- and 35-ml capacity are commonly employed for work with the photoelectric spectrograph. For work at either low or high temperatures a Dewar flask with plane windows and suitable cooling jacket are substituted for the sample and filter arrangement shown in Fig. 1.

Figure 2 shows a reproduction of a photoelectric spectrogram of benzene, excited by λ4358 which was obtained with the source-sample arrangement shown in Fig. 1. The photoelectric spectrograph used was that described by Rank and Wiegand.[6] The galvanometer and photographic recorder formerly used were replaced by a 5-mv Brown electronic recorder operated from the same electrometer d.c. amplifier previously employed to drive the galvanometer. For the production of Fig. 2 the slit width used was 12 cm^{-1}. With smaller slit widths it has been possible to resolve three of the isotopic fine structure components of the totally symmetric vibration of CCl_4 (separation 3.1 cm^{-1}). The fine structure of the 992-cm^{-1} frequency of benzene has also been resolved with this apparatus.

Inspection of Fig. 2 shows that with the present apparatus the signal from the scattered light is sufficiently strong so that the gain of the electronic detection system can be kept much smaller than that required to produce a noise signal on the recorder with no light on the photo-tube. The light noise shown on the record arises from Rayleigh scattering of the continuous background radiation of the arc, parasitic light, and probably a small amount of fluorescence from the benzene sample. It should be pointed out that a.c. amplification would not remove this background scattering to the slightest extent since it would have the identical phase as the desired radiation. It should be observed that the 992 cm^{-1} frequency shift appears on the record Fig. 2 excited by the λ4358, λ4347 and λ4339 lines of Hg. The measured intensity ratio of these three lines in the present source under above quoted operating conditions is 115:2.7:1.0. With moderately high pressure commercial arcs, one would observe the 992 cm^{-1} frequency shift excited by λ4339 to have approximately the same intensity as the 847 cm^{-1} frequency shift excited by λ4358.

POLARIZATION MEASUREMENTS

It is immediately obvious that Edsall and Wilson's[4] method of measuring depolarization factors¶ will yield

[5] B. L. Crawford, Jr., and W. Horowitz, J. Chem. Phys. **15**, 268 (1947).

‡ Lamps of this type were developed by H. L. Welsh and M. F. Crawford at the University of Toronto and described in a paper delivered by Professor Welsh at the Montreal meeting of the Am. Phys. Soc. in 1947.

[6] D. H. Rank and R. Wiegand, J. Opt. Soc. Am. **36**, 325 (1946).

¶ This method consists in illuminating the sample circularly symmetrically with light polarized horizontally and then with light polarized vertically. The intensity of the completely depolarized scattered spectra are measured for each type of polarized exciting light and the ratio of the intensity of the spectra, i.e., corresponding lines yields the ρ for the line in question. The polarization of the incident light is achieved by means of polaroid cylinders with the polarizing axis suitably oriented to produce the desired type of polarized transmitted light. The polarizing cylinders are made to fit snugly to the outside wall of the scattering tube.

inaccurate results if applied directly to the apparatus shown in Fig. 1. The inaccuracy of the ρ-values will be occasioned by the fact that the polarized incident light does not impinge upon the sample perpendicularly to the axis of the sample tube. This so called convergence error will cause the observed value of the depolarization factor ρ_0, to be considerably larger than the true value ρ_t.

Placzek[7] has shown that for polarized incident light the intensity of radiation $I_{\parallel}$ scattered parallel to the direction of vibration of the electric vector of the incident light is given by

$$I_{\parallel}=6\gamma_{VV'}{}^2kI_0, \tag{1}$$

where k is a constant, I_0 the intensity of the incident light, $\gamma_{VV'}{}^2$ is the matrix element between the vibrational states V and V'.

The intensity of radiation $I_{\perp}$ which is scattered perpendicular to the direction of the incident electric vector is given by

$$I_{\perp}=(5A_{VV'}{}^2+7\gamma_{VV'}{}^2)kI_0, \tag{2}$$

where

$$\gamma^2=\tfrac{1}{2}[(C_1-C_2)^2+(C_2-C_3)^2+(C_3-C_1)^2]$$

and

$$A^2=(C_1+C_2+C_3)^2,$$

in which expressions C_1, C_2, and C_3 are the principle values of the polarizability tensor of the scattering molecule which is executing the vibration.

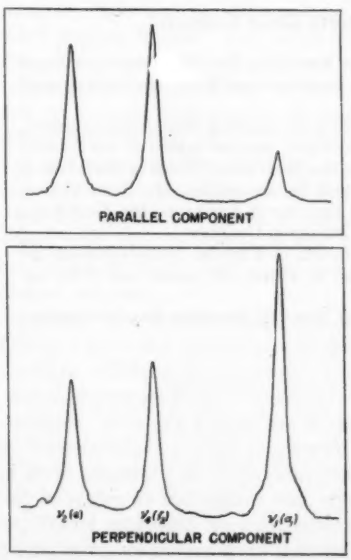

FIG. 3. Reproduction of records made with the photoelectric spectrograph of the strong lines of the Raman spectrum of CCl_4. The upper record was made with parallel polarized exciting light, the lower record with perpendicularly polarized exciting light.

[7] G. Placzek, Marx, *Handbuch der Radiologie* (Akademische Verlagsgesellshaft, Leipzig, 1934) Vol. VI, Part II, p. 205.

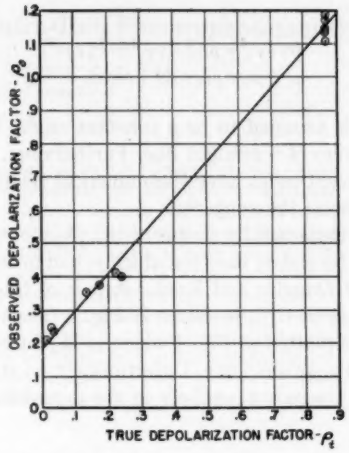

FIG. 4. A plot of the depolarization factors actually observed (ρ_0) for a number of Raman lines against the true value ρ_t. The curve shown in the figure is a least squares solution of the data.

The true theoretical depolarization factor ρ_t is given by

$$\rho_t=\frac{I_{\parallel}}{I_{\perp}}=\frac{6\gamma_{VV'}{}^2}{(5A_{VV'}{}^2+7\gamma_{VV'}{}^2)}. \tag{3}$$

It can be seen that when that polaroid cylinder is in position which restricts the plane of vibration of the electric vector of the incident light to planes perpendicular to the axis of the sample tube (i.e., horizontally polarized light) one actually observes the true value of $I_{\perp}$. It is easy to see that all the light transmitted by this polaroid cylinder is polarized horizontally regardless of its obliquity to planes parallel to the horizontal plane. The second polaroid cylinder whose function it is to produce vertically polarized light will only be able to perform this function when the incident light is perpendicular to the axis of the scattering tube. If the incident rays make an angle θ with planes parallel to the horizontal plane, the transmitted polarized light will consist of two components namely $I_0\cos\theta$ and $I_0\sin\theta$ which are polarized vertically and horizontally respectively.

An exact calculation of ρ_0 would involve exact knowledge of the distribution of intensity of all the rays inclined to planes parallel to the horizontal plane. From Fig. 1 it is obvious that we cannot make such a strict calculation. In order to calculate ρ_0 we shall make the most simple assumption possible, namely that all of the light is incident on the scattering tube at an average angle Θ with planes parallel to the horizontal plane. Making use of this assumption and Eqs. (1), (2), and (3) we obtain

$$\rho_0=\frac{I_{\parallel}\text{obs.}}{I_{\perp}\text{obs.}}=\frac{6\gamma_{VV'}{}^2\cos\Theta+(5A_{VV'}{}^2+7\gamma_{VV'}{}^2)\sin\Theta}{5A_{VV'}{}^2+7\gamma_{VV'}{}^2}, \tag{4}$$

since

$$6\gamma_{VV'}{}^2=\rho_i(5A_{VV'}{}^2+7\gamma_{VV'}{}^2)$$
$$\rho_0=\rho_i\cos\Theta+\sin\Theta. \quad (5)$$

Since Θ is assumed to be a constant angle, Eq. (5) is the equation of a straight line. Furthermore, the slope and intercept must have the numerical relationship of cos and sin of the angle Θ.

ρ_0 was measured by means of the photoelectric spectrograph for strong lines for which ρ_i had been obtained earlier by Douglas and Rank.[1] A pair of traces of the strong lines of CCl_4 is shown in Fig. 3. The results obtained are plotted in Fig. 4 where ρ_0 is plotted as ordinates and ρ_i as abscissae. Unfortunately no strong lines had been measured precisely in the ρ_i region of 0.3 to 0.8 and thus we do not know exactly whether ρ_0 values in this region will fall on the straight line shown in Fig. 4. A least squares solution of the data yields a value of 0.179 and 1.13 for intercept and slope of the straight line respectively. It can be seen that experimentally the expected sin and cos relationship between intercept and slope of the curve has not been quite realized. However, the agreement between theory and experiment is eminently satisfactory when one considers the unavoidable crudeness of the assumptions necessary to derive Eq. (5).

In conclusion, it is easy to see that very acceptable depolarization measurements can be made by the apparatus and method described in this paper by empirically constructing a correction curve which is of very simple form: namely, a straight line.

1950 Annual Meeting of the Inter-Society Color Council

ON March 8, 1950, in the Keystone Room, Hotel Statler, New York City, the 19th annual meeting of the Inter-Society Color Council will be held. Members of the Inter-Society Color Council's 19 member bodies are cordially invited to attend.

Committee discussions and the annual business session will be held in the morning. The afternoon session, arranged by representatives of the four design, decoration, and architect member bodies of the Council, will be held under the title, "Color as Used in Architecture, Design, and Decoration." Each of the following speakers will present the color viewpoint of practicing members of his association: Mr. Scott Wilson, American Designers' Institute; Mr. Waldron Faulkner, American Institute of Architects; Mr. Karl Bock, American Institute of Decorators; Mr. Egmont Arens, Society of Industrial Designers.

A dinner meeting, "I. S. C. C. Operation Rainbow," is being arranged by a special committee under the chairmanship of Mrs. Helen D. Taylor. In the evening Mr. Ralph M. Evans will present one of his unusually fine illustrated lectures, "Seeing Light and Color."

For further information address the Inter-Society Color Council, Box 155, Benjamin Franklin Station, Washington 4, D. C.

JOURNAL OF THE OPTICAL SOCIETY OF AMERICA VOLUME 40, NUMBER 2 FEBRUARY, 1950

Performance of a Double-Beam Recording Infra-Red Spectrophotometer

JOHN U. WHITE* AND MAX D. LISTON†
The Perkin-Elmer Corporation, Glenbrook, Connecticut

(Received October 17, 1949)

The performance of the Perkin-Elmer Model 21 Recording Infra-Red Spectrophotometer has been tested by measuring known spectra under a wide variety of operating conditions. A complete infra-red spectrum in the rock salt region can be recorded as a graph of percent transmittance *vs.* wave-length in less than 10 minutes. At slower speeds resolving power can be varied from the normal of 30 percent to 40 percent up to about 60 percent of the Rayleigh limit. For extreme resolution or stability, the r.m.s. noise level of 10^{-9} volts or 2×10^{-10} watts at the fastest response speed can be reduced as far as 2×10^{-10} volts or 4×10^{-11} watts by increasing the response time. The extreme ranges of the operating conditions are: response time, 4.5 to 110 seconds for full scale; scanning rate, 0.5 to 400 minutes per micron; chart scale length, 1 to 50 inches per micron; slit width, to give constant energy levels between. 01 and 2 r.m.s. microvolts full scale. The effects of scattered light and atmospheric absorption bands are less than 3 percent throughout. Operation is automatic after the conditions are selected and the instrument turned on. These features are illustrated in photographic reproductions of original records with more detailed data on the independent performance of the instrument's more critical parts.

INTRODUCTION

THE double-beam recording infra-red spectrophotometer described in the two previous papers[1,2] has been in operation for a period of nine months. During this time it has repeatedly been adjusted, tested, and altered until its performance appears to be close to the limit obtainable from an instrument of its design and components. The resolving power is close to the Rayleigh limit, the noise level approaches that of the Johnson noise in the thermocouple, and the speed of response is the best obtainable from available recorder motors. However, the low energy available from infra-red sources makes it impossible to combine these features simultaneously in high speed, stable recording at high resolution. Stability increases as more time is used to average out random fluctuations, so that smooth records can only be obtained by sacrificing resolution to get energy or by recording very slowly. When the resolution and stability are specified they determine the slit widths and speed of response. The scanning speed must then be chosen so that the wedge and pen have time to follow and record the spectrum with the desired accuracy.

Matched groups of operating conditions are shown in Table I, which gives the conditions necessary to follow most spectra within a few percent at all points. Required scanning time increases linearly with response time and inversely with slit width, the latter because more detail is resolvable in the spectrum with narrower slits. Noise level expressed as equivalent noise in the input circuit increases as the square root of the speed of response. When expressed as a percentage of full scale deflection, it varies inversely as the square of the slit width and inversely as the square root of the response time. The table is limited at the top by the maximum slit width and scanning rate, at the bottom by excessive noise, at the right by the slowest possible speeds of response and scanning, and at the left by the fastest response speed. Near the bottom of the table, the limit of the monochromator's resolving power is reached, and further reduction of slit width gives little additional detail in the spectrum. The combinations shown are useful for most purposes.

This performance has been evaluated in terms of speed, accuracy, stability, and versatility in measuring and recording infra-red spectra. The results show it to be generally superior to the performance previously reported for comparable single or double beam infra-red spectrometers.[3] The materials used to illustrate its performance were selected for their general interest and for the large amount of work that has already been done on them by others.[3] They were also chosen to show the special advantages resulting from the use of the double beam principle.

SCANNING SPEED

For survey work, when incomplete following of the spectrum is permissible, fast response and scanning speeds are used. For quantitative recording of the peak intensities of an absorption spectrum, wider slits, less gain and longer scanning times are useful. For accurate measurement of points on the sides of bands, even longer times are needed. For higher resolution and reasonable accuracy, narrower slits and much slower speeds are necessary. Scanning speeds are generally limited by the most detailed parts of the spectrum. The use of faster scanning speeds in other parts of the spectrum, made possible by the speed suppressor, may re-

* Present address: 90 Lincoln Avenue, Stamford, Connecticut—Consulting physicist and instrument designer.
† Present address: Liston-Folb Instrument Company, Post Office Box 1334, Stamford, Connecticut.

[1] J. U. White and M. D. Liston, J. Opt. Soc. Am. **40**, 29 (1950).
[2] M. D. Liston and J. U. White, J. Opt. Soc. Am. **40**, 36 (1950).

[3] For a survey of comparative results on other instruments and general information on infra-red spectroscopy the reader is referred to a review article by V. Z. Williams, Rev. Sci. Inst. **19**, 135 (1948).

TABLE I. Scanning rate and peak-to-peak noise level for different slit schedules and response times. Noise is expressed as percent of full scale and scanning rate in minutes per micron.

Response time for full scale deflection in seconds			4.5		14		38		110	
Slit schedule	Slit width at 10.5	Nominal energy in r.m.s. microvolts for full-scale deflection	Rate	Noise	Rate	Noise	Rate	Noise	Rate	Noise
1	0.328 mm	2	0.5	0.1	1	0.1	3	0.1	10	0.1
2	0.232	1	0.5	0.2	1.4	0.1	4.5	0.1	14	0.1
3	0.164	0.4	0.7	0.4	2	0.25	6	0.14	19	0.1
4	0.116	0.17	1	1	3	0.6	9	0.3	27	0.2
5	0.083	0.06	1.4	3	4	1.7	13	0.9	38	0.5
6	0.060	0.02					18	2.8	54	1.6
7	0.042	0.01							70	3.3

duce the total scanning time by about a half, depending on the nature of the spectrum.

The performance under survey conditions is illustrated by the benzene spectrum shown in Fig. 1. The sensitivity is 0.2 r.m.s. microvolts and the response time 4.5 seconds for full scale deflection. This gives a peak to peak noise level of approximately 1 percent of full scale deflection and permits recording all the major bands in the infra-red spectrum between two and fifteen microns in about 8 minutes. While the intensities of the bands are not exactly the same as they would be at a slower scanning speed, the breadth of the benzene absorption bands makes this record suitable for survey work and approximate analysis. Automatic suppression of the scanning speed was used in both this and the following spectra.

With a more detailed spectrum like ammonia, only slightly more scanning time is required. Figure 2 shows a record of its complete spectrum measured from 2 to 15 microns in 9.5 minutes. In this time the instrument was able to follow the individual absorption lines reasonably accurately, as is shown by the resolution of the doublet at 10.5 microns. The slits at this point were about 0.116 millimeters wide, giving a sensitivity of about 0.2 microvolts for full scale deflection.

The ethylene spectrum, because of its resolvable rotation lines, is particularly good for illustrating the selection of the best scanning speed. Figure 3 shows four records of its spectrum measured under identical conditions except for scanning time and degree of suppression. The slowest took 25 minutes and appeared to follow all the detail resolved in the spectrum. The 10-minute spectrum shows as many lines as the slower one, but because it does not quite follow at the peaks, it would be less suitable for quantitative transmission measurements. The 7-minute spectrum is obviously too fast for anything but survey work. These three spectra were measured with uniform scanning rates. In the fourth, requiring only 5½ minutes, the automatic scanning speed suppression was used. In this case, the wave-length drive motor was automatically slowed down whenever the pen and wedge failed to follow the details in the spectrum. This spectrum shows better following of all the individual lines in the bands than the 7-minute one and appears comparable to the 10-minute one. Its performance is slightly better than the latter for the stronger absorption lines around 10 and 11 microns but slightly worse for the weak ones near 5 microns. This spectrum is suitable for survey work and semi-quantitative analyses. In general, the speed suppression is more effective for strong bands that produce appreciable off balance signals. With the use of suppression, the scanning time for the complete spectrum depends on the nature of the spectrum, being most effective when sharp bands are present.

I_0 STABILITY

A blank spectrum recorded without a sample is included in Figs. 1 and 2 to show the flatness of the I_0 line. Between 6 and 15 microns it departs less than ±1 percent from a level line. At shorter wave-lengths it drops off gradually until it is 2 percent low at 2 microns. The atmospheric water vapor and carbon dioxide bands are present only to about 1 percent, even though the optical path for this experiment included 20 inches of room air in each beam. The rest of the path was enclosed and desiccated with sodium hydroxide pellets.

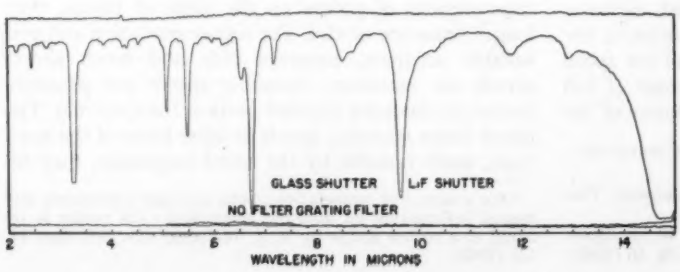

FIG. 1. Benzene spectrum showing I_0 and scattered light using grating filter; 0.025-mm cell, 0.2μv full scale, 8 minutes per run.

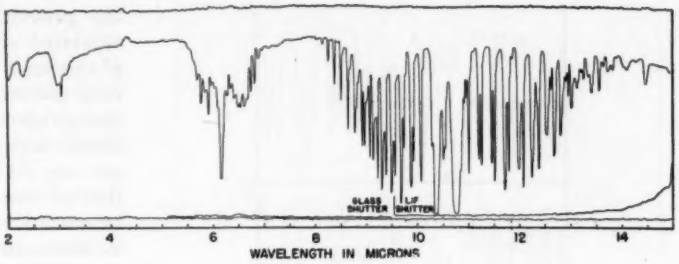

FIG. 2. Ammonia spectrum showing scattered light without filter; 0.2μv full scale, 9½ minutes per run.

When the whole path was exposed to room air, good compensation for the atmospheric bands was impossible.

SCATTERED LIGHT

The amount of scattered light in the monochromator is shown in Figs. 1 and 2. The benzene spectrum was measured using the grating filter to remove scattered light at wave-lengths longer than 7.5 microns. The filter was not used for the ammonia spectrum. In each, the amount of scattered light was measured with a glass shutter from 5 to 9.5 microns and with an LiF shutter from 9.5 to 15 microns. The two curves show that at 14.9 microns there was 12 percent of scattered light in the instrument without the filter and 2.3 percent with it. The reliability of the LiF shutter in determining scattered light can be checked by the intense long wave-length absorption band of benzene, which indicates the presence of 3.5 percent of scattered light when the filter was used. The 1.2 percent difference between this and the LiF shutter measurement represents scattered light not transmitted by the shutter, i.e., partially reflection losses on the shutter and partially scattered light of wave-lengths greater than 6 microns. If the total scattered light decreases with wave-length at the same rate as that measured with the LiF shutter, it becomes less than ½ percent at wave-lengths shorter than 13 microns.

RESOLUTION

The resolution of a spectrometer is limited by the size and dispersion of the prism and by the slit width necessary for adequate speed and stability. To get high resolution approaching the Rayleigh limit, the slits must be closed until the thermocouple voltages are extremely small. For fast scanning the slits are opened until the effective resolution is about a third of the theoretical limit for the prism. They are controlled by a cam that may be adjusted stepwise over a wide range of incremental factors of the square root of 2 in width, giving thermocouple voltages differing by factors between two and three from 2 to 0.01 microvolts for full scale deflection. The use and effect of this variable is illustrated in Fig. 4, which shows five spectra of the center of the 10 micron ammonia band measured at different resolutions. The slits in each case were varied continuously throughout the run, being adjusted to give energy levels of 0.4, 0.17, 0.06, 0.03, and 0.01 microvolts for full scale deflection. The slit widths at 10.5 microns were 0.164, 0.116, 0.083, 0.060, and 0.043 millimeters. The closest resolved pairs of lines are indicated on the first three curves. The resolution is obviously better on each of the next two curves. On the fifth a single line indicates another absorption line that has been well resolved. Because of the slope, the positions of the lines on each side of it are not obvious. The separations between these lines is about 1.8 cm^{-1}. The individual lines between 10.4 and 10.5 microns are separated by about 1.5 cm^{-1}.[4] While they are not clearly indicated in this figure, they have occasionally been observed. The theoretical resolution for 2 traversals of a 75-mm rock salt prism at this wave-length is 1 cm^{-1}.

In recording this group of curves, it was necessary to make other compensating adjustments to correct for the reduction in energy when the slit widths were reduced. Increasing the gain to compensate for the loss in energy increased the noise level proportionately. To maintain a reasonable noise level and following accuracy, both the response time and scanning time were increased.

WAVE-LENGTH SCALE

The spectra are recorded on a uniform wave-length scale that can be adjusted in length to suit the features of the spectrum being measured. The scale of 2 in.

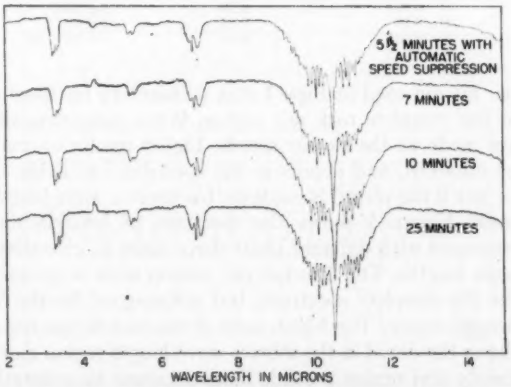

FIG. 3. Ethylene spectrum measured at different speeds; 10-cm gas cell, 0.3μv full scale.

[4] Private communication from Darwin L. Wood.

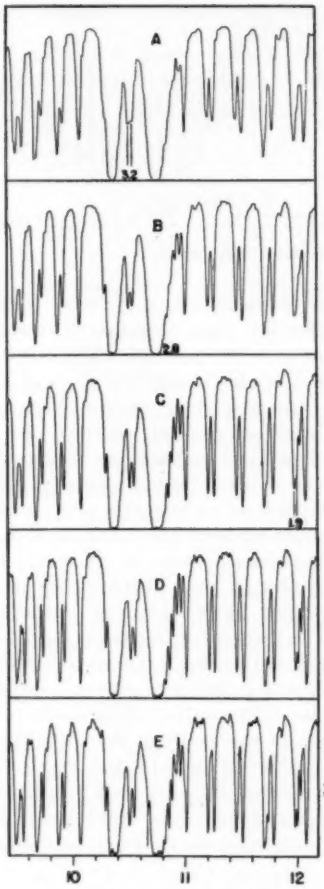

FIG. 4. Resolution of the 10μ ammonia band at different slit widths.

	Slit width at 10.5	Energy full scale	Time per micron
A	0.164 mm	0.4	42 sec.
B	0.116	0.17	2.6 min.
C	0.083	0.06	9.5 min.
D	0.60	0.03	1.2 hr.
E	0.042	0.01	5.2 hr.

per micron used in Figs. 1–3 is satisfactory for spectra of the complete rock salt region. When measurements are made at the slower speeds, higher resolution may be obtained, and details in the spectrum are liable to be lost if the record is made on too short a wave-length scale. Figure 5 shows the spectrum of benzylamine measured with different chart drive gears to give three scale lengths. The 2 inches per micron scale is suitable for the complete spectrum, but not so good for the 3-micron region. The 5-inch scale of the middle spectrum shows the detail in the shorter wave-length region more clearly and makes possible more accurate wave-length readings. This is the scale used in the ammonia spectra of Fig. 4. The lowest spectrum shows the 3-micron region expanded to 10 inches per micron. On this record, the individual hydrogen valence vibrations are well separated and easy to identify. Additional expansion of this scale is possible up to 50 inches per micron but does not seem justified with a rock salt prism. The bottom spectrum was measured with narrower slits and slower response than the other two in order to bring out any additional detail that might exist. The fact that no new bands are isolated even though they are known to exist from high resolution measurements indicates that the slit width is not limiting the resolution at this wave-length. The other extreme from these expanded scales is one of 1 inch per micron, giving a total length of 14 inches for the spectrum from 1 to 15 microns. If small records are desired to simplify reproduction and filing, they may be made on this scale by changing the size of the pulley on the pen drive and using half the chart as full scale to give records approximately 5 in. $\times$ 14 in. Naturally, this size does not give the same accuracy as the regular size.

COMPENSATION FOR SOLVENTS AND SCATTERING

In a double beam spectrophotometer, the absorption by a solvent in a solution may be compensated for by placing the proper amount of the solvent in the reference beam. The instrument then records the spectrum of the impurity free from the spectrum of the solvent. Figure 6 shows this type of operation with nujol taken as the solvent and 25 percent of toluene added as the solute. The lowest spectrum is that of nujol alone, the next above it nujol plus 25 percent toluene, the next the same amount of toluene alone, and finally at the top, the spectrum of 25 percent toluene in nujol compensated with the same amount of nujol in the reference beam. This spectrum is obviously adequate to identify the toluene and to determine how much is present. It

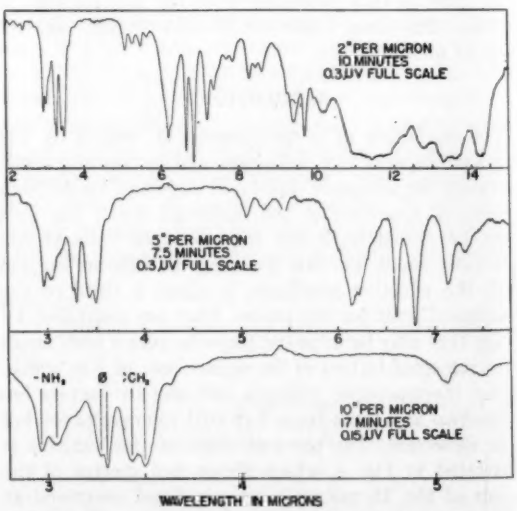

FIG. 5. Infra-red spectrum of benzylamine on three different wave-length scales.

shows that all except the strongest nujol bands have been eliminated, the more conspicuous corrections being around 2.5, 8.5, 10.5, and 13 microns. At 3.5, 6.9, and 7.3 microns, the nujol bands absorbed so much of the light that the instrument became inoperative, and not only were the bands removed but aslo the toluene bands in the region were concealed.

These bands illustrate a serious problem in measuring differential spectra. If too much energy is absorbed from the reference beam, the off-balance signals become too small to operate the pen motor and the instrument becomes dead. This can be overcome by readjusting the amplifier gain or by making the instrument's response less sensitive to energy level. A further discussion of the permissible range of energy level and the effects of changing it is given below in the section on noise.

Figure 7 shows another spectrum of one component in a mixture isolated by the use of a compensating cell

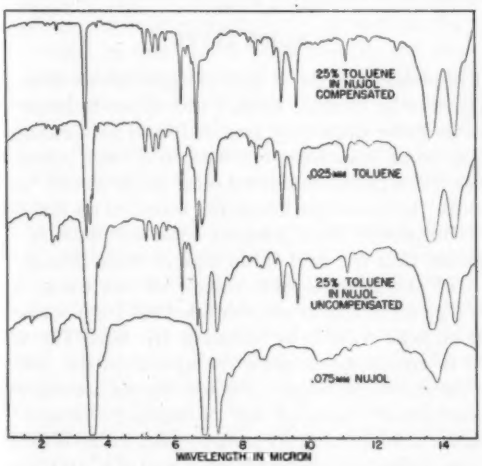

FIG. 6. Compensation of solvents; 0.5mμv full scale, 8–9 minutes per spectrum.

in the reference beam. The top spectrum is that of a penicillin null in nujol; the middle one is the same sample slightly over-compensated with nujol in the reference beam; and the bottom one is the spectrum of the nujol that was used to compensate the middle one. The effects of removing the two nujol bands near 7 microns are clearly seen. Good operation was obtained throughout this region. The penicillin spectrum in the 3.6 micron region was largely concealed by the strong C—H absorption of the nujol, even though it was pretty well compensated. The upward bend of the spectrum on the long wave-length side of this band probably indicates overcompensation by the use of too much nujol. The adjustment of the amount of nujol in the reference beam was quite difficult for the thin layers that were necessary.

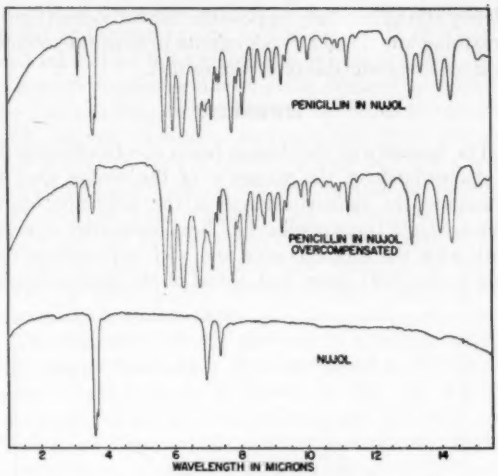

FIG. 7. Compensation of solvents; 0.5μv full scale, 8–9 minutes per run.

The same principle can be applied to permit partial compensation for scattering in a powder sample by use of a ground salt plate in the reference beam.

FIXED WAVE-LENGTH RECORDING

In addition to its use in scanning spectra, the instrument may be operated at a fixed wave-length to record changes in a stream of sample flowing through an absorption cell. An illustration is given in Fig. 8 where the wave-length was set to the 4.3-micron carbon dioxide absorption band and the operator breathed through the absorption cell. The instrument followed the carbon dioxide content in the breath, plotting the changes continuously, including the irregularities. In the middle spectrum, breathing was controlled voluntarily at 15 per minute to show how the instrument followed a changing signal of this frequency. The timed breathing was deeper to flush out the absorption cell more com-

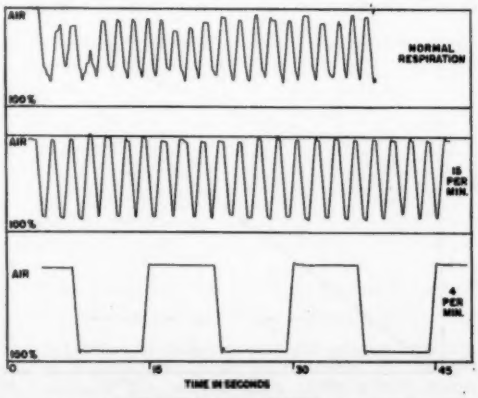

FIG. 8. Fixed wave-length absorption by CO_2 in breadth with 10-cm cell.

pletely and as regularly as possible. In the bottom figure, breathing was timed at 4 per minute to show the smoothness and reproducibility of the record.

LINEARITY

The linearity of the double beam spectrophotometer is determined by the accuracy of the wedge used to attenuate the radiant energy in the reference beam. The wedge's transmission has been measured directly both with the thermocouple and with a photronic cell held in the light beam just ahead of the thermocouple.

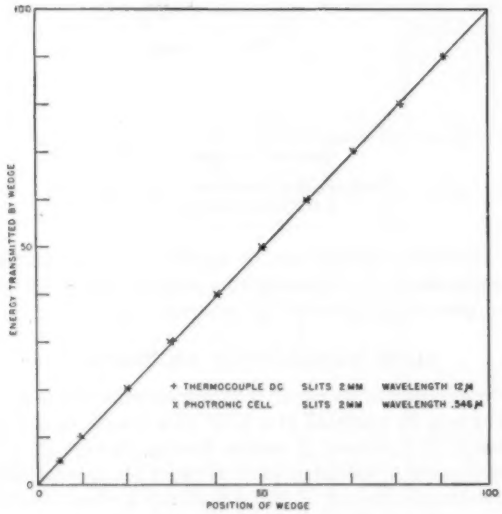

FIG. 9. Linearity of wedge aperture.

For the photo-cell measurements a 10-ohm load resistance was used. In each case the output voltages were measured potentiometrically at very low light levels with a breaker amplifier and meter as the null indicator. Figure 9 shows the relationship between comb position and the energy transmitted by it. The data indicate the comb to be linear within a few tenths of a percent. Measurements at a number of different wave-lengths and slit widths show no systematic variations.

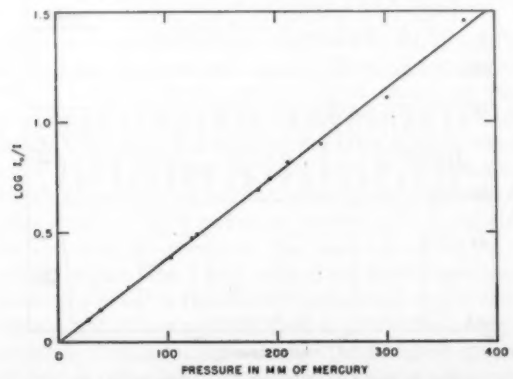

FIG. 10. Linearity in measuring 6.8 propane absorption band.

The linearity of the whole instrument has been tested by measuring the intensity of the 6.8-micron absorption band of propane at a number of different pressures. In Fig. 10 the values of $\log I_0/I$ calculated from these measurements are plotted against pressure. The departures from the straight line in this graph appear to be random and all correspond to less than 1 percent error in transmission. The mean departure from the line for all the points corresponds to 0.3 percent in transmission.

More important than linearity is the ability of the spectrometer to reproduce its readings from one time to the next. Figure 11 shows two repeat runs of the isooctane spectrum in the region from 6 to 14 microns. The records are within a few line widths of each other at all points, indicating that with suitable adjustment and calibration very accurate measurements are possible.

NOISE LEVEL

The principal cause of instability of the recorder pen appears to be random noise. Other types of instability such as those caused by zero drift and gain change in single beam spectrometers have not been observed. Noise levels can be measured most easily as the "peak-to-peak" height of the instability recorded on the chart. For comparison with Johnson noise calculations, it is assumed that the root mean square noise level is one fifth of the peak-to-peak value. All the r.m.s. noise levels given in this paper were derived from measured peak-to-peak values by dividing by five. The units used to express r.m.s. noise are equivalent d.c. volts in the thermocouple circuit. The test signals are expressed as the r.m.s. values of the alternating voltages. To measure a noise level, its peak-to-peak value is divided by the deflection produced by a unit a.c. test signal, multiplied by 2.8 to convert from the r.m.s. test signal voltage scale to the d.c. voltage scale, and divided by five to convert from peak-to-peak to r.m.s. noise. This value may be further converted to equivalent noise input by dividing by five, the thermocouple's sensitivity in volts per watt.

Figure 12 is a record of detector and amplifier performance at the four different speeds of response. It shows the noise level, the time of a seven-inch deflection for a 0.018-microvolt test signal and the equivalent noise expressed as microvolts output from the thermocouple and as watts of radiant energy on the thermocouple. The gain and chart speed are the same throughout, the only changes being in the electrical filtering and in the mechanical speed reduction between the balance motor and the comb. With speed reduction ratios changing by steps of 3, times of response were measured corresponding to 4.5, 14, 38, and 110 seconds for full scale deflection.

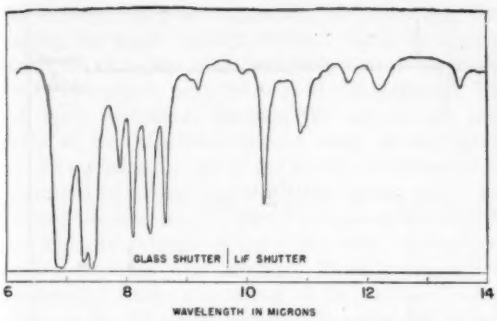

FIG. 11. Two repeat runs of isooctane spectrum showing I_0 and scattered light using grating filter; 0.1-mm cell, 0.4μV full scale, 5 minutes per run.

The relationship between amplifier gain, speed of response and noise is important. The pen balancing system includes a closed servo loop operating through the wedge, light beam, detector, amplifier and balance motor, and has the general properties of such servo loops. Its response characteristics depend on the loop gain, which in this case is adjustable by the amplifier gain control and by the monochromator slit width. At low gains, the response is sluggish and liable to have a dead spot. At high gains, the response becomes fast and jumpy until the system finally breaks into oscillation. The best operating point is between these extremes.

The effect of changing the amplifier gain is illustrated in Fig. 13 for each of the four response speed settings. Each curve shows how the high gain at the upper left end produces a high noise level. Curve 1, for the fastest response speed was not carried higher because of oscillation. As the gain is reduced along each curve, the noise level goes down without loss in response speed until a critical point is reached. Further reduction in gain reduces the noise less rapidly and causes a great increase in the response time. The best operation is obtained at the bend point in the curves. If less gain is used for further noise reduction, the operation is likely to become unreliable due to static friction. In addition the speed of response and hence the required scanning speed are very dependent on the energy level. The only time when this type of operation may be trusted is for short spectral intervals when enough noise is present to keep the pen from sticking. This is illustrated in Fig. 4E, where the gain was reduced to about half of that in Fig. 4D. The noise at the same energy level was reduced by about a half, and the required scanning time increased about five times.

The response curve of the pen to a sudden impulse is a straight line with a little curvature as the balance point is approached, as shown in Fig. 12. For the calculation of noise levels and response times in curve tracing, only the part of the response curve near balance is significant, as large off-balance signals do not occur. As the response curve appears to be roughly exponential for small deflections, time constants have been calculated as half the time required for a 5-division deflection. The Johnson noise calculated on this assumption for a ten-ohm thermocouple at 40°C is shown in Fig. 13 as a straight line with a slope of one-half. The observed noise levels at the most favorable gain settings are all less than 1.5 times the Johnson noise, indicating that little further reduction in noise is possible.

The relationship between the energy falling on the thermocouple and the noise and response properties at fixed gain is different from that shown in Fig. 13. As this determines the amount of absorption by a solvent that may be compensated for by the use of the solvent in the reference beam, it is illustrated in Fig. 14. This shows a group of noise level runs at different known energy levels. On each run transient impulses

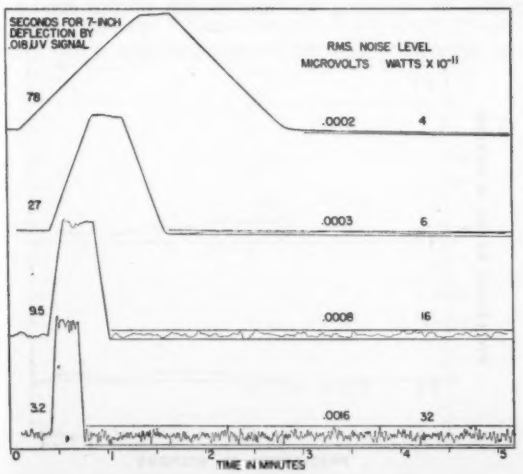

FIG. 12. Noise level and speed of response.

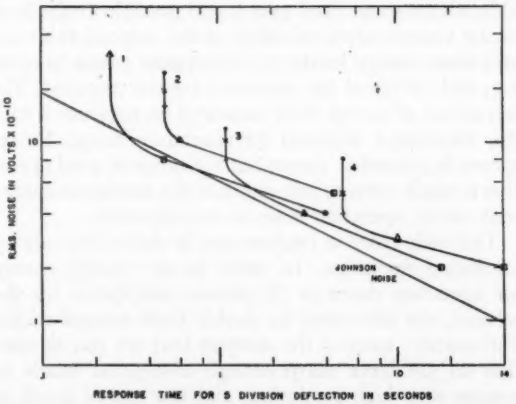

FIG. 13. Effect of change in amplifier gain on noise level and speed of response. The curves are numbered for their response speed settings. The relative gains of the plotted points are: ●, 100 percent; ×, 88 percent; +, 57 percent; △, 37 percent; □, 19 percent; ○, 9 percent.

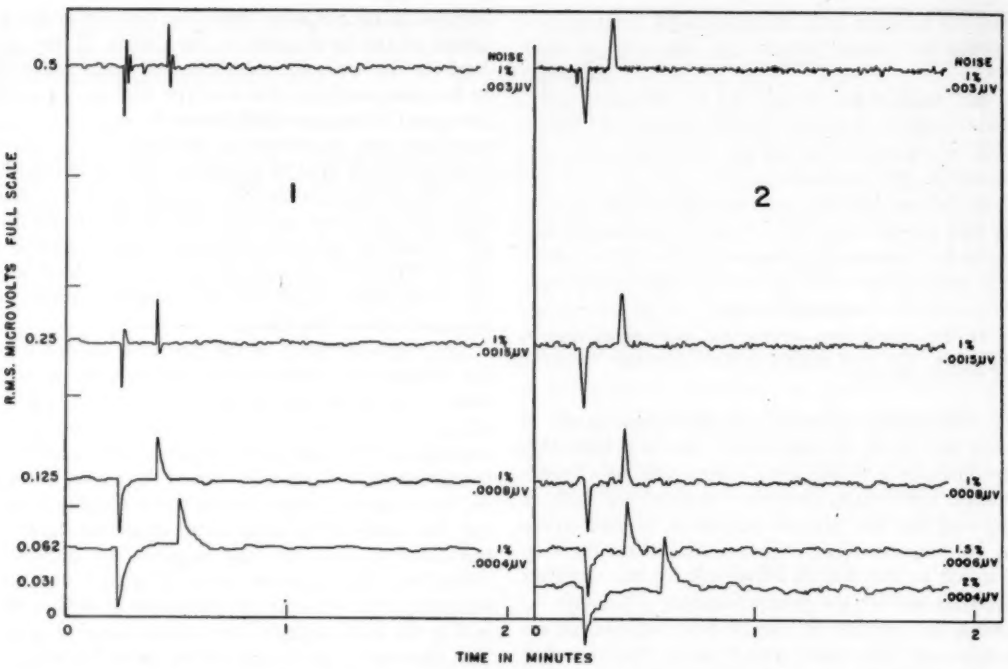

FIG. 14. Noise and response to transient impulses at fixed gain and different energy levels. Response 1 is adjusted for minimum noise, response 2 for maximum range of operability. Percent noise is peak-to-peak percentage of full scale. Microvolt noise is r.m.s.

are included to show the speed and nature of the response. The first set of curves was measured on response 1 with the instrument adjusted for minimum noise. With the gain set to the maximum permissible for the energy level of the top curve, good response to transient impulses in each direction was possible when the energy fell to a quarter of its initial value. The top curve is on the verge of hunting. Slower operation probably with a small dead spot is still possible at the level of the lowest curve, an eighth of the original value. At still lower energy levels, the instrument ceases to operate, and details of the spectrum are not recorded. The second set of curves were measured on response 2 with the instrument adjusted for maximum range. Its response is somewhat slower but the range of good operation extends down to one-eighth of the maximum energy with slower operation down to one-sixteenth.

This wide range of performance is obtainable only by sacrificing resolution. In order to get enough energy for operation down to 75 percent absorption by the solvent, the slits must be double their normal width. Fortunately, most of the samples that are run in solution do not have sharp enough absorption bands to require very high resolution, and the loss of detail in the spectrum resulting from the use of wide slits is not too serious. Approximate measurements similar to those shown in Fig. 14 indicate that depending on the electrical filter used, the slower speeds of response have a wider range of permissible operation and less tendency to hunt at high energy levels.

WAVE-LENGTH AND SLIT CAMS

The wave-length cam and its adjustments are designed to permit the use of prisms whose apex angles differ slightly from the nominal 60°. The resulting small variations in the total length of the spectrum are corrected by changing the arm length of the cam fol-

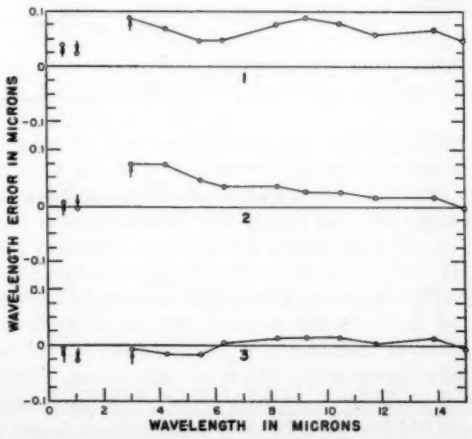

FIG. 15. Adjustment and performance of wave-length cam.

lower between its point of contact and its pivot, thus changing the angle through which it turns for a given amount of cam rise and correcting the wave-length scale at two points near the ends of the spectrum. The small error introduced because the cam is not used exactly at its calculated contact angle is not significant. An additional point in the middle of the spectrum is corrected by adjusting the Littrow mirror angle. For adjusting the arm length, the 15 micron carbon dioxide band and the average of the 1.014 and 1.129 micron mercury arc lines were selected. These points fall at wave-lengths where the slopes of the cam are equal, and hence the difference in their indicated wave-lengths is independent of small errors in the Littrow mirror angle. For setting the mirror angle, the mercury green line and the 3-micron branch of the ammonia absorption band are used. This adjustment is fairly independent of small errors in the arm length. Figure 15 shows the wave-length errors remaining when the cam is adjusted as well as possible and the errors present after the last two previous approximations in the adjustment. In the top curve, the Littrow arm is too long and the mirror angle is incorrect. In the middle curve, the arm length has been adjusted until the errors are equal at the two wave-lengths indicated by the arrows pointing down, but the mirror angle has not been changed. In the bottom curve, adjustment of the mirror angle has removed the error at the wave-lengths indicated by the arrows pointing up, but has thrown the other adjustment slightly off. Further adjustment does not appear practical, as any change would merely redistribute the residual errors.

The performance of the slit cam is indicated in Fig. 16, where the energy equivalent to full scale deflection, neglecting atmospheric absorption bands, is plotted as a function of wave-length for 6 different settings of the resolution control. For slit schedules 2, 3, 4, and 5, the maximum range of energy in each is less than a factor of 2. For schedule 1, the energy range is three times and for schedule 6, it is four times. Schedule 7 could not be measured accurately because the energy was less than the smallest test signal. The total range of energies included by the six slit schedules at 10 microns is about 100. As the slit widths change by the square root of two between each schedule, the energy change might be expected to be 32 instead of 100. As this factor is approached fairly closely at the longer wave-lengths and wider slits, the difference may be due to energy losses at narrow slit widths, such as those due to diffraction and to a "tunnel vision" effect caused by the finite width of the edges of the slit jaws.

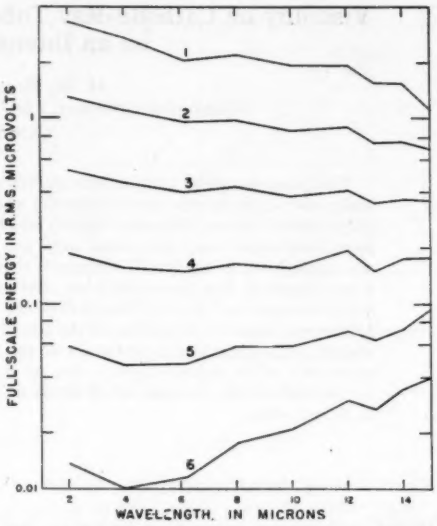

FIG. 16. Spectral energy distribution for six different settings of the slit cam.

ACKNOWLEDGMENTS

In conclusion of these three papers, the authors wish to thank the American Cyanamid Company and the Esso Laboratories for samples, to acknowledge the help of George Brueske in the design of the new instrument, and to thank the other members of the Perkin-Elmer Corporation for their help in constructing and testing it.

Visibility on Cathode-Ray Tube Screens: Positive *vs.* Negative Signals on an Intensity Modulated Scope*

M. W. Harriman and S. B. Williams
Psychological Laboratory, The Johns Hopkins University, Baltimore, Maryland
(Received October 6, 1949)

This paper compares two methods of presenting targets on CRT screens of modern radar. One method makes use of grid targets (positive signals) which appear brighter than their background, and the other employs cathode targets (negative signals) which appear darker than their background. Data were collected from three subjects on a very small target and on one of moderate size. A third target, intermediate in area, was studied, but in less detail. The results show: (1) The visibility of a cathode target is better than that of a grid target at bias levels which are relatively bright. The amount by which cathode targets are more visible is from 1 to 9 db. (2) There is evidence that the dimmest bias at which the cathode target is superior to the grid target is a function of the size of the target. (3) The optimal bias for a very small target is shifted to a brighter level by about a volt and a half when target voltage is injected at the cathode. (4) The superiority of the cathode target is due, not to any inherent advantage of dark-on-light targets, but rather to a property of the phosphor which allows the phosphor to work on a portion of its response curve favorable to human vision.

I. INTRODUCTION

THERE are two ways in which a signal (pip) may be displayed on the cathode-ray tube screen of an intensity modulated radar scope. The usual method is to put the signal voltage on the grid of the *CRT*, thus producing a pip which appears brighter than its background. The other technique, one which has not heretofore been tested in any systematic manner, is to inject the signal voltage at the cathode. This produces a pip darker than its background. The study reported here compared the visibility of the two kinds of targets at various levels of background brightness (volts bias). The *CRT* screen used for the experiment is an intensity modulated *PPI* (Plan Position Indicator), a type commonly employed in modern radar. The screen is 7 inches in diameter, and is coated with a *P*-7 phosphor.

A study by Williams, Bartlett, and King[1] on the light output of a *P*-7 phosphor as a function of *CRT* bias is relevant to this problem. Results obtained by these investigators show that successive increases in the logarithm of brightness grow continuously smaller as bias is reduced; or in other words, with continued reduction in bias the phosphor screen approaches saturation. The curve, then, is a negatively accelerated one.

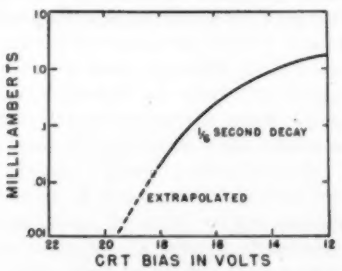

FIG. 1. Brightness of the phosphor screen measured one-sixth second after electrical excitation. (See reference 1.)

The brightness characteristics of the phosphor as described by this curve (Fig. 1) have an important bearing on what can be gained by using negative signals. If, for example, a signal is introduced at a bias level represented along the lower or steeper section of the curve, the brightness increment concomitant with an increased flow of electrons (positive signal) will be about equal to the decrement accompanied by a reduced flow of electrons (negative signal). However, for a voltage applied at a bias represented along the flatter portion of the curve, the brightness decrement attending a reduced flow of electrons will be greater than the increment accompanying an increased flow. Furthermore, the brighter bias levels represented by the flattened portion of the curve are approaching light levels at which the eye is most sensitive. Therefore, an improvement in the visibility of a signal might be expected if its voltage were injected at the cathode.

II. APPARATUS AND PROCEDURE

A detailed account of the apparatus and experimental conditions may be obtained elsewhere.[2] The radar parameters for this experiment, however, were as follows: sweep rotation rate, 20 r.p.m.; pulse repetition rate, 667 p.p.s.; distance of target from center of the scope, half the scope's radius. The screen background was fairly uniform; no video noise was added to the signal.

Three target sizes were used: (a) 1-microsecond pulse length and 1-degree beam width; (b) 2-microsecond pulse length and 2-degree beam width; (c) 7½-microsecond pulse length and 10-degree beam width. Here-

* This research was carried out under Contract N5ori-166, Task Order I, between Special Devices Center, Office of Naval Research, and The Johns Hopkins University. This is Report No. 166-I-102, Project Designation No. NR-784-001, under that contract.

[1] Williams, Bartlett, and King, J. Psychol. **25**, 455 (1948).

[2] S. B. Williams and N. R. Bartlett, J. Psychol. **25**, 401 (1948).

after the targets will be referred to as small (a), medium (b), and large (c). The angular subtense of the small target was 3′29″ by 7′31″, that of the medium target 6′56″ by 14′58″, and that of the large target 26′6″ by 74′52″. The targets were viewed at a distance of 12 inches.

Eight-volt signals were used. They could be attenuated by telephonic instructions to the experimenter's control room. The attenuation system at the disposal of the experimenter could attenuate accurately any signal up to 99 db in ½, 1, or 10-db steps.

III. PROCEDURE

The psychophysical method used was an adaptation of the method of average error. A trained observer adjusted a signal in intensity until he was satisfied it was just barely visible. The strength of the just visible trace in decibels of attenuation below the initial 8-volt strength was the basic datum of the experiment.

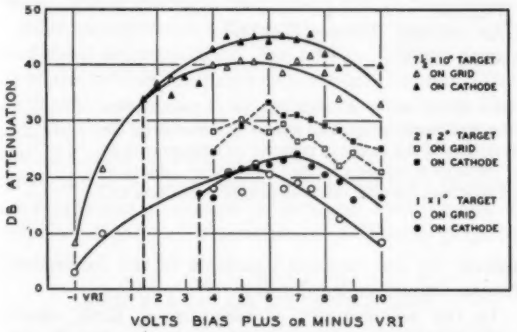

FIG. 2. Visibility of large and small targets when displayed as positive and negative signals. Curves represent attenuation of an 8-volt signal strength at which signal was just visible.

Data were obtained from three observers. The experimental routine was varied only slightly in the 10-day period needed to collect the data. In a typical session each subject observed targets of two sizes. He observed each target at four bias voltages, and at every bias he observed each target as a grid target and also as a cathode target.

At the beginning of every session a visual reference intensity (*VRI*) was obtained by having the observer dark adapt and then adjust the bias until the sweep line was just visible. This bias was taken to be the *VRI*, and the bias voltages for the session were determined by adding voltage to, or subtracting voltage from, the *VRI*. This procedure was adopted because previous experimental work done at this laboratory has shown the *VRI* to be a stable reference for individual observers, and relatively free from the effects of equipment variability.

At least 12 bias voltages were used for the small target and the large. The medium target was not studied in as great detail, and the bias voltages at which it was observed were fewer in number.

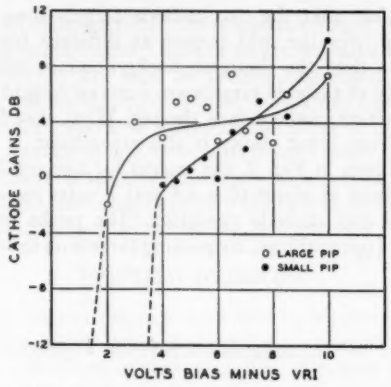

FIG. 3. Gains in visibility of negative signal over positive signal.

IV. RESULTS

The results of this experiment are plotted in Fig. 2. The curves in the upper portion of the figure are for the large target, while those in the lower part are for the small target. In these two sets of data, points for biases of plus 4 and 7.5 volts inclusive are means of eight observations; the other points are means of four observations. The third pair of curves, computed from a few observations of the medium target were obtained merely for the purpose of ascertaining where, in relation to the other two, a target of intermediate size would fall. The conclusions drawn from the experiment are based principally on the smallest and largest targets studied.

Previous studies[1,2] have shown that high brightnesses on cathode-ray screens are favorable to visibility. Figure 2 shows clearly that at such brightnesses negative signals are more visible than positive signals. In fact at brightnesses at which there is high visibility of the conventional positive signal, visibility is still further increased by 3 to 8 db with the use of negative (cathode) signals. At the dimmer biases, on the other hand, cathode operation is less efficient than grid operation. The large target could not be seen when the bias was lower than 1.5; the small target was not visible below a bias of 3.5.

The data in Fig. 2 can be used to calculate db gains for cathode operation by computing the mean db difference between each kind of target at each bias level. The results of these computations are shown in Fig. 3. Certain differences in the two functions are apparent. For the small target the positive and negative signals are equally visible at about 5 volts above the *VRI*. At biases brighter than that the cathode target is increasingly advantageous, varying in amount from 1 to 9 db. For the large target, however, cathode operation is superior to grid operation at biases much closer to the *VRI*. As the background is made brighter the cathode advantage increases in a somewhat irregular manner.

The fact that the two cathode targets show an advantage over the grid targets at different bias levels suggests that the dimmest background at which the visibility of cathode targets are superior to grid targets is a function of the size of the pip. What that function is, however, is not shown in this experiment.

As shown in Fig. 2, the curves for the small target show peaks at about plus 5.5 and 7 volts respectively for grid and cathode operation. The peaks represent points of optimal bias. By putting targets on the cathode the optimal bias has been shifted toward a brighter level by approximately a volt and a half. It may be noted here also that visibility at the optimum bias for cathode targets is better than visibility at the same bias for the grid target. No such well-defined peaks can be seen in the curves for the large target. Rather, best visibility is evident over a range of biases. However, the bias at which visibility begins to grow poorer for the negative signal is brighter than that for the positive signal.

JOURNAL OF THE OPTICAL SOCIETY OF AMERICA VOLUME 40, NUMBER 2 FEBRUARY, 1950

Objectives and Methods of Density Measurement in Sensitometry of Color Films*

FRANKLIN C. WILLIAMS
Kodak Research Laboratories, Eastman Kodak Company, Rochester, New York
(Received November 14, 1949)

Density measurements used in the sensitometry of color films can be divided into two broad classes: Integral densitometry, which provides a description of the multilayer image as a whole in terms of its absorptions; and analytical densitometry, which gives a description of the image in terms of its components by determining their individual density values. Each class contains subclasses formed by special definitions of density. Terms and units are defined for each class and subclass; for each one, the field of usefulness and methods of measurement are briefly discussed.

SENSITOMETRIC testing plays an important part in controlling the manufacture, the processing, and in many cases the use of film for color photography. Its undoubted success in the field of black-and-white photography has led to the reasonable expectation that it would help solve the grave problems met in the introduction and expansion of color photography. To a limited but broadening extent, it has done so. It has been particularly useful in operations with multilayer subtractive color films, those in which (usually) three differently sensitized layers, coated on the same supporting base, form three differently colored dye images, one of which is primarily red-absorbing, another is primarily green-absorbing, and the third primarily blue-absorbing.

The purpose of sensitometric testing is to determine relationships between photographic images and the factors which affect their formation. If the established relationships are to be of much value, they must be expressed quantitatively. The sensitometric method of determining and expressing such quantitative relationships involves exposing the film to known amounts of light of known quality, processing the exposed film through the required developer or developers and other solutions, and obtaining measurements of the light-absorption properties of the developed images. Since, in black-and-white sensitometry, the silver image absorbs light of all visible wave-lengths nearly equally, its light-absorption can be expressed by a single number, usually by the common logarithm of the reciprocal of transmittance, called density.

In the sensitometry of silver-image films, density originally was intended not only to express the effectiveness of the silver deposit as a light-absorber, but also to be a measure of the amount of silver contained in the image. Now, also in the sensitometry of films used in color photography, density is the unit most often used in sensitometric description of the image, and here again densities are used to express both the effectiveness of the deposits as light-absorbers and the amounts of colorants contained in the images. But the problems of measuring the dye images of color films are more difficult than those encountered in measuring the silver images of black-and-white films. The dye images of color photography are highly selective with respect to wave-length. Their usefulness depends upon their spectral selectivity, and the measurements which must be made of these images must take proper account of it. The specification of what constitutes "proper account" defines the objectives of color densitometry.

FUNCTIONAL CLASSIFICATION OF COLOR DENSITOMETRY

Sensitometry has two main purposes, exclusive of the objective study of the photographic process: (1) To describe a photographic material in terms of its function—how it looks or acts as a photographic positive or negative—in numbers derived from physical measurements. This functional description is the purpose of product evaluation. It may be required for comparison

* Communication No. 1298 from the Kodak Research Laboratories.

of the product with an ideal, with a standard, or with another product. (2) To furnish quantitative information helpful in maintaining at a fixed level the photographic characteristics of the film or the quality of its processed images. This is the purpose of product or processing control; it is especially important in the film-manufacturing plant and in the processing laboratory.

To fulfill these two purposes, many systems of color densitometry have been developed. Each one has been designed to obtain the most significant data possible to answer one or both of two questions: (1) What will be the action of the developed image as an element of the optical system in which it will be used? (2) Of what is this developed image composed? The first question is most often asked in the course of product evaluation, and the second more frequently in product control. These questions have given rise to two classes of color densitometry: "integral densitometry," and "analytical densitometry." The first determines densities of the multilayer image as a whole; the second determines the amounts of its component absorbers. The methods used in the two types of determination are generally quite dissimilar. Each of these classes is further divisible, since special definitions have resulted in several kinds of integral density and several kinds of analytical density. A classification of these is given in Fig. 1.

INTEGRAL COLOR DENSITOMETRY

When a color-film transparency is inserted in a printer, a projector, or other optical system, each elementary area acts as an optical filter, that is, it absorbs radiant energy. If we want to determine the effect of this filter in the optical system, we are interested not in its components but only in its integral action. The kind of density in which this action is expressed is integral density; its measurement is called integral densitometry.

Classically, density is defined as

$$D=\log_{10}(1/T),$$

where T is the transmittance of the sample. The definition of the American Standard for Diffuse Transmission Density Z38.2.5—1946 is

$$D=\log_{10}(P_0/P_t),$$

where P_0 is the radiant energy incident on the sample, and P_t is the radiant energy transmitted by the sample. Density, then, expresses the effect of an absorber on the total energy of the light beam on which it acts. To measure it in conformance with this simple definition requires that all the energy transmitted by the sample be collected and equally evaluated by the receiver of the measuring instrument.

This definition of density is inadequate for integral color densitometry. In most cases, no useful information can be obtained from an instrument which weights equally all components of the transmitted light without regard to wave-length. Color films are not used in such systems. They are used to control responses, photographic, photoelectric, or visual, which are highly selective with respect to wave-length. There is no satisfactory way to obtain information applicable to such systems from measurements made with equal weighting. A particular, precisely defined weighting must be used, and it must be performed by the densitometer.

PRINTING DENSITIES

In any normal use of a color-film transparency each of its elementary areas is required to control one or more of a small set of responses. The responses may be photographic or visual. In making a black-and-white print of a color transparency, one response alone is controlled, the latent-image formation in the single print material. In making a color print on a three-emulsion material, three responses are controlled. If the transparency is projected or otherwise viewed, each elemental area will, in terms of the trichromatic concept of color vision, control three color-stimulus responses.

These responses must be considered as always of the same kind, regardless of the wave-length of the light which stimulates them; they change only in magnitude. If, for example, the response is cyan dye formation, it must always be cyan dye formation. Then, two energies, even though as different in kind as red and blue light, can be said to be equal in amount if they produce equal responses of the required kind. Thus, a red and a green light are said to have equal luminous intensities if, under the same conditions, they produce equal sensations of brightness; they would have equal photographic intensities if they could produce, in a given photographic system, equal image densities.

By evaluation in terms of the required kind of response, it is possible to compare the intensity of energy incident on a filter with the intensity of the energy transmitted by the filter, even though the qualities of the incident and transmitted light are made dissimilar by selective absorption of the filter. One can thus determine the ratio of incident photographic intensity to transmitted photographic intensity. This is a ratio of energies—energies evaluated according to their ability to produce a fixed response. It is not a ratio of responses, unless those responses happen to be proportional to the stimulating energies.

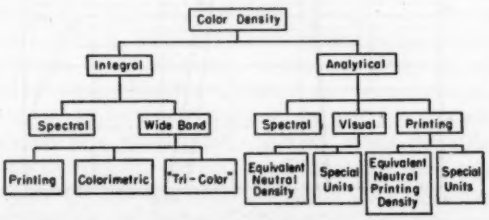

FIG. 1. A classification of color densities.

If a transparency is to be used as an intermediate step in a photographic process, i.e., if it is to control the exposure of a print, its integral absorptions are most significantly evaluated by measurement of its effect on the photographic intensity of the printing light. This effect is expressed by its printing density, the $\log_{10}$ of the ratio of incident to transmitted photographic intensities:

$$D_p = \log_{10}(\phi_0/\phi_t),$$

where ϕ_0 is the photographic intensity of energy incident on the sample, and ϕ_t is the photographic intensity of energy transmitted by the sample.

In black-and-white sensitometry, printing densities are also used[1] and can be defined in the same way. The essential difference lies in the difficulty of determining the photographic intensity of the light. In photographic color printing, sharp selectivity with respect to wavelength usually exists either in the sensitivity of the print material or in the energy content of the printing light, or both. There also is sharp selectivity in the spectral transmittance of the absorbers to be measured. Unless the system for measuring printing density accurately weights the spectrum of the measuring light in conformance with the weighting which exists in the printing system, the effective density of a selective absorber will be incorrectly determined.

The requirements of correct weighting are rather easily derived. The simplest device for measurement of D_p consists of a light source, a filter, and a photo-cell,

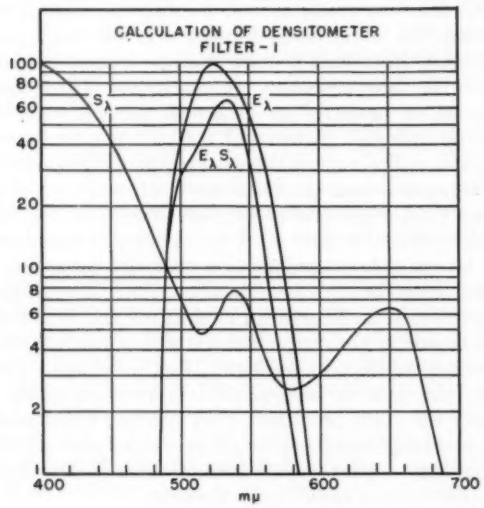

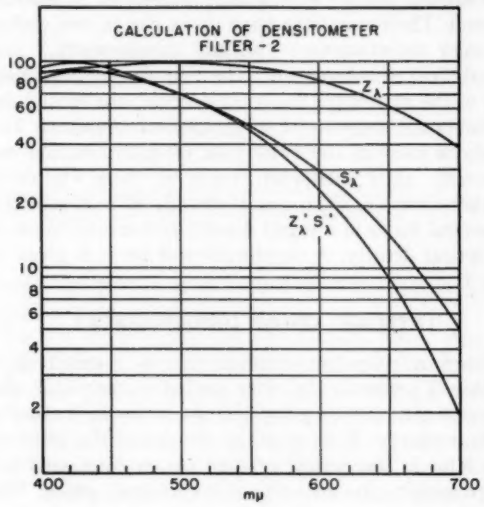

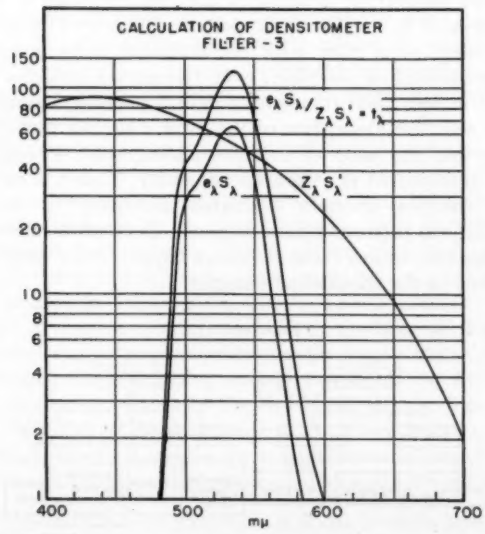

FIG. 2. A typical determination of the spectral transmittance distribution of a filter required for a densitometer to measure printing densities. (a) Light sources in printer and in densitometer are in this case the same; J_λ and J_λ' cancel. Relative e_λ is shown; it is largely governed by use of a Wratten No. 60 filter in this printer. S_λ shows relative spectral sensitivities of print film. 10× the product $e_\lambda S_\lambda$ is shown. (b) Fixed densitometer factors Z_λ (relative spectral efficiency) and S_λ' (photo-tube sensitivity) are shown, and their product. (c) The product of the printer terms is divided by product of densitometer fixed terms to determine required distribution of filter transmittance.

[1] J. G. Frayne, J. Soc. Mot. Pict. Eng. **36**, 622 (1941).

with a means of determining the photo-cell output. This instrument is required to measure the densities which a film transparency would have if it were placed in a printer optical system consisting of a light source, a filter, and a print material. Inserting the sample in the optical system of the densitometer must reduce the photo-cell output in the same degree to which the photographic intensity of the printing light would be reduced if the sample were inserted in the printer optical system. For simplicity, it is assumed that, for energy of any one kind, the photo-cell output is proportional to the intensity of its irradiation.

Let J_λ be the spectral radiant intensity of the printer lamp, e_λ the relative spectral efficiency of the entire optical system of the printer, and S_λ the spectral sensitivity of the print material. The spectral transmittance of the film sample is T_λ. The photographic transmittance of the film sample, that is, its transmittance as determined by its effect on the photographic response, is given by

$$\frac{\int J_\lambda e_\lambda S_\lambda(T_\lambda)d\lambda}{\int J_\lambda e_\lambda S_\lambda d\lambda},$$

and the printing density of the sample is the $\log_{10}$ of the reciprocal of that ratio. Also, let J' be the spectral radiant intensity of the densitometer lamp, e' the relative spectral efficiency of the densitometer optical system, and S' the spectral sensitivity of the densitometer photo-cell. The integrated transmittance of the film sample as determined by its effect on the photo-cell response is given by

$$\frac{\int J_\lambda' e_\lambda' S_\lambda'(T_\lambda)d\lambda}{\int J_\lambda' e_\lambda' S_\lambda' d\lambda}.$$

The densitometer is graduated in density units based on this integrated transmittance, that is, $\log_{10}$ of the reciprocal of this latter ratio. These units will be printing densities if these two ratios are equal. Theoretically, they can be made equal by innumerable combinations of functions, but, since T_λ varies widely and independently of the other factors, the only condition which will dependably satisfy the spectral requirements is

$$J_\lambda' e_\lambda' S_\lambda' = k(J_\lambda e_\lambda S_\lambda)$$

at all wave-lengths; that is, the spectral distribution of densitometer response must be proportional to the spectral distribution of the printer response.

The densitometer designer usually must consider the printer characteristics, J_λ and e_λ, fixed for each required type of reading; at least they are not variable for his purposes. Since the densitometer is being designed for a given S_λ, the entire right-hand member of the equation is fixed. In the left-hand member, only a rough variation is practical in the selection of J_λ' and S_λ' through the choice of the densitometer lamp and photo-cell. The remaining variable is e_λ', the relative efficiency of the densitometer optical system in transferring spectral energy from the source to the photo-cell. It is specified by

$$e_\lambda' = k\frac{J_\lambda e_\lambda S_\lambda}{J_\lambda' S_\lambda'}.$$

In the simple instrument used as example here, the spectral efficiency is most easily controlled by inserting a filter. The efficiency e_λ' then will be determined by two factors, the fixed selectivity of the densitometer's original optical system and the transmittance of this filter. Call these factors Z_λ and t_λ; then the required transmittance of the filter, t_λ, is specified by

$$t_\lambda = k\frac{J_\lambda e_\lambda S_\lambda}{J_\lambda' S_\lambda' Z_\lambda}.$$

Figure 2 shows the steps of computing the desired characteristics of a filter to be used in a densitometer in order to read densities in terms of printing green-record matrices on Eastman Pan Matrix Film, assuming certain printer characteristics.

Many color-printing operations involve making three prints through the same transparency. The three prints are dissimilar because (a) the three print materials are differently sensitized (i.e., they are red-, green-, and blue-sensitive), or three different filters are used in making the prints, or both, and because (b) each area element of the transparency has three, usually different, integral densities corresponding to these three printing conditions. The densitometer is required to make three density determinations on a test sample, corresponding to these three printing densities. It must be possible, therefore, in such densitometers to shift rapidly among three functions, e_λ'. In the simple case considered here, this could be done by providing three filters, each with transmittance correct for one of the required instrument responses.

Note that in the design of such a densitometer no account is taken of the spectral transmittance of the sample, T_λ. There is, therefore, no restriction on the nature of T_λ in samples to be read by the instrument. This type of densitometer, if properly designed, will read printing density values of any non-fluorescing material, in terms of printing on one specific print material in a given printer system. If all its optical characteristics are correct, it will measure, with equal facility, the printing densities of an area of a color transparency, a black-and-white silver negative, or a dyed-gelatin filter. This flexibility is in marked contra-

distinction to the limitations of some other types of color densitometer.

COLORIMETRIC DENSITIES

Printing densities are of primary interest only in materials which are used in an intermediate step in a photographic process. Many color transparencies are intended for direct viewing. These include 8- and 16-mm direct-reversal color films, the positive prints from motion-picture color processes, and color slides of all

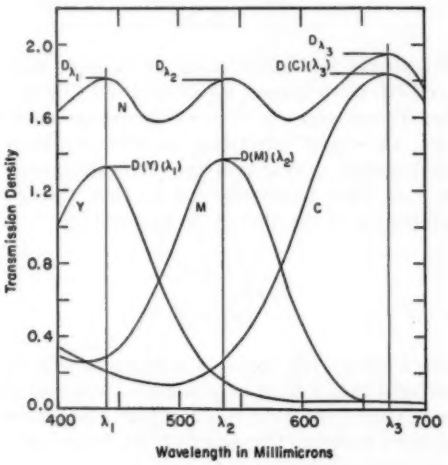

FIG. 3. Spectral density curves of (N) a gray area of a processed image in a typical multilayer subtractive color film, and of the (Y) yellow, (M) magenta, and (C) cyan component absorbers which combine to form the gray image.

types. Integral densitometry for films of these types should describe the image in terms significant in color perception, i.e., by a colorimetric system.

Other authors have discussed the principles involved and problems encountered in the direct determination of colorimetric stimulus values. They need not be reviewed here except to state that the principles are fundamentally the same as those involved in the determination of printing densities. In the design equations the spectral sensitivity of the print material is replaced by a stimulus function of some accepted colorimetric system. In colorimetry, this type of direct measurement is rarely made with any claim to high accuracy, excepting measurements of nearly nonselective materials. In color sensitometry it is made even more difficult by the requirement that a wide range of densities and a wide range of colors must be handled, but the requirements of accuracy are frequently less rigid. Satisfactory density values can usually be obtained from transmittance measurements which are subject to errors of two percent or more. Research in product development may, of course, demand higher accuracy. Well-known indirect methods are available for such work.

As a result of the difficulties of design and construction of densitometers for accurate determination of printing or colorimetric densities, there has arisen a widely used type of density measurement which can loosely be placed under the heading of tricolor densitometry. This type of measurement results from the use of nondescript red, green, and blue filters, frequently chosen for no better reason than that they are at hand. For some purposes, this type of densitometry is quite satisfactory. It determines the ability of the transparency to transmit blue, green, and red light of uncertain specification. This determination is adequate to test the identity of two samples of the same product, if, as in most cases, the product can form each color in only one way. If each color can be formed by only one set of colorant components, that color will always produce identical stimulus values in any measurement system. The limitations of such a densitometer must be realized, however, if it is to be used not for simple establishment of identities but to determine the direction and amount of deviation from a previously determined standard, or for the direct establishment of some image characteristics. Although densities measured by red, green, and blue light of any qualities will frequently give rough approximations to printing densities in terms of printing on red-, green-, and blue-sensitive materials, it is dangerous to assume that the approximation is adequate. It is particularly dangerous for samples exhibiting a high degree of selectivity throughout the spectrum, such as occurs in high densities of almost all transparency materials and in all densities, high and low, of products containing colored couplers. The same remarks apply to the assumption that these red, green, and blue densities constitute an adequate approximation to colorimetric densities. Large errors of interpretation are frequently made, not only in estimating the purity of the image but also in determination of its hue.

An attempt is now being made by the photographic industry to discourage widespread, indiscriminate use of this type of densitometry. By collective effort under the agency of the American Standards Association, certain standards of integral color densitometry are being set up to provide specifications of acceptable common practice.

SPECTRAL DENSITIES

Spectral densities are a special type of integral density. The spectral density of a sample is defined as its density to spectrally homogeneous light. By standard definition, this density is

$$D_\lambda = \log_{10} \frac{P_0(\lambda)}{P_t(\lambda)},$$

where D_λ = spectral density at wave-length λ, $P_0(\lambda)$ = radiant flux of wave-length λ incident on the sample, and $P_t(\lambda)$ = radiant flux of wave-length λ transmitted by the sample. Spectral densities are accurately deter-

mined by using as the source of energy "lines" from an atomic spectrum. These are sometimes used in color densitometers; those most frequently used are the lines at 436 mμ and 546 mμ from the mercury arc spectrum, and 644 mμ from the cadmium arc spectrum. Use also is made of narrow bands selected from spectra dispersed by prisms or gratings, as is done in spectrophotometers. If these bands are pure and sufficiently narrow, their use also will produce density values in excellent agreement with densities the sample would have if rigorously homogeneous energy were used, even when the sample is highly selective. Approximations satisfactory for most sensitometric purposes are obtained by using filters to pass narrow spectrum bands. This method has widespread use, largely because simpler instruments can be made with incandescent sources and filters than can be made with arc sources or dispersion devices.

Whatever the source, even though it is a spectrum line, the radiant energy it produces covers a spectrum band and is not a single wave-length. The spectral integral density, therefore, can be expressed by the general definition of integral density,

$$D=\log_{10}\frac{\int J_\lambda' e_\lambda' S_\lambda' d\lambda}{\int J_\lambda' e_\lambda' S_\lambda' T_\lambda d\lambda}.$$

An integral density is a spectral density only if there are no significantly large values of either the numerator or the denominator integrands outside a small range of λ. This is easily accomplished for the numerator, but in the denominator the highly selective nature of the transmittance, T_λ, in some samples makes the problem more difficult. In measuring high densities of a yellow dye with blue light, for example, the value of T_λ for the intended measuring wave-lengths is sometimes less than one-thousandth part of its value in the red end of the spectrum. Then even if the instrument response to red light is only one-thousandth of its response to the blue, the transmitted red light will contribute more than the transmitted blue light will to the total response. The density determination, intended to be only in terms of blue light, will be grossly incorrect. In densitometers of high accuracy, capable of reading densities approaching 4.00, if more than a few parts per million of the summation of $J_\lambda' e_\lambda' S_\lambda'$ are contributed by wave-lengths far removed from the intended pass band, the density determinations will be appreciably in error. Since energy in the near-infra-red region is freely transmitted by most dyes used in color transparencies, special care must be taken to exclude infra-red energy from the measuring beam.

The choice of wave-lengths in measurements of this kind depends upon the intended use of the data. Figure 3 shows density-wave-length curves of component absorbers of a typical subtractive color film and, as curve N, their sum. The amounts of the components have been adjusted to form a gray, of which N is the spectrophotometric curve. Wave-lengths λ1, λ2, and λ3 have been chosen at the positions of the maximum absorption of each of the component absorbers. The integral spectral density of this neutral absorber is shown as $D_{\lambda 1}$ for wave-length 1, etc. By use of wave-lengths chosen at these positions, the integral spectral densities become most sensitive to variations in each of the components.

Other sets of wave-lengths may be chosen for other specific reasons. Frequently an otherwise free choice of wave-lengths is restricted by such densitometer characteristics as lack of range, or lack of sensitivity.

ANALYTICAL COLOR DENSITOMETRY

For many control operations, and for much investigative work, it is not sufficient to know the integral absorptions of the test samples. If a color film has three superimposed layers, each containing a different dye, all three dyes will contribute to all the integral densities of every area, even though some of the contributions may be small. In Fig. 3, curve N shows the spectral densities of an image made up of component dye deposits, Y, M, and C; these components are typical subtractive process dyes. It is evident that measuring the integral densities of the sample, N, with blue, green, and red light will not directly measure the yellow, magenta, and cyan components of N. Suppose a series of three-dye deposits being investigated is intended to vary only in component C. Integral density measurements of the series will not directly reveal whether C alone varies or whether other components also vary, since all integral densities will show change. But by special methods it is generally possible to determine, from integral density measurements of the composite image, which of the component absorbers are changing, and to determine the amounts and magnitudes of the changes; in fact, it is possible to assign to the components of a multi-dye image the magnitudes each must have in order that they will combine to make up the measured image. The process is called "analytical color densitometry."

The assumption that analytical color densitometry is possible involves the following secondary assumptions which should be recognized, even though they may later be ignored:

(1) It must be assumed that the image is composed of discrete absorbing components, with different spectral absorption properties, and that not more than a certain finite number of these components exist. If subtractive color images were simply composed of deposits of three dyes, the logical image components would be these dye deposits, and not more than three could exist in any image. But this is not true. Other absorbers always exist in a color film. Some of these are

stains, residual or process-formed, in the dye-containing layers, or in the pelloid layer, or the subbing, interemulsion, or filter layers. Surface reflections also act as absorbers. Some of these non-dye absorptions are constant; others vary as a function of image formation.

(2) In practical methods of image analysis it is assumed that the image is composed of components of known characteristics. It is therefore assumed that predetermination of these characteristics is possible. Some instruments require knowledge of certain spectral absorptions of the components. Others require that the components, usually dye deposits, be physically separated or individually formed on separate support sheets so that each can be introduced into the densitometer optical system in various amounts. The complex nature of color images and of the processes which form them frequently makes either exact isolation or exact measurement of the true components extremely difficult if not impossible.

In spite of these difficulties, however, analytical color densitometry is widely used. Where accurate determinations or isolation of components is impractical, approximations are used, and for most purposes the results are satisfactory. It may be adequate for the scope of this paper to describe the general procedures in use with only brief mention of the difficulties and approximations involved.

Since it is the object of most color processes to accomplish color variation in transparencies by varying the amounts of three dyes, it is the object of most analyses to determine the image content by measuring the amounts of three dyes. Suppose we assume a simple process in which this can be done, and further assume that the dye deposits can be formed individually on separate sheets of film.

In such a case, the absorptions of any uniform image formed by the process can be exactly matched by combining the separate sheets containing the separate dye deposits. It is only required for the match that the correct amount of each dye deposit be used; there is only one combination which will exactly match the transparency image. One type of analytical densitometer determines image contents by making such a match. It is provided with wedged deposits of each of the dyes. These can be inserted in one beam of a comparator. In the other (identical) beam of the comparator is the sample to be matched. The positions of the dye wedges are adjusted until comparison indicates that the sample and its synthetic counterpart are identical. Then the dye contents of the sample under test must be the same as those used in the matching wedge set. The amounts of these are known from previous wedge calibration. They are expressed in units described farther on in this paper.

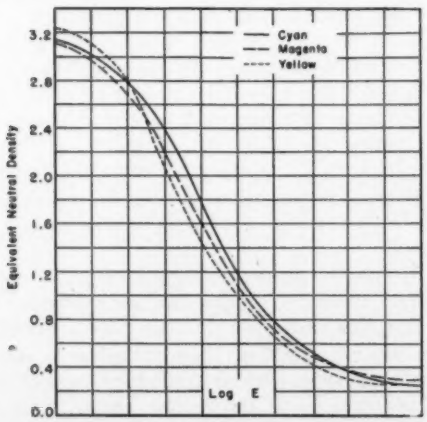

FIG. 4. Gray-scale characteristic curves of a sample of a professional sheet color film, using equivalent neutral density units for the density ordinate scale.

This method of analytical color densitometry is called "image synthesis." If it were done with an instrument having two exactly identical beams, and if the wedges in the synthesizing beam represented exactly the only three components of the measured image, at the condition of match the two halves of the comparator would present spectroradiometrically identical energies. They would match in color, and the condition of match could be determined visually. They would match in any three-stimulus system. Photo-cells responding to blue, green, and red light are frequently used to determine the existence of a match. If visual determination of a color match is used, it unfortunately is usually required that the color match be made at whatever color each transparency appears in the optical system employed. It is possible but inconvenient to avoid making matches at high saturations.

Evans[2] has described an instrument, also using dye wedges, which permits color matches always to be made at a fixed luminance level of gray. In this instrument a constant comparison color is matched by the color of light, initially the same as that in the comparison beam, which passes through the sample under test and also through three dye wedges and a fourth, neutral, wedge. The dye wedges are formed of the process dyes; the neutral wedge is a silver image deposit. The chromaticity of the comparison color is matched by adding to the absorptions of the light passing through the sample under test the absorptions of the just-required amounts of not more than two of the dye wedges. If the sample is, for example, too yellow, cyan and magenta wedges are added. The neutral wedge is also adjusted to complete the color match by making the brightness of the field illuminated by the measuring beam equal to that of the field illuminated by the comparison beam. The dye contents of the measured sample are determined from the settings of the wedges required to form with that sample the required fixed absorptions.

The use of dye wedges is avoided in another type of analytical densitometer in which the image is analyzed

[2] R. M. Evans, J. Soc. Mot. Pict. Eng. 31, 194 (1938).

by use of abridged spectrophotometry. Assuming, still, that the dyes of the process are the only absorbers in the image, and that deposits of these dyes can be formed separately, it is in this case necessary also to assume that for each member of a concentration series of each of the individual dye deposits, linear relationships exist among three spectral densities, usually the densities to wave-lengths near maximum absorption of each of the three dyes. These relationships are usually almost but not quite direct proportionalities. For any one combination of the three dyes, there can be only one set of integral spectral densities at the three wave-lengths chosen. Conversely, any image with a given set of three integral spectral densities must be formed of dyes of a unique set of concentrations. From mathematical relationships based on the linear spectral density functions of the component dyes, simple equations can be derived which permit rapid computation of the concentration values of this set, using as data only the integral spectral density values.

It is notable that in each of these methods of analysis the existence of match between the measured image and the sum of its determined component parts is ascertained by three and only three tests. If the method of image synthesis is used, with a visually determined color match as determination of identity, it is required that the measured image and its synthetic duplicate equally affect each of the observer's three color responses. If the synthesis is determined by photo-electric measurement, it is required that the measured and synthetic images equally affect the response of a photocell, whether it is covered by a red, a green, or a blue filter—again a three-variable match. The Evans densitometer requires visual, and therefore presumably trichromatic, determination of match. Analysis by abridged spectrophotometry customarily requires that at three wave-lengths the integral spectral densities of the measured image shall be matched by the sum of the spectral densities of the components.

If the measured image and its supposed synthetic counterpart need match in only three absorption attributes, the match can be achieved by combinations of components quite different from those of the measured image. The analytical description of the image will then be in serious error; but if the components assumed for the analysis are truly the variables of the measured image, the image and its synthetic counterpart will exhibit identical absorptions throughout the spectrum. The validity of the assumed components can be determined, at least in part, by examining whether or not spectrophotometric identity of absorption does exist. The results of such examination generally show that no set of three variables will by itself satisfactorily account for all the absorption distributions exhibited by the images of an actual color process. Better approximation results from assuming four absorbers, one of which may be constant. This is frequently done. Further elaboration of the analytical method may introduce severe requirements in the precision of density measurement.

It should also be noted that the individual dye deposits of the process are not the only possible analytical variables. Others have been used, such as the absorbers formed in an image by separate elements of the processing sequence. The variables chosen for any particular application should be those giving the most valuable data for the job at hand.

The unit in which analytical densities are expressed is of great importance in determining the usefulness of the data. In Fig. 3, curve *N* shows the spectral densities of a deposit formed of the assumed component dye deposits, Y, M, and C. Spectrophotometric analysis of this deposit, using wave-lengths λ_1, λ_2, and λ_3, will show a yellow component density equal to $D(\mathrm{Y})(\lambda_1)$, a magenta component density equal to $D(\mathrm{M})(\lambda_2)$, and a cyan component density equal to $D(\mathrm{C})(\lambda_3)$. Their values are 1.34 for the yellow density, 1.38 for the magenta density, and 1.84 for the cyan density. If these components are combined, they form a gray deposit of density 1.72, but this fact is hardly obvious from the individual density values. Since the formation of gray deposits is a highly important function of many color films, it is useful to know just what gray density can be formed with a given deposit of a component absorber. To provide this information, the concept of equivalent density (or equivalent gray density, or equivalent neutral density) was developed by Heymer and Sundhoff[3] and independently by Evans.[2] In effect, Evans defined the equivalent neutral density of a component of a subtractive color process as the visual density it would have if it were converted to a neutral gray by superimposing the just-required amounts of the other absorbers of the process.

It is generally accepted practice to use equivalent neutral densities to express the amounts of individual components in films intended for direct viewing. A typical set of analytical characteristic curves is shown in Fig. 4. These are the components of a gray scale of a professional sheet film. The gray-scale images of this product are (intentionally) not exactly gray. If they were, the three component densities of each point on the scale would be identical; the result would be a single curve or, rather, three congruent curves. In the actual scale, where the cyan component is adequate to form a gray deposit of density 2.00, it is accompanied in the gray-scale image by magenta adequate to make a gray of density 1.80, and yellow adequate for a density of 1.64. The relationship of these densities indicates that the gray-scale image at this point is actually blue, and to a lesser extent, green.

Equivalent neutral densities can be read directly from the wedge settings of image-syntheses densitometers. They are easily derived from the wedge settings of Evans densitometers. Since they usually are

[3] G. Heymer and D. Sundhoff, Veröffentl. wiss. Zentral-Labs. phot. Abt. I. G. Farbenind. Akt-Ges. AGFA **5**, 62 (1937).

nearly linear functions of single-element monochromatic densities (not quite proportional to them), they can be directly determined by the spectral-density analysis method. In this last case, the direct computation of equivalent neutral densities from (usually three) integral spectral densities can be performed rapidly by rather simple electrical analog computers. The process is a type of coordinate transformation and is frequently called "density coordinate conversion."

EQUIVALENT NEUTRAL PRINTING DENSITIES

Not all color films are intended for direct viewing. Many are intended to control the exposure of other photographic materials; these are the materials for which printing densities serve as a functional description. For them, the concept of equivalent neutral density has been expanded to specify the term "equivalent neutral printing density." It is directly analogous to the parent term. It may be defined as follows: *The equivalent neutral printing density of a component of a subtractive color process is the printing density of the (nonselective) neutral absorber which would be matched by adding to that component the just-required amounts of the other components of the process to form a combination with all printing densities equal.* This is merely the original definition of equivalent neutral density, with the observer replaced by a print material; instead of the observer judging visually that a composite image effects equal reductions of all color stimuli, the print material is used to indicate that the composite image has effected equal reductions of all print exposures.

Analytical curves plotted in this density unit have this important advantage: To close approximation, identical prints can be made from any two samples of a product which have the same intercomponent density differences, simply by intensity adjustment of the print exposures. Direct determination of equivalent neutral printing density can be made with an image-synthesis wedge instrument, if the wedges are calibrated properly. Direct determination by the Evans densitometer requires provision for color-matching with a triple response system equivalent to that formed by the print material sensitivities. Direct determination can be performed with the spectral-density analysis system if equivalent neutral printing densities can be assumed to be linear functions of single-element monochromatic densities. The assumption is frequently justified.

Complete density description of a color-film gray scale requires determination of both, functional properties and composition of the image set. Only the fundamental concepts underlying such determinations have been discussed here. Little discussion has been presented of the many difficulties involved in the actual application of these fundamental concepts.

JOURNAL OF THE OPTICAL SOCIETY OF AMERICA VOLUME 40, NUMBER 2 FEBRUARY, 1950

Some Considerations in the Design of Double-Beam Analyzers for Industrial Control*

GILBERT KIVENSON
Mellon Institute, Pittsburgh, Pennsylvania
(Received January 3, 1950)

The design and constructional features of infra-red and ultraviolet double-beam analyzers are discussed. Various optical and electronic arrangements are described and the most commonly used methods of evaluation listed. Some recommendations for future research have been made.

A. INTRODUCTION

WITH the increased use of double-beam analyzers for the control of plant stream compositions and the gradual appearance of commercial instruments, considerable interest has arisen in the various constructional features of this specialized type of spectrometric equipment. Recent literature descriptions of double-beam analyzers[1–7] have demonstrated a wide variety of designs, some representing successive stages in the development, others being specifically intended for a given application. There are, however, several basic factors in the design of infra-red and ultraviolet analyzers† which can be considered and which will be of

* This work is part of the program sponsored by the Office of Rubber Reserve, Reconstruction Finance Corporation, and has been approved by that office for publication.

[1] H. Schmick, U. S. Patent No. 1,758,088.
[2] N. Wright and L. W. Herscher, J. Opt. Soc. Am. 36, 198 (1946).
[3] W. G. Fastie and A. H. Pfund, J. Opt. Soc. Am. 37, 762 (1947).
[4] R. C. Fowler, Rev. Sci. Inst. 20, 175 (1949).
[5] Kivenson, Steinback, and Rider, J. Opt. Soc. Am. 38, 1086 (1948).
[6] V. F. Hanson, Ind. Eng. Chem., Anal. Ed. 13, 119 (1941).
[7] I. M. Klotz and M. Dole, Ind. Eng. Chem., Anal. Ed. 18, 741 (1946).

† The term "double-beam analyzer" as used in this discussion designates those instruments which employ liquid or gaseous filters in the infra-red or ultraviolet, are intended for continuous plant operation on flowing streams, and measure small transmission differences between a standard sample, not necessarily a pure solvent, and the material under consideration. In these respects they differ from the laboratory colorimeter which is generally operated with solid filter from the laboratory colorimeter which is generally operated with solid filters in the visible region. Some similarities will exist, however, in the physical equipment for both types of instruments.

service in the purchasing or building of an instrument. The considerations to be discussed are sufficiently removed from those involved in the construction of the usual spectrophotometers to justify separate treatment.

B. OPTICAL SYSTEMS AND TYPES OF BEAM INTERRUPTERS

A double-beam analyzer utilizes a comparatively simple optical system. Since no dispersion is employed, the optical requirements consist only of means to split radiation into two discrete beams, to pass it through the requisite number of cells and focus the two beams on one or two sensitive receivers. Figure 1(a) shows a simple arrangement for accomplishing this.[2] The radiation from a selected source is focused on two bolometers or thermopiles by means of a lens of suitable material. If the receivers have large sensitive-areas, the non-critical focus afforded by the lens is not a serious objection. In other variations of this design, the lens has been replaced by a pair of off-axis paraboloid mirrors with front surfacing; or the focusing means eliminated entirely and the radiation "funneled" to a pair of receivers by means of highly reflecting instrument walls.[3] Many designs involve a light interruption system to provide an alternating current signal at the receiver. The chopping methods used up to the present time fall into three general types: (1) non-reflecting choppers; (2) reflecting, diagonally placed interrupter disks; and (3) vibrating reflectors.

Figures 1(b) to 1(e) illustrate four arrangements utilizing non-reflecting disks. As pictured, a single source and receiver are employed, but instruments involving double sources or double receivers have been constructed.[1] Of the non-reflecting arrangements, those shown in Figs. 1(b) and 1(e) are the simplest, requiring a minimum of optical components. The type shown in Fig. 1(d) does not use off-axis parabolic mirrors, but the collimated radiation is divided by the source housing so that a crescent-shaped beam is passed through each cell.[8] Both types 1(d) and 1(e) permit a closer superpositioning of the two beams on the receiver for a given cell size. With large, enclosed receivers (such as photo-tubes) where some reflection and scattering may occur at the surface of the enclosing material, this advantage has great importance.

Diagonally placed reflecting chopper disks have come into use in several commercially available infra-red spectrophotometers.[9,10] In double-beam analyzers, where over-all size is sometimes of significance, they may permit a more compact arrangement of the entire optical system and a subsequent size decrease in the necessary housing.

In type 2(a), the field of the receiver is divided in half, so that the receiver views each beam from a slightly different angle. The feasibility of this arrangement and of the focusing lens depends on the particular application, the type of receiver required, and the range of wave-lengths employed. For cases where it is necessary that both beams be brought into exact alignment, the system of Fig. 2(b)[11] (using a disk silvered on both surfaces) may be used.

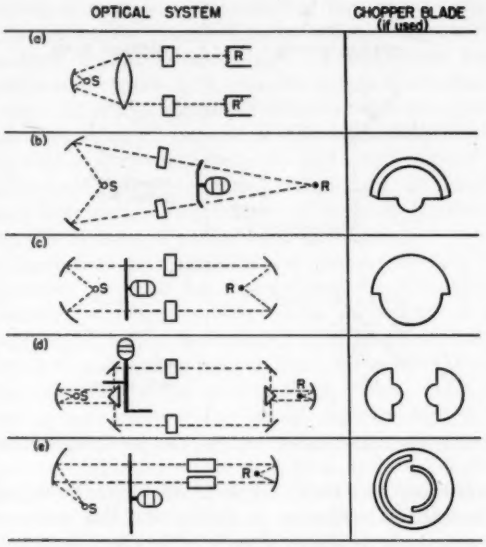

FIG. 1. Continuous radiation and non-reflecting chopper arrangements.

It is essential that the reflecting surfaces of diagonally placed disks be precision-polished and carefully silvered. A spurious signal during one-half of the cycle can usually be traced to an imperfect reflecting surface. Under the continuous operating conditions of industrial service, creep of the rotating member may sometimes distort the surface.

A third type of interruption arrangement consists of a vibrator-driven reflecting prism.[12] The incident radiation is focused on the prism, reflected to a pair of inclined plane mirrors and passes from these through the absorption cells. This system has an advantage in that an optical level principle can be employed, so that a large separation in light beam positions is obtained for a small vibratory amplitude.

The presence of a motor-driven interrupter device has presented some problems in the attaining of maximum signal-to-noise ratio. Many of the infra-red and ultra-violet receivers in common use show some microphonic response and are thus affected by motor vibration. In addition, the slight heating of the chopper disk and subsequent radiation may prove troublesome when very sensitive infra-red detectors are employed. The

[8] Jamison, Kohler, and Koppius, J. Opt. Soc. Am. **38**, 1099A (1948).
[9] Baird, O'Bryan, Odgen, and Lee, J. Opt. Soc. Am. **37**, 754 (1947).
[10] J. U. White and M. D. Liston, J. Opt. Soc. Am. **38**, 1098A (1948).
[11] Private communication from H. H. Cary, Applied Physics Corporation, Pasadena, California.
[12] W. A. Darrah, U. S. Patent No. 1,746, 525.

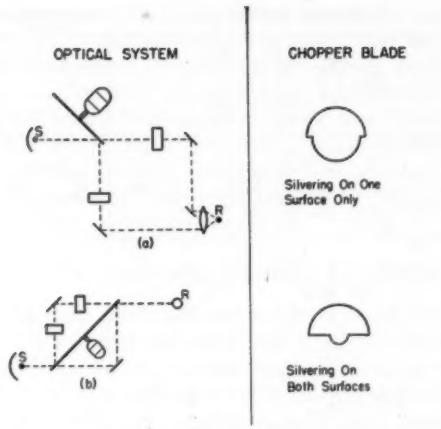

FIG. 2. Diagonally placed, reflecting chopper arrangements.

use of tuned amplifiers and electronic filters (Section E) is sometimes ineffective in eliminating this source of noise since the undesired signal is of the tuned frequency. Several interesting possibilities in this respect are open to further investigation. These include the use of Kerr cells for light pulsing, thyratron-operated gas tubes such as are employed in infra-red telephony for sources; and the modulation of a Nernst glower.[13]

C. SOURCES, CELLS, AND BEAM ATTENUATORS

Infra-red sources for double-beam analyzers present little difficulty when properly constructed. The requirement of blackbody conditions and low reflectivity at greater wave-lengths has not been as important as in the infra-red spectrophotometers. Successful use has been made of Nichrome coils, flat ribbons, spirals, and cones.[3, 5] It is necessary, however, that the glowing element be of sufficient rigidity and mounted sturdily enough so that it will not sag or bend when in use for long periods of time.

Adequate regulation of the emitted radiation may be accomplished by a transformer type of voltage regulator. The use of the double-beam principle and the interruption of the beams limits drift caused by minor voltage fluctuations and emissivity changes.

The application of ultraviolet gas discharge tubes in double-beam analyzers is complicated by the high temperature coefficient of resistance and de-ionizing rate of these tubes. The former makes the tube difficult to regulate and the latter permits undesirable modulation from inadequately filtered power supplies. Over-all instrument thermostating and the introduction of a monitoring photo-tube circuit‡ would probably help to eliminate ambient temperature effects. The utilization of high audiofrequency a.c. power with gas-filled tubes might permit the needed smoothing of the modulation.

Gas cells for double-beam analyzers have usually consisted simply of brass or steel containers with apertures in opposite walls. Cell windows of silver chloride or rocksalt have been attached with glyptal cement. Liquid cells suitable for streams at pressures close to atmospheric are described by Wright and Herscher.[2] Some applications of infra-red analyzers have been made to moderate-pressure liquid flows using quartz windows, but extension to greater wave-lengths in the infra-red has been seriously limited by the lack of window materials having both the required transmission characteristics and strengths.

A factor to be considered in the design of industrial analyzers is the accumulation on cell windows of solid material from the stream being samples. If a two-cell arrangement is used for gas analyses, one cell contains a stationary comparison standard, while the other holds the flowing unknown. Minute particles of dust will accumulate on the analytical cell window, causing an apparent drift as the transmission through one side of the instrument is continually decreased. The amount retained by the window is a function of the flow rate, the efficiency of filters placed in the gas stream, and the position of the cell window with respect to vertical. The comparison cell will suffer no deposit in this case. In liquid sampling, using the same cell arrangement, solid particles in suspension may also be deposited. If a considerable temperature difference exists between the outside surface of the cell window and the entering liquid, dissolved solids of low solubility will sometimes precipitate. In addition, liquid systems of high polymerizing power will deposit gummy residues on the window surfaces of the standard cell, this phenomenon being favored by the long immobility of the standard and occasionally by higher temperatures and actinic light in the ultraviolet instruments. Some measures in the design and operation of the analyzer can be taken to reduce such effects. Analyzer arrangements which use double cells such that the material being sampled passes a window surface in each beam are preferable. Placement of the instrument so that cell windows are vertical has been found to increase considerably the "on-stream" time for gas analyzers.

Automatic restandardization mechanisms which periodically turn off a liquid sample stream and force the comparison material or a solvent from a storage tank through one or more of the cells, can eliminate serious errors in analysis by preventing a consistent build-up of solid material. In addition, these devices will automatically correct for other cumulative errors such as drift due to aging of the source, changes in flow rate, etc. The mechanism of a restandardization unit is readily assembled. It consists of a sequence timer controlling a bank of switches, several solenoid valves, a balance-detecting relay, a reversible motor, and a potentiometer-battery nulling system. The period of restandardization is determined by the maximum error permitted in the analysis, and can be set to the desired value by adjustment of the sequence timer.

[13] R. E. Stark and D. E. Stark, U. S. Patent No. 2,389,649.

‡ Hanovia Chemical and Manufacturing Company, Newark, New Jersey.

Differences in optical alignment, cell thicknesses, and source intensity in each beam are usually balanced in double-beam instruments by the use of beam attenuators. These are often very simple in form, in some cases consisting only of small bolts which can be advanced, thread by thread, into the beam. The shadow thus created appears in proportionately reduced size on the receiver and decreases the amount of energy from that beam on the receiving area. In chopped-light instruments, the optical balance of the two beams is more critical and in this case the attenuators can be made in the form of gear-driven shutters with calibrated adjusting dials.[8] The edge of the shutter is so cut that the percentage reduction in light beam size is a linear function of the number of revolutions of the dial. This arrangement provides a valuable laboratory feature, since the transmission of various components in the stream to be sampled can be measured in terms of the "equivalent percentage of light beam decrease." The measurement is obtained by introducing the material in one beam and bringing the instrument back to null by use of the attenuator in the opposite beam. The results obtained represent a series of integrated transmission values for each material in the wave-length range, and under the conditions that the instrument will be operated in the plant application. These transmission figures are valuable in any preliminary calculations as to the feasibility of analysis of a given material by a double-beam analyzer.

D. RECEIVERS

Much has been written on both infra-red and ultraviolet radiation detectors. In recent years many new devices and improvements have appeared. Theoretical treatments of detector performance have also been made for many of the existing types. The designer of double-beam analyzers is fortunate in the respect that his classification of radiation detectors generally consists of only two major divisions: non-selective and selective receivers. The terms, "negative filtering" and "positive filtering" have also been used to designate these types. A non-selective receiver can be any one of the detectors commonly employed in infra-red or ultraviolet spectroscopy, with a desirable characteristic being that its variation of response with wave-length at constant radiation intensity is essentially flat or constant. In a double-beam instrument, it would, therefore, measure the unabsorbed energy in each beam and compute the ratio electrically. If, however, a suitable semi-opaque solid is interposed between the receiver and the beam so that solid and receiver are in thermal contact, the detector will then sense only that fraction of the two beams which is absorbed by the solid. If a dilute solution of the solid in a solvent is now placed in either beam, the response of the detector will change in proportion to the amount of solid present, and the signal will not be affected under ideal conditions by the presence of the solvent. The receiver, if used directly, would sense, not only the absorption of the solid, but that of the solvent in its characteristic bands. Concentration changes would therefore appear as small signal differences in large background signals for a non-selective receiver, and as a more discernible signal difference for selective operation. The potential increase in sensitivity thus afforded can enable analyses to be performed which depend on differences in fine structure, rather than on discrete band differences. This feature of positive filtering is valuable in cases of partial band overlapping.

Conversion of a non-selective receiver to selective operation can also be accomplished by placing the detector in thermal contact with the vapor of the material for which the analysis is to be made, but in such a position that neither beam strikes it directly. The gas absorbs the radiation selectively, indirectly heating the receiver.[14] The over-all time constant of the detecting system may be increased by this arrangement and some difficulty might be encountered in a chopped-light instrument. By the use, however, of very small gas chambers and rapid detectors such as the thermistor bolometer, this "offset" method of selective operation could theoretically be accomplished and the advantages of interrupted radiation retained.

Other methods of constructing positive filtering systems utilize the fact that a pressure rise accompanies selective absorption by a gas. Pfund[15] used a gas thermometer, consisting of two chambers connected by capillary tubing. Both chambers are filled with the sensitizing gas and an oil drop in the capillary indicates relative pressure. Radiation enters both chambers through cemented windows of suitable material. Changes in beam intensity can then be measured by the position of the oil drop. The apparatus is a version of Weber's microradiometer,[16] in which a conducting liquid is placed in the capillary and resistance changes are measured through sealed-in electrodes. Kidder and Berry[17] have adapted the Pfund apparatus to automatic recording by employing a long-filament lamp and photo-cell combination to measure the position of the oil drop. Barnes[18] utilizes the fact that only a portion of the radiation is absorbed in a positive filtering system and places several receivers in series. If each receiver is filled with a pure component gas, automatic multi-component analysis can readily be accomplished.

The adaptation of the pressure-measuring method to chopped-light instruments has been made by Luft,[19,20] Veingerov,[21–24] and others. The audiofrequency sound

[14] N. Wright, U. S. Patent No. 2,386,831.
[15] A. H. Pfund, U. S. Patent No. 2,212,211.
[16] Weber, Arch. sci. phys. et nat. [3] **18**, 347 (1887).
[17] R. E. Kidder and J. W. Berry, U. S. Patent No. 2,443,427.
[18] R. B. Barnes, U. S. Patent No. 2,431,019.
[19] K. F. Luft, Zeits. f. tech. Physik **5**, 97 (1947).
[20] K. F. Luft in "Study of the industrial processing instrument industry in Germany," U. S. Department of Commerce, Report No. PB-4600.
[21] M. L. Veingerov, Comptes Rendus U.S.S.R. **19**, 687 (1938).
[22] M. L. Veingerov, Izvest. Akad. Nauk. **4**, 94 (1940), Fig. 4.
[23] M. L. Veingerov, Comptes Rendus U.S.S.R. **46**, 182 (1945).
[24] M. L. Veingerov, Comptes Rendus U.S.S.R. **51**, 195 (1946).

produced by chopping the radiation is measured by means of a microphone. In the Luft apparatus a thin diaphragm forms a seal in a tube connecting a pair of gas-filled chambers. A perforated disk placed within 0.002 of an inch of the diaphragm forms the back plate of a condenser microphone. Two sources, simultaneously interrupted, heat the gas in the right and left chambers. When the beams are in balance, no movement of the diaphragm occurs and the capacitance of the condenser remains constant. When an absorbing material is introduced into either beam, the unequal heating of the gases in the detector chambers causes the diaphragm to distend and a measurable capacitance change to occur. The Veingerov unit is somewhat similar, but uses alternate chopping (the "flicker" system) and a dynamic microphone. The Hayes[25] and Golay[26] cells, although not designed as selective receivers, utilize the principle of pressure measurement and their conversion to selective operation would not be difficult.

Although data which could be used for comparative calculations of the merits of various detectors and selective receiver arrangements are now meager, the increasing number of instruments being tested in laboratories for application to plant analysis and control problems should provide sufficient information for such computations to be eventually made. In the final evaluation, not only would minimum detectable power, stability, and speed of each receiver need to be compared, but also such features as ruggedness and constancy of response under continuous operating conditions. From considerations of the fundamental limits of electronic equipment, it would not appear that positive filtering receivers are capable of lower detection thresholds than the negative filtering type. It is entirely possible, however, that the effective sensitivity of the former for a given problem can be made many times greater than that of the latter.

Recent work on infra-red photo-cells has produced several whose range extends somewhat beyond 3.5μ.[27–29] These are the lead sulfide, lead selenide, and lead telluride photo-conductive cells. The lead sulfide cell is now commercially available.** The use of a photo-cell in a double-beam analyzer not only affords greater sensitivity, but also permits higher chopping speeds. This makes the construction of stable tuned amplifiers and band pass filters a more simple task than for lower audio frequencies. In addition, the noise voltage of a photo-tube falls off with frequency and higher signal-to-noise ratios could theoretically be obtained. Although photo-cells are not selective, their higher sensitivity may allow the use of longer filter cell paths.

In the ultraviolet, the detector problem is much less involved. Excellent ultraviolet-sensitive photo-tubes and photo-multipliers have been commercially available for some time. In addition, the types of problems for which ultraviolet analyzers have been used in preference to infra-red machines are those involving one strongly absorbing material, so that the question of selectivity does not need to be considered. The potentialities of double-beam ultraviolet analyzers for continuous plant analysis have not been explored thoroughly enough, however, for a complete analysis of optimum detector requirements to be made.

E. AMPLIFICATION AND RECORDING SYSTEMS

The advantages of a.c. amplification have been well defined and it is generally employed in most double-beam analyzers. Since the signal from a source-receiver system is inherently d.c., it is necessary to convert the signal voltage prior to amplification. This has been done, in existing instruments, in three general ways: (1) use of an a.c.-driven bolometer bridge; (2) interruption of the signal from the receiver by a vibrating relay to give a pulsating direct current; and (3) light chopping.

Method 1 is subject to the effects of stray fields, and extra precautions must be taken in the shielding and grounding of both the output and power supply. Method 2 has been used to convert the output of thermopile bridges to a.c. As developed in the General Motors amplifier,[30] it has reached a high degree of perfection, permitting the detection and measurement of extremely low d.c. voltage levels. A mechanical interruption device is also incorporated in some commercial electronic recorders so that it is not necessary in many cases to provide a separate amplifier. If a sufficiently high frequency of interruption is used, it is possible to chop the output of an a.c. bridge, as in method 1. A novel way of converting the d.c. output of a photo-tube is given by Kalmus,[31] who pulses the emission of the cathode by means of a coil surrounding the tube and an audio oscillator.

Both methods 1 and 2 have the disadvantage that no discrimination is made against scattered light which enters the receiver. In method 3, if the radiation is chopped after being collimated and passed through the cells, the d.c. effect of scattered light on the receiver can be almost entirely eliminated. Methods 2 and 3 lend themselves readily to the use of tuned amplification, which is a powerful method of eliminating the effect of extraneous electrical disturbances and zero drift on the output signal. The narrower that the band pass is made, the less will be the effect of electrical pick-up and noise but, as Harrison *et al.*[32] point out, the increase in overall response time of the system places a practical limit on the extent to which the band pass can be decreased.

The availability of commercial electronic recorders having a high degree of dependability has made this

[25] H. V. Hayes, Rev. Sci. Inst. **7**, 202 (1936).
[26] H. A. Zohl and Marcel Golay, Rev. Sci. Inst. **17**, 511 (1946).
[27] R. J. Cashman, J. Opt. Soc. Am. **36**, 356 A (1946).
[28] J. Starkiewicz, J. Opt. Soc. Am. **38**, 481 (1948).
[29] T. S. Moss, Nature **161**, 766 (1948).
** Continental Electric Company, Geneva, Illinois.

[30] M. D. Liston, J. Opt. Soc. Am. **37**, 515A (1947).
[31] H. P. Kalmus and G. O. Striker, Rev. Sci. Inst. **19**, 79 (1948).
[32] Harrison, Lord, and Loofbourow, *Practical Spectroscopy* (Prentice-Hall, Inc., New York, 1948), p. 312.

means of recording the most popular. Their use is convenient from another standpoint. In many cases, unitized control systems are available which fit into or operate directly from the electronic recorders. It is therefore a simple matter to adapt a double-beam instrument to control after a preliminary test period as a recording analyzer.

For applications where control and remote reading features are not necessary, some reduction in housing requirements may be made by the use of recording milliammeters or millivoltmeters. These are less expensive, but have the disadvantage that the response time is a delicate function of the pen balance, the density of the ink used, and capillary adhesion between pen and paper. Since the time constant of a chopped-light double-beam instrument itself is generally low, the over-all response time is, in many cases, determined by that of the recorder.

The use of "servo" optical balancing and recording systems has not as yet been exploited in double-beam analyzers, although it has been used for some time in spectrophotometers. In the latter instruments[23] it permits operation of the receiver at or near an electrical null condition. In a double-beam analyzer, an automatic optical balancing system would provide a good method of eliminating changeover or transition signal. The latter will be discussed.

Two devices which may have promise for double-beam analyzers are the magnetic amplifier and the electronic switch. The magnetic amplifier or saturable core reactor permits the control of a.c. currents by means of comparatively feeble d.c. signals. Resembling a transformer in construction, it uses no vacuum tubes and has an upper frequency cut-off of approximately 400 cycles per second. When used in conjunction with an electronic preamplifier and a dry disk type of rectifier bridge, it has potential uses as a simple and reliable amplifying system for the output signals of various detectors. Electronic switches would permit multi-channel operation so that the intensities of two or more beams could be compared to that of the beam through a standard cell.

F. SYNCHRONOUS RECTIFIERS

In an instrument utilizing a single source and receiver, the beam being alternated by means of a chopper disk, an undesirable signal is generated at the detector (when both beams are of equal intensity) when the transition of the cycle occurs. The angle through which the chopper disk must turn before complete changeover is accomplished determines the relative length of the signal and is a function of the size of the beams and the diameter of the disk. The changeover signal is fairly high because it is generated either by both beams striking the detector simultaneously or by the complete absence of radiation on the receiver surface. When amplified and rectified, it appears on the recording device as a background voltage level and decreases the signal-to-noise ratio. It is non-random in the sense that it can be reproduced quantitatively in the instrument by duplicating the conditions at which it was originally measured, but it will vary in magnitude with concentration changes of the material under test. Three devices are in common use for reducing the effect of changeover signal: (1) a potentiometer-battery nulling system in the recorder circuit; (2) a commutator rectifier on the chopping disk drive shaft; and (3) a pulse generator driven by the chopping motor.

A nulling system merely enables the recorder output to be placed at zero when the beams are in balance. The rectification in this case is usually accomplished by a dry disk bridge of the copper oxide or germanium type. This arrangement does not use phase discrimination, so that the direction of a change in concentration is not indicated. By using a comparison sample of suitably low or high concentration of the desired component, the analyzer can be made to operate satisfactorily, and changes measured in one direction only.

The commutator method combines the rectifying and changeover-signal-elimination mechanism in one apparatus. The segments of the commutator are so placed that the signal is short circuited during the period of transition. The recorder inertia prevents oscillation during the short intervals of the transition periods. Since the device rectifies during other parts of the cycle and is in synchronism with the chopping disk, the polarity of the output d.c. depends on the direction of concentration change, so that the analyzer does not need to be operated undirectionally.

A simple a.c. generator attached to the chopper motor can be made to produce pulses equal in amplitude, of opposing polarity, and over the same interval as the changeover signals. In this way the latter are cancelled out and do not appear after subsequent rectification.

Of the three methods described, the nulling system is the simplest and most readily constructed. It does not compensate for changes in the transition signal with beam intensity changes. The commutator is the best from the latter standpoint, but is subject to failure from segment and brush erosion. The generator method is very reliable, but requires considerable care in the initial installation.

G. EVALUATION OF PERFORMANCE

The estimation of relative figures of merit for double-beam analyzers would enable comparison of various instruments to be made. It would also permit a logical choice whenever a given problem is under consideration. The large number of variables involved, however, make comparative calculations of such quantities difficult and unreliable. The best that can be done at present is the citing of various performance data on a particular instrument under specialized conditions.

The most obvious method of describing performance

[23] N. Wright and L. W. Herscher, J. Opt. Soc. Am. **37**, 211 (1947).

is in terms of ultimate sensitivity. Thus, information often appears on the minimum concentration change in a specific gas mixture, such as carbon dioxide in dry air, which can be detected by the instrument. Unless the prospective user intends to purchase the instrument for use with the same gas mixture, in a similar concentration range, this figure is difficult to interpret. A test gas could be accepted as a standard and applied to all instruments, but this will not take into account such indeterminate factors as source temperature, amplifier gain, band pass, speed of response, noise level, drift, etc., which would modify the figures obtained. Another method of evaluating sensitivity, used frequently in infra-red analyzers, is to state the change in resistance of the detector which is required to give full scale deflection of the recording device. Again, this does not give any information about the noise level, drift, etc. A sensitivity stated in this way may serve as a convenient reference for reproducing amplifier gain conditions in the same type of instrument, but cannot be used in reproducing optical conditions. The latter situation is somewhat improved with the use of calibrated trimmers and the stating of sensitivity in terms of the percent of reduction in the size of one light beam required to give full scale deflection of the recorder, since this measurement will be independent of light beam intensity.[8] The interpretation of such a figure with respect to the instrument response to various gases and liquids is, however, very difficult and depends to a large extent on the wave-length range being utilized.

If electronic performance is to be evaluated, a valuable index of merit is the signal-to-noise ratio. This can be measured by operating the instrument at the maximum practical amplifier gain with typical materials in the cells. The noise level can be measured from the recorder trace, a statistical mean calculated and compared to the sensitivity as obtained by any one of the above methods. The minimum detectable change in concentration of a given component can then be calculated. This figure measures the limitations imposed on the analysis (of the given material only) by the noise level of the complete electronic system, including the source, the receiver, the amplifier and recorder.

In some instruments, drift of the zero point occurs and this must also be evaluated in stating performance and in computing a restandardization schedule. The drift can be measured at the same time that the noise level is determined. When the average value of the recorder trace (arithmetic mean of the noise amplitude) changes by an amount equal to one-half the mean noise amplitude, a restandardization must be made if the full potentialities of the instrument are to be realized. The effects of recorder damping do much to complicate the situation, since the noise level appears very small and the drift rate is not altered.

Insufficient data are available on selective instruments to permit comparative figures of merit to be made, but it is apparent that new performance criteria will need to be adopted for this type of analyzer before a true comparison can be made with the non-selective type.

Present methods of evaluation of double-beam instruments leave much to be desired. As a direct result of this, experimental work with several types of instruments for each given application is becoming standard procedure. With the greater accumulation of data on a wide variety of substances under differing conditions, it may be possible in the future to derive a more suitable method of performance evaluation.

H. MISCELLANEOUS FEATURES

Complete thermostating of double-beam analyzers has come into general use. The additional cost has been more than justified by the gain in instrument stability.

The thermostating systems are of the usual "on-off" type and are set at temperatures of 30 to 40°C. An unusual difficulty occurs in the case of liquid streams. If the stream temperature is considerably lower or higher than that of the instrument, variations in flow rate will cause temperature changes in the liquid and an erratic behavior of the transmission measurement. Uniform stream temperatures can be had by the use of an auxiliary heat exchanger maintained at instrument temperature and the control of the liquid flow rate.

The need for explosion-proofing of analyzers in some applications introduces another complicating factor in design. Presently available housings, which meet the requirements of various safety codes, are limited in size. It might therefore be desirable to take the inside area of available explosion-proof housing, as the "base plate size" of a proposed new instrument.

I. CONCLUSIONS

The double-beam analyzer is a versatile tool of growing importance and its design and component features have been subject to much improvement and variation within recent years. The adaptation of optical methods to the needs of chemical plant control problems has been a slow process and much needs to be done; but the great progress of spectroscopy, the many wartime developments in optics, and the general wider acceptance of optical methods by industry will continue to yield improved instruments of this type.

J. ACKNOWLEDGMENTS

The author wishes to thank R. T. Steinback and M. A. Rider of this laboratory for their direct aid, and to acknowledge the many helpful suggestions of O. W. Burke of the Office of Rubber Reserve, and H. H. Cary of the Applied Physics Corporation. The author would also like to thank G. H. Young for help in the writing of this paper.

Letters to the Editor

Abridged Spectrophotometric Colorimetry with Photo-Cells

J. W. PERRY
Hilger and Watts, Ltd., London, England
November 9, 1949

THE paper by Hardy and Young in a recent issue of this Journal[1] describes a procedure in which a high degree of color control is obtained by spectrophotometric observation at a limited number of wave-lengths related by previous calculation to the supposedly known spectrophotometric distribution of the standard color. The method considerably simplifies the routine spectrophotometric control of color products. It may be of interest to describe how, in the course of improving photoelectric differential colorimeters of the cell and filter type[2] especially applicable in cases of spectrophotometric similarity, we have applied a somewhat similar procedure, with some essential differences, as indicated below.

A considerable gain in information of value to the colorimetrist and incidentally in colorimetric accuracy may be derived from photoelectric measurements of this type in which the range of the correcting filter is subdivided, or, more generally, in which the whole spectrum range is divided, with reference to (a) the correcting filters for X, Y, Z, or an equivalent system of other suitably chosen units, and (b) the conditions for an adequate distribution of spectrophotometric control from a colorimetric point of view. The relative potency of different regions of the spectrum in influencing the resulting color is a very important factor in this respect. This may in special cases (for example, of relatively high selectivity) involve detailed consideration of the spectrophotometric properties of the coloring constituents, but color relationships themselves influence the proper distribution of observations, as is obvious from Hardy's selected ordinate method of colorimetric reduction.

Utilizing this principle, the following outlines generally, from a colorimetric point of view, the basis of measurement upon which the instruments referred to, now being developed, depend, in their application to such purposes, but in application the working procedure may be abbreviated. The measurements enable a substantial measure of spectrophotometric control to be effected, provide measurements of chromaticity and brightness factor to first-order accuracy, and determine differences in these quantities to a high degree of accuracy, thus considerably extending the scope of usefulness of the differential colorimeter.

Let the spectrophotometric curve of the reference sample be given by $f(\lambda)$. $f(\lambda)$ may be equated severally to three other functions denoted by $\xi(X)$, $\eta(Y)$, and $\zeta(Z)$ where

$$X(\lambda)=\int_0^\lambda E\bar{x}d\lambda, \quad Y(\lambda)=\int_0^\lambda E\bar{y}d\lambda, \quad Z(\lambda)=\int_0^\lambda E\bar{z}d\lambda, \qquad (1)$$

in terms of which selected ordinates are linearly interpolated. With a photo-cell of spectral sensitivity $\phi(\lambda)=\psi(X)$ for the X summation, and a set of filters of transmission $\theta_j(\lambda)=\vartheta_j(X)$, designed to satisfy the conditions:

$$\int_0^\infty E\phi\theta d\lambda=\frac{1}{n}\int_0^\infty E\bar{x}d\lambda\cdots \qquad (2)$$

and $X_i=X_j$, where

$$X_i=(2i+1)/(2n)\int_0^\infty E\bar{x}d\lambda\cdots(i=0 \text{ to } n-1)$$

and

$$X_j=\int_0^\infty \vartheta\psi X dX \Big/ \int_0^\infty \vartheta\psi dX,$$

observations are taken to obtain

$$g_j(\lambda)=\int_0^\infty fE\phi\theta_j d\lambda$$

and provide corresponding values ξ_j', and similarly η_j' and ζ_j'. Corrections in the event of $X_i\neq X_j$ may be applied by interpolation. Thus, summations of the form $\Sigma\alpha_j\xi_j'$, $\Sigma\beta_{j'}\eta_j'$, $\Sigma\gamma_{j''}\zeta_j'$ are obtained for the X, Y, and Z sums, respectively, α_j, $\beta_{j'}$, and $\gamma_{j''}$ being constant coefficients, exact for illuminant E. The chromaticity is thus directly determined and the luminance factor, w, may similarly be found.

When variations $\delta\xi_j'$, $\delta\eta_{j'}'$, and $\delta\zeta_j'$ occur in ξ_j', $\eta_{j'}'$, and $\zeta_{j''}'$ with varying samples, the color difference determined as a differential is given directly to a high approximation by:

$$\delta x=(y+z)(y/wD)\Sigma\alpha_j\delta\xi_j'-x(y/wD)\Sigma(\beta_{j'}\delta\eta_{j'}'+\gamma_{j''}\delta\zeta_{j''}')$$

where x, y, and z are the chromaticity coordinates, w is the luminance factor, $D=\int_0^\infty E\bar{y}d\lambda$, and similar expressions obtain for δy and δz. Hence the color differences corresponding to the spectrophotometric variation observed in g_j may be expressed in the form $\delta x=\Sigma(\alpha_j'\delta\xi_j'-\beta_{j'}'\delta\eta_j'-\gamma_{j''}'\delta\zeta_{j''}')$ where α_j', $\beta_{j'}'$, and $\gamma_{j''}'$ have obvious derived values. On referring ξ_j', η_j' and ζ_j' back to their corresponding g_j values, we may reduce this to: $\delta x=\Sigma\epsilon_j\delta g_j$ and similarly for δy. The luminance factor variation may likewise be similarly expressed and thus the color variation is obtained directly from observations of δg.

As an example of the spectrophotometric application of this, commencing from a knowledge of the coloring constituents for the practical assessment of spectrophotometric color tolerances, one may attach suitable relative weights to the component terms in the final summations in order to adjust appropriately the stringency of the tolerance to the scientific and economic needs of the control procedure.

Space here does not allow a detailed consideration of the effect of small errors upon the measurement, but it is clear that the principle applying in the design of the differential colorimeters known as "Blancometers"[2] (*viz.*, that errors affecting absolute values cause inaccuracies in differential readings only in the second order) secures here likewise a correspondingly high degree of accuracy in the determination of the color coordinate differences δx, etc. A full description of the new form of instrument referred to herein will be published in due course.

[1] A. C. Hardy and F. M. Young, J. Opt. Soc. Am. **39**, 460 (1949).
[2] J. W. Perry, J. Sci. Inst. **15**, 270 (1938).

On the Effect of Slit Dimensions on Collimated Beam Intensity

LOUIS GOLD
Department of Physics, University of Colorado, Boulder, Colorado
November 2, 1949

THIS note is intended to make available a method for estimating the reduction of beam intensity which results from collimation. Where one is dealing with an inherently weak radiation it often becomes of vital concern as to the optimum compromise between the degree of collimation and the net intensity. The practice generally has been to approach this problem in a more or less arbitrary fashion; the present report may be helpful in eliminating this situation.

Recently Counter[1] has derived a relation for the power received by a detector placed at the base of a cylinder whose dimensions are negligible compared with the radius of a sphere which has a uniform brightness B. The expression which applies for the stated geometry is

$$P=(\pi a^2B/4)[(1+k^2)^{\frac{1}{2}}-k]^2, \qquad (1)$$

where a is the radius of the cylinder and k is the ratio $l/2a$, l being the length of the cylinder.

Now the limiting angle for radiation to pass through the cylindrical aperture (assuming that the walls are perfectly absorbing) is defined by the relation

$$\tan\phi=2a/l=1/k. \qquad (2)$$

Accordingly, the ratio of the power transmitted through the cylinder (P^*) to that which would be incident on a flat disk (P_0)

is given by the expression

$$P^*/P_0=[(1+\cot^2\phi)^{\frac{1}{2}}-\cot\phi]^2. \quad (3)$$

Relation (3) may also be written as

$$P^*/P_0=(1-\cos\phi)/(1+\cos\phi). \quad (4)$$

For the instance of the collimation of an x-ray beam ϕ is generally quite small so that an approximate form of (4) is

$$P^*/P_0=\phi^2/4. \quad (5)$$

Putting in the approximation $\phi\simeq\tan\phi=1/k$, we get finally

$$P^*/P_0=(a/l)^2, \quad (6)$$

a relation which may be used to estimate the effect of beam collimation on intensity. This, for a cylindrical slit whose diameter is 1 mm and length 1 cm, a beam angle of approximately 5° is achieved at the expense of a reduction of intensity of about 2.5×10^{-3}.

[1] V. A. Counter, AMC Report No. 1, Upper Air Research Program, pp. 152–158 (September 1, 1947).

Maximum Attainable Luminous Efficiency of Various Chromaticities

DAVID L. MACADAM
Research Laboratories, Eastman Kodak Company, Rochester, New York
November 30, 1949

ANY desired chromaticity can be obtained with any of an infinite variety of spectral energy distributions. One of those distributions yields that chromaticity with a greater efficiency—lumens per watt—than any of the others. Figure 1 shows this upper limit for all chromaticities. This limit can be obtained in only one way, by mixture of suitable intensities of a single pair of wave-lengths. Except for blue and purple colors of very high purity, the shorter of the two wave-lengths required for maximum efficiency is in the range from 448 to 470 mμ. The maximum luminous efficiencies for various wave-lengths of the spectrum, indicated at the spectrum locus in Fig. 1, are the standard luminosity values (ICI $\bar{y}$) multiplied by 680 lumens per watt. The latter is the maximum luminous efficiency (for 555 mμ) based on the new standard value of $c_2=1.438$ cm degrees, in Planck's blackbody radiation formula.

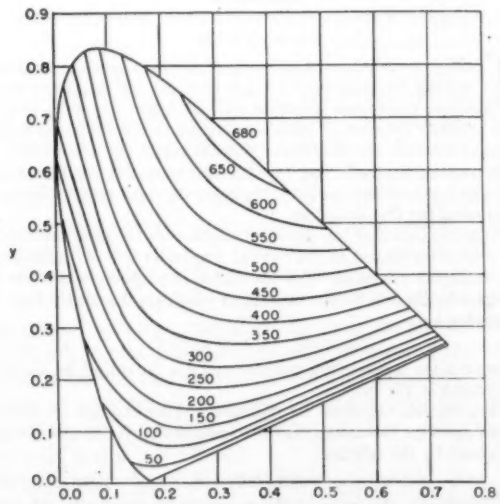

FIG. 1. Maximum possible luminous efficiency (lumens per watt) shown on ICI 1931 chromaticity diagram.

As an example of the use of Fig. 1, standard artificial daylight ($x=0.3101$, $y=0.3163$) obtained by filtering the energy from a tungsten filament lamp, has the continuous, but complicated spectral distribution tabulated for source *C* by the International Commission on Illumination. The same chromaticity can also be obtained by a mixture of any one of the pairs of complementary wave-lengths listed in the *M.I.T. Handbook of Colorimetry*.* It can also be obtained by a mixture of suitable intensities of any three wave-lengths, provided only that one is longer and a second shorter than the complementary of the shortest wave-length. Similarly, ICI source *C* can be matched with an infinite variety of intensity distributions among four or more wave-lengths, provided that some three of them satisfy the above requirement. Finally, an infinite variety of continuous spectral distributions can give the same chromaticity as ICI source *C*. By definition, the colors of sources having these different distributions are not distinguishable by a normal observer. Such chromatically identical sources are said to be metameric. Although they all match each other, they do not, in general, produce the same colors when they are used to illuminate any selectively reflecting or transmitting material. Consequently, the mixture of 448 and 568.7 mμ, which yields the same chromaticity as ICI source *C* at the maximum possible luminous efficiency (400 lumens per watt), would not be a satisfactory source of artificial daylight illumination. As a stimulus to be viewed directly for its own sake, such as in a television receiver, this most efficient mixture would be chromatically indistinguishable from daylight. However, color fringes due to chromatic aberration of the lenses of the eyes of the observer would be noticeable and militate against such use of that mixture. A similar objection could be raised against the use of the most efficient source of any other chromaticity, in most applications. However, like the maximum possible luminous transmittance data published some years ago,[1] the results for the maximum possible luminous efficiencies indicate absolute limits against which efficiencies of practical sources can be compared, and possibilities for major improvements assessed.

* *M.I.T. Handbook of Colorimetry*, Table VIII, p. 31.
[1] D. L. MacAdam, J. Opt. Soc. Am. **25**, 361 (1935).

Cadmium Spectra

K. C. MAZUMDER
The New Control and Research Laboratory, Tatanagar, India
September 13, 1949

A PAPER entitled "Cadmium spectra" was published in the March, 1949, issue of the Journal by A. G. Shenstone and J. T. Pittenger. An analysis of the Cd III spectrum was included in this paper. I published a paper on "Spectrum of doubly ionized cadmium" in the Indian Journal of Physics [Vol. 17, Part 4 (August, 1943)]. The experimental part of this investigation was carried out in Professor Siegbahn's Laboratory at Upsala, Sweden, in 1931–32. An abstract of my paper was duly published in the Physics Abstract **1311**, 118 (June, 1944). There was sufficient indication in this abstract of the nature of the work reported in the Indian Journal. I am sending you a copy of the reprints of my paper from which you will find that the group of lines arising out of the combination of the $4d^95p$ and $4d^96s$ terms given by Shenstone and Pittenger is exactly the same as in my paper. I calculated the ionization potential from the $5s-5p$ and $5p-6s$ groups of lines and put it approximately to 38 volts whereas Shenstone found it to be 37.6 volts. All the $6s$ terms and some of the $5d$ terms are about the same if $4d^{10}\,{}^1S_0$ is taken as zero. They differ only by 9 to 12 units. There are several cases in which reference has been made to my paper, e.g. "Spectroscopy past, present and future," J. Opt. Soc. Am. **36**, 431 (1946).

Cadmium Spectra

A. G. SHENSTONE
Palmer Physical Laboratory, Princeton University, Princeton, New Jersey
September 27, 1949

I REGRET very much that I failed to notice the paper by Dr. K. C. Mazumder referred to in his letter. I can attribute this lapse only to the fact that our work was done in 1940 and that I had no contact with ordinary scientific literature for the five years from 1940 to 1945.

Dr. Mazumder's paper, as he points out, correctly identifies the levels $4d^9 6s$ and, therefore, the ionization potential. He apparently failed to notice Rasmussen's paper of 1940 in which the $4d^9 5s^2$ levels of Ag II are given and he therefore did not identify the corresponding levels in Cd III. Of Mazumder's levels attributed to $4d^9 5d$, only half are real. A comparison with Pd I and Ag II reveals this fact. Also, an examination of his unidentified levels indicates that they, too, are unreal, since they fall chiefly in regions where no further even levels should exist.

Reflectance as a Measure of Absorption in Solid Crystalline Materials

PETER D. JOHNSON AND FRANK J. STUDER
Research Laboratory, General Electric Company, Schenectady, New York
January 9, 1950

IT is a common practice among workers in the field of luminescence to compare the reflectance of powdered crystalline phosphors with that of a standard material such as MgO in order to determine the spectral regions of strong absorption. The absorption characteristics thus obtained are often used in the correlation and interpretation of luminescence phenomena. In view of the prevalence of these procedures and since there appears to be practically no information in the literature comparing true absorption characteristics with reflectance data on the same material[1] in the range of ultraviolet wave-lengths of greatest interest in the study of luminescence (2000–4000A), we have compared the transmission of clear single crystals of phosphors with the reflectance from powders formed by pulverizing samples of the same material.

The phosphor selected for the preliminary work was KBr:Tl because of the interesting bands in its absorption spectrum.[2] Large crystals of this and other phosphors have been prepared in this laboratory from the melt in an apparatus similar to that described by Strong.[3] All optical measurements were made on a recording grating spectroradiometer designed by Studer, to be described in a later publication. A low voltage hydrogen discharge tube with a fluorite window provided continuous ultraviolet radiation in the region from 1850A to 4000A. The reflectance at wave-lengths longer than 2800A is not reported here since the emission of KBr:Tl begins at this wave-length.

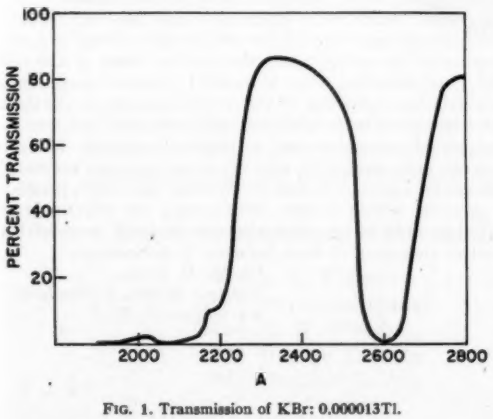

FIG. 1. Transmission of KBr: 0.000013Tl.

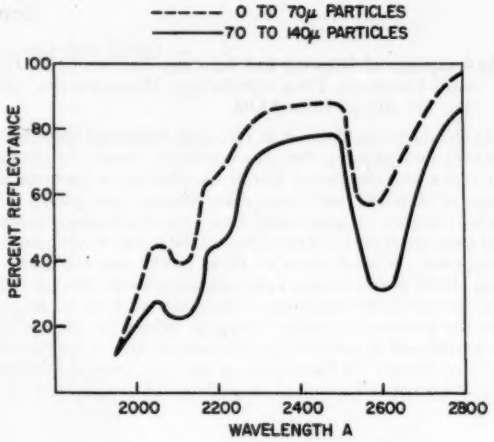

FIG. 2. Reflectance of KBr: 0.000013Tl.

Figure 1 gives the percent transmission of a KBr:0.000013 Tl crystal 5.0 mm thick obtained by comparing the spectroradiometer recordings with and without the crystal between the source and the entrance slit of the instrument. In Fig. 2 is shown the percent reflectance of the powdered phosphor of two different ranges of particle size compared with freshly prepared MgO. It is seen that all of the absorption and transmission bands observable in the transmission curve are found in both of the reflectance curves. This provides justification for using reflectance data to obtain absorption characteristics. In the actual spectroradiometer recordings the absorption peak at 2100A and the shoulder at 2180A were much more obvious in the reflectance than in the transmission curve.

It is reasonably certain that "holes" in the reflectance correspond to absorption peaks. However, the converse may not be true; a lack of reflectance holes may not be proof of the absence of absorption bands. It is seen from Fig. 2 that at smaller particle sizes the "holes" in the reflectance curves tend to be filled. Since most sulfide, silicate and other phosphors of commerical value are prepared with particle diameters averaging around 20μ or smaller, reflectance holes present in these materials may be nearly filled under certain circumstances. The particle diameter in addition to its effect on reflectance in regions of strong absorption also has a pronounced effect at wave-lengths where absorption is weak. Preliminary calculations indicate that these effects depend on the average length of path of the light in the phosphor before emerging. This path length is a function of the particle size and other physical characteristics of the material.

In a subsequent publication the apparatus and experimental techniques will be described more completely, and additional data will be presented and discussed.

[1] Urbach, Hemmendinger, and Pearlman, *Preparation and Characteristics of Solid Luminescent Materials*, G. Fonda and F. Seitz, Editors (John Wiley and Sons, Inc., New York, 1948), p. 279.
[2] N. Lorenz, Zeits f. Physik **46**, 558 (1928); W. Koch, Zeits. f. Physik, (a) **57**, 638 (1929); (b) **59**, 378 (1930).
[3] Strong, Phys. Rev. **36**, 1663 (1930).

Book Review

The Language of Drawing and Painting. ARTHUR POPE, Harvard University Press, Cambridge, Massachusetts, 1949. Pp. 162 plus xi. Price $5.00.

It should be understood at the outset that the language of drawing and painting does not consist of words. To produce a visual effect the painter has at his disposal, not words, but areas of different positions, sizes, shapes, and colors. The various modes of organizing these positions, sizes, shapes, and colors to express his meaning are the words in the painter's vocabulary. Several score of these modes are explained in some detail in this compact and scholarly book. Most of them have an arbitrary character. They may have to be learned like the words of a spoken language before the picture can be interpreted as intended by the painter. One of the simpler of these "words" is illustrated on the title page of the book (Fig. 1), a reproduction of an etching "Artist and Model,"

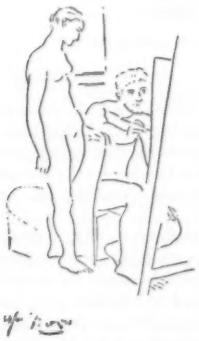

FIG. 1. "Artist and Model" by Picasso (reproduced by permission of the author).

by Picasso. You see there a painter in front of a window applying brush to an easel in the foreground with the model looking over his shoulder. That is, you see it that way if you have already learned an important "word" in the vocabulary of line drawing. Pope calls this word, "omission of detail for the expression of planes forward and back." If you have not learned this word, it will seem to you that the artist in the picture has only two-thirds of a face.

The "omission of detail for the expression of planes forward and back" is one "word" in one of the "languages" of drawing, that is, the language of line drawing. Other modes of drawing are form drawing and color-value drawing. Some of the modes having abstract or arbitrary meaning discussed in this book are: expressionism, calligraphic quality, linear expression, plastic expression, mode of line and local tone, mode of relief, pictorial mode, mode of the total visual effect, and normal, telescopic, and impressionistic handling of detail. The discussion of these rather difficult ideas is made intelligible by reference to a series of 67 black-and-white reproductions of drawings and paintings chosen to illustrate the different modes. You have to read a sentence, then study one of the plates for a minute or two, then probably read the sentence over again. It is fascinating but slow. One of Pope's main points is that much criticism of paintings is meaningless because the critic does not know the language of the painter; how then can he hope to read the message and judge whether or not it is well expressed! Maybe this is so. At any rate the pictures without the text are just as unintelligible to an amateur critic, like the reviewer, as the text without the pictures. But put them together and they make sense.

There are also modes of using color in painting that have arbitrary or symbolic meaning. Discussion of these takes up about half of the book. That they can be dealt with at all arises from the fact that the relations of the colors are described in terms of a three-dimensional diagram of color perceptions called a "working tone solid." This color solid is illustrated by four plates in chromatic color and corresponds so closely to what a normal observer perceives by looking at the Munsell book of color in daylight that it may most easily be described by telling what the differences are. The hues to be placed opposite one another are chosen on the basis of pigment mixture; that is, violet is placed opposite yellow instead of opposite its optical complementary greenish yellow; blue is placed opposite orange, and so on. For convenience, the most saturated color perception of each hue is diagrammed at the same distance from the gray axis, instead of using distances proportional to the contrast with the equivalent gray. And, finally, the color perceptions corresponding to colors of constant purity are represented by straight lines passing through the point representing the perception of black. This condition, met exactly by the organization of the original Atlas of the Munsell color system, is only approximately met by the present Munsell book of color. Pope uses intensity to indicate the saturation of a color perception, constant intensity at constant hue being indicated by vertical lines in the working tone solid. He uses value to indicate the lightness of the color perception, constant value being indicated by horizontal planes in the solid. And he uses brilliance as a name for the quality that is constant along straight lines passing through the white point. It is pointed out that it is impossible to paint a color chart that would be perceived exactly in accord with these requirements. This is an imaginary arrangement of color perceptions deliberately simplified for more convenient use. And it is used very well indeed in more than 50 explanatory diagrams. An object in light, half-light, and shadow usually yields colors of constant purity. One conventional substitute for this color sequence is the series of constant brilliance, in which the shadowed areas are represented by maximum instead of minimum saturations.

The basic limitation of painting is that the contrast ratios producible by pigments fall far short of those found in a scene illuminated by sunlight and shadow. In terms of the color solid Pope describes what is meant by normal rendering of value relations, crowding of the darks, crowding of the lights, and crowding of both lights and darks. He also indicates how exaggerated saturations and artificially systematic hue relations can make up for the effect of value contrasts necessarily deficient because of pigment limitations. The effects produced by painting within limited color ranges are effectively described in terms of the color solid and the book closes with an excellent treatment of color harmony in pure design.

DEANE B. JUDD
National Bureau of Standards
Washington 25, D. C.

The Frederic Ives Medal for 1949

Awarded by the Optical Society of America to

George Russell Harrison

for distinguished work in optics.

This medal, awarded biennially, was endowed in 1928 in honor of Frederic Ives, distinguished for his pioneer contributions to color photography, photo-engraving, three-color process printing, and other branches of applied optics.

The previous recipients of this medal have been

1929 E. L. Nichols	**1939 A. H. Pfund**
1931 Theodore Lyman	**1941 Selig Hecht**
1933 R. W. Wood	**1943 Loyd A. Jones**
1935 George E. Hale	**1945 W. W. Coblentz**
1937 Herbert E. Ives	**1947 W. F. Meggers**

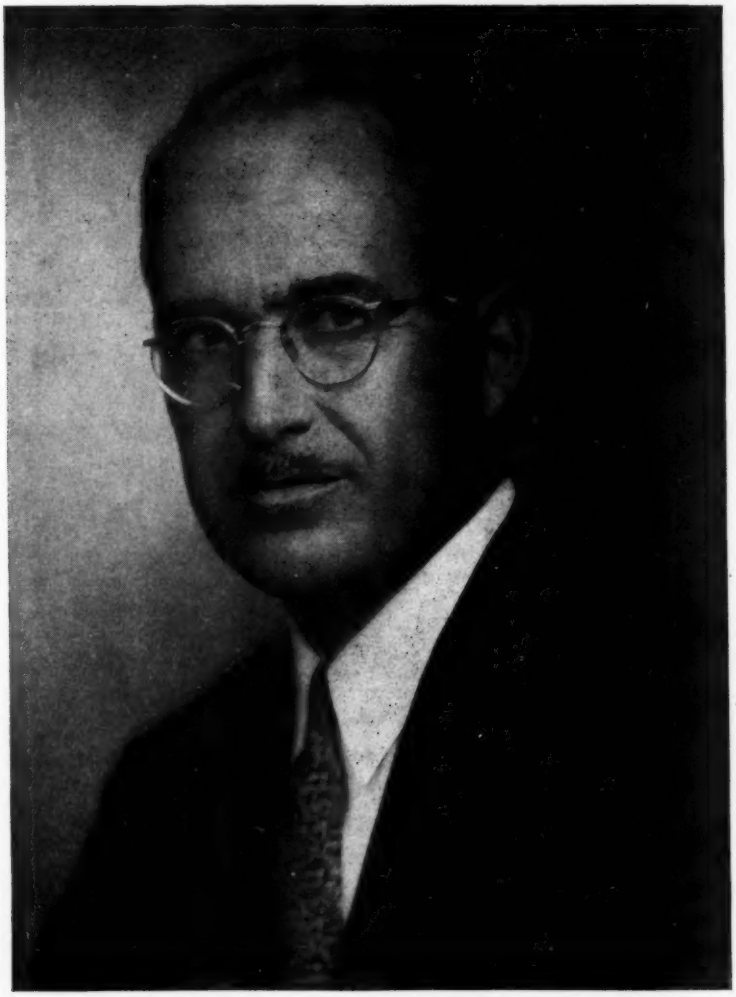

Fabian Bachrach

Dean George Russell Harrison

Frederic Ives Medalist for 1949

President of the Optical Society of America, 1945–1947

Editor of the Journal of the Optical Society of America, 1940–1950